

IDENTIFICATION AND CHARACTERIZATION OF A SMALL MOLECULE INHIBITOR
OF IMP-1 THAT DECREASES EXPRESSION OF IMP-1 TARGET MRNAS AND INHIBITS
PROLIFERATION OF IMP-1 POSITIVE CANCER CELLS

BY

LILY MAHAPATRA

DISSERTATION

Submitted in partial fulfillment of the requirements
for the degree of Doctor of Philosophy in Molecular and Integrative Physiology
in the Graduate College of the
University of Illinois at Urbana-Champaign, 2016

Urbana, Illinois

Doctoral Committee:

Professor David J. Shapiro, Chair and Director of Research
Associate Professor Jongsook Kim Kemper
Assistant Professor Eric Bolton
Assistant Professor Sayeepriyadarshini Anakk

ABSTRACT

RNA-binding proteins control a variety of biological processes ranging from messenger RNA splicing to transport and translation. These post-transcriptional events are critical for proper cell function. One emerging class of proteins functions in several of these capacities. The VICKZ family of RNA-binding proteins is involved in translation control, mRNA localization and mRNA stability. I have studied the Insulin-like Growth Factor-2 mRNA-Binding Protein 1 (IGF2BP1/IMP-1/CRD-BP). IMP-1 exhibits an oncofetal pattern of expression, where it is expressed in embryonic development and its expression is repressed shortly after birth. However, the IMP-1 gene is reactivated in many different human cancers. Overexpression of IMP-1 leads to increased levels of proteins that promote tumor growth, metastasis, and resistance to anticancer drugs and is associated with a poor prognosis. IMP-1 enhances proliferation and migration of cancer cells by binding to and stabilizing mRNAs important in cancer, such as c-Myc. Although the role of c-Myc in cancer has been well established, it has remained an elusive therapeutic target because of its role as a transcription factor in non-neoplastic proliferating cells. Given its oncofetal pattern of expression, targeting IMP-1 presents a novel approach to targeting c-Myc. To identify new chemical entities with therapeutic potential in IMP-1 positive cancer, we carried out a pilot screen using an *in vitro* fluorescence anisotropy microplate assay (FAMA) and found that this approach was robust and appropriate for high throughput screening. We then carried out a high throughput screen of approximately 150,000 small molecules. Reported here is BTYNB, the first small molecule inhibitor of IMP-1, BTYNB decreases levels of IMP-1 target mRNAs, inhibits proliferation of IMP-1 positive cancer cells, and functions through the unique mechanism of decreasing oncogene mRNA stability. We believe that BTYNB not only can be developed as a potential

therapeutic agent, but also serves as a useful molecular tool, with which we can probe the actions of IMP-1 in cancer cells. In addition to identifying and characterizing the first small molecule inhibitor of IMP-1, we were also interested in identifying novel molecular targets of IMP-1. Using *in silico* analysis of publically available microarrays where IMP-1 was knocked down, we identified a panel of candidate target genes. Using qRTPCR and Western blot analysis, we then confirmed whether or not the mRNAs of candidate genes were decreased with IMP-1 knockdown and identified Protein Kinase C α (PKC α) as a new molecular target of IMP-1.

Overall, this work has led to the identification and characterization of the first small molecule inhibitor of IMP-1 and has demonstrated that despite the fact that studies of the role of IMP-1 in cancer are rapidly expanding, there still remain novel molecular targets, such as PKC α , which may play critical roles in IMP-1 action in cancer cells.

*To my Mother, Dipti Rekha Mahapatra,
and Father, Rabindra Nath Mahapatra*

ACKNOWLEDGEMENTS

They say it takes a village to raise a graduate student. In this regard, I have so many people to thank who have extended their kindness, encouragement, and generosity of time on my path to earning a PhD.

First, I would like to thank my advisor, Dr. David Shapiro, for providing me with an excellent opportunity to conduct meaningful research and providing guidance and support on a daily basis in my pursuit of MD/PhD training. From the first day I stepped foot on University of Illinois campus (during the MCB/MSP interview weekend) and he was on my interview panel asking me the “tough questions” to our weekly lab meetings, Dr. Shapiro has challenged and strengthened my scientific thinking. His patience and love for science have been instrumental to my development as a scientist.

I would like to extend a heartfelt thank you to my doctoral committee members, Dr. Kemper, Dr. Bolton, and Dr. Anakk for your time and diligent effort in guiding my thesis work. Their feedback and support has proved invaluable over the course of my research project.

Thanks to the Medical Scholars Program for granting me an opportunity to pursue dual degree training, especially, Dr. Tony Jimenez, Dr. Nora Few, Dr. Jim Hall, and Professor Jim Schlauch. Your support and guidance has been excellent and I appreciate all of the time and effort you put into nurturing students.

Thank you to the members of the Shapiro lab for the friendship, fun, and cats! To Dr. Chengjian Mao thank you for sharing your knowledge of critical techniques that I used in the making of this thesis. I have enjoyed your friendship and calm presence you bring to lab each and every day. To former member Dr. Milu Cherian, thank you for your patience, friendship, and encouragement during my early years in the lab. You taught me a lot—from proper execution of FAMA to knitting, you are a jack of all trades! To Dr. Neal Andruska and Mat Cherian for the laughter we shared and for showing me the ropes in lab. Thanks for taking me under your wing and giving me awesome guidance both in lab and medical school—I couldn’t imagine my time at UIUC without you! To Xiaobin, Liqun, Mara, and Ji—you have been a joy to work with and I cannot wait to see what amazing work you will accomplish!

To the members of the Laboratory of Parasitic Diseases at the NIH, I would not be in an MD/PhD program if it were not for you. Thank you to Dr. Tom Nutman for allowing me to conduct research as a Post Bac IRTA for two and a half years in your lab and to shadow physicians in the LPD clinical unit at the NIH Clinical Center. To Dr. Roshanak Semnani—you remain one of the most generous, kindest people I know and your support and encouragement changed the course of my life. Thank you for giving me such an excellent foundation in molecular laboratory techniques and tissue culture. In the long run, it pays off learning how to be fastidious at the bench (even when working with parasitic worms)! To Drs. Sasi Bennaru and Simon Metinou—thanks for making science fun and teaching me not to take myself too seriously! Each and every one of you taught me so much and I am so thankful that I had the opportunity to learn in such a nurturing and productive environment.

To all of my friends at UIUC (especially Neal, Rachel, Mat, Carleigh, Itamar, Luke, and Chris) thank you for all of your help and support—whether it was with trouble shooting experiments, taking classes together, or laughing over lunch, your friendship has been instrumental in keeping me happy and hopeful throughout the course of my PhD training, which I will be forever grateful for.

Above all else, I must thank my family for their unwavering love, support, and faith. Thank you Ashis, Tara, Rohan, Ritu, Bob, Dad & Mom! Bob, our Sunday night calls were the most therapeutic part of my week and you always helped me see the brighter side of things. Additionally, your unsolicited advice is beyond reproach. You are such a joyful, kind and intelligent person—I really couldn't have a better role model in life! To my Nunna, thanks for being my “co-advisor” and always bestowing your wisdom and knowledge upon me. You are an inspiration to me and remind me that it is never too late to accomplish your goals. Thinking back on it, I can't believe how you were able to simultaneously work, earn a PhD and be a stellar Dad. Thanks for taking care of me when I had the chickenpox in second grade and you had to write your prelim paper (it is only now that I can fully appreciate this sacrifice). And finally, I would like to thank my number one fan, my Bou. There is an old proverb saying that “God couldn't be everywhere and therefore he made mothers.” Mom, you have been with me every step of this journey and nothing would be possible without your love, selflessness, and support. Thanks for always believing in me and my dreams—you are the best!

TABLE OF CONTENTS

LIST OF ABBREVIATIONS.....	viii
LIST OF FIGURES AND TABLES.....	ix
CHAPTER 1: BACKGROUND.....	1
CHAPTER 2: HIGH-THROUGHPUT FLUORESCENCE ANISOTROPY SCREEN FOR INHIBITORS OF THE ONCOGENIC MRNA BINDING PROTEIN, IMP-1.....	15
CHAPTER 3: A SMALL MOLECULE INHIBITOR OF THE ONCOGENIC MRNA BINDING PROTEIN IMP-1/IGF2BP1/CRD-BP TARGETS C-MYC MRNA AND INHIBITS PROLIFERATION OF CANCER CELLS.....	42
CHAPTER 4: IMP-1 REGULATES PROTEIN KINASE C ALPHA MRNA AND PROTEIN LEVELS.....	80
CHAPTER 5: DISCUSSION.....	100
CHAPTER 6: REFERENCES CITED.....	108

LIST OF ABBREVIATIONS

bp	Base pairs
BSA	Bovine serum albumin
CMV	Cytomegalovirus
CRD	<i>c-myc</i> mRNA Coding Region instability Determinant
CRD-BP	CRD-binding protein
DMSO	Dimethyl sulfoxide
DOX	Doxycycline
EC50/IC50	Half-maximal effective/inhibitory concentration
ER	Estrogen receptor
ERE	Estrogen response elements
FAMA	Fluorescence anisotropy/polarization microplate assay
HTS	High Throughput Screen
IGF-II	Insulin-like growth factor II
IMP1	IGF-II mRNA binding protein
KH	K-homology domain
MAPK	Mitogen-activated Protein Kinase
MMTV	Mouse mammary tumor virus
mRNA	Messenger RNA
PBS	Phosphate buffered saline
PCR	Polymerase chain reaction
PKC α	Protein Kinase C alpha
qRT-PCR	Quantitative RT-PCR
RNA	Ribonucleic acid
RT-PCR	Reverse transcription PCR
RRM	RNA recognition motif
SDS	Sodium dodecyl sulfate
SEM	Standard error of the mean
UTR	Untranslated region
VgIRBP	VgI RNA binding protein
ZBP1	Zipcode binding protein 1
Z'-factor	A measure of statistical effect size ranging from 0-1

LIST OF FIGURES AND TABLES

Figure 1.1 Alignment of KH RNA-binding domains of IMP-1 and related proteins.....	2
Table 1.1 The VICKZ family of RNA Binding Proteins.....	3
Figure 1.2 Domain structure of IMP-1.....	4
Figure 1.3 Schematic representation of IMP-1 action.....	7
Figure 1.4 Kaplan Meier analysis of overall survival in patients with ovarian, lung, or colorectal cancer that is IMP-1/CRD-BP positive or negative.....	10
Table 1.2 Expression of IMP-1 in human cancers.....	11
Figure 1.5 Specificity of IMP-1 and IMP-3 antibodies in detecting recombinant purified IGF2BPs.....	12
Table 2. 1 Summary of Statistical Data from the Pilot Screen.....	32
Figure 2.1 Schematic representation of Fluorescence Anisotropy Microplate Assay (FAMA) to evaluate binding of IMP-1 protein to fl-Myc RNA probe.....	33
Figure 2.2 Purification of IMP-1.....	34
Figure 2.3 Specific, high affinity binding of IMP-1 to fl-Myc RNA.....	35
Figure 2.4 Assay validation and high throughput screening results.....	37
Figure 2.5 Evaluation of hits for potency and specificity.....	38
Figure 2.6 IMP-1 knockdown inhibits cell proliferation in IMP-1 positive cells.....	39
Figure 2.7 Scheme for categorizing representative compounds from the pilot screen.....	40
Figure 2.8 Scatter plot of Z-scores from the plate containing the lead inhibitor.....	41
Figure 3.1. Scheme for identification and characterization of small molecule inhibitors of IMP-1.....	67
Figure 3.2. Dose-response studies show BTYNB is a sequence and structure selective inhibitor of IMP-1 binding to fl-Myc.....	68

Figure 3.3. Structural relatives of BTYNB have little or no ability to inhibit binding of IMP-1 to fl-Myc.....	69
Figure 3.4. IMP-1/IGF2BP1/CRD-BP protein expression in 31 cancer cell lines.....	70
Figure 3.5. BTYNB decreases IMP-1 levels in IMP-1 positive cell lines.....	71
Figure 3.6. BTYNB decreases expression of IMP-1 mRNA targets.....	72
Figure 3.7. Knockdown of IMP-1 and treatment with BTYNB decrease expression of eEF2.....	73
Figure 3.8. BTYNB decreases the stability of c-Myc mRNA, reducing expression of c-Myc mRNA and protein.....	74
Figure 3.9. IMP-1 knockdown blocks proliferation of IMP-1 positive cells with no effect in IMP-1 negative cells.....	75
Figure 3.10. BTYNB is a dose-dependent inhibitor of IMP-1 positive cancer cell proliferation.....	76
Figure 3.11. Compound 5226752, a structural relative of BTYNB, does not inhibit proliferation of IMP-1 positive or IMP-1 negative cells.....	77
Figure 3.12. Overexpression of IMP-1 reverses BTYNB inhibition of cell proliferation.....	78
Figure 3.13. BTYNB inhibits anchorage-independent growth of IMP-1 positive cells in soft agar.....	79
Table 4.1 Downregulated transcripts in IMP-1—depleted HEK 293T cells from microarray analysis.....	91
Table 4.2 PKC α and its roles in multiple types of cancer cells.....	92
Table 4.3 Predicted miRNA sites on PRKCA mRNA 3' UTR region produced by miRWalk and other programs.....	93
Figure 4.1. Knockdown of IMP-1 decreases PKC α mRNA.....	94
Figure 4.2. Knockdown of IMP-1 decreases PKC α and ERK protein.....	95
Figure 4.3. Knockdown of IMP-1 leads to a decrease in PKC α protein while overexpression of IMP-1 leads to an increase in PKC α protein in HEK 293T cells.....	96

Figure 4.4. Putative binding sites for miR-340 and IMP-1 in the 3'UTR of PKC α mRNA.....	97
Figure 4.5. miR-340 regulates PKC α protein levels.....	98
Figure 4.6. IMP-1 knock-down in IGROV-1 cells reduces NF- κ B luciferase activity.....	99

CHAPTER 1

BACKGROUND

RNA-Binding Proteins

Post-transcriptional modifications of mRNA transcripts at the 5' and 3' ends stabilize and protect the mRNAs from nucleolytic attack by degradative enzymes. RNA-binding proteins also play a critical role in protecting mRNAs, by binding to and protecting mRNAs from nucleases (1). Although RNA-binding proteins are known to play a role in regulating translation, little is known about the specific interactions that allow for this regulation (2). There is extensive RNA-binding protein involvement in the posttranscriptional processing of mRNAs, whereby RNA-binding proteins recognize specific features in the mRNAs and bind nascent transcripts at specific times during the processing of the mRNA (2). There are a variety of motifs that the RNA-binding proteins use to recognize and bind to RNA. Their ability to regulate gene expression and mRNA levels means that RNA binding protein overexpression has been identified in many diseases, including cancer (3,4). An example of an mRNA-binding protein that has emerged as a key regulator of oncogenes is IGF2BP1 (Insulin-like Growth Factor 2 mRNA Binding Protein 1), also known as IMP-1.

Insulin Like Growth Factor 2 mRNA Binding Protein (IGF2BP1/IMP-1) Orthologs

IGF2BP1, also known as IMP-1 (human) and Coding Region Determinant-Binding Protein (CRD-BP; mouse) belongs to a highly conserved family of RNA binding proteins called VICKZ (Vg1RBP/Vera, IMP-1,2,3, CRD-BP, KOC, ZBP-1) (5,6). Figure 1.1 shows the amino acid alignment of heterogeneous nuclear Ribonucleoproteins-K-homology (KH) domains for IMP-1

and related proteins. Discussed in more detail in a later section, the KH domains of IMP-1 are necessary for binding to appropriate RNA targets. Interestingly, there is >98% structural similarity between human IMP-1 and mouse CRD-BP. The strong evolutionary conservation of this protein family highlights the biological importance of their many proposed functions.

```

hCRDBP 1 PLRLLVPTQYVGAIIGKEGATIRNITKQTQSKIDVHRKENAGAAEKA..ISVHS
mCRDBP 1 PLRLLVPTQYVGAIIGKEGATIRNITKQTQSKIDVHRKENAGAAEKA..ISVHS
chZBP1 1 PLRLLVPTQYVGAIIGKEGATIRNITKQTQSKIDVHRKENAGAAEKA..ISIHS
hKOC 1 PLRLLVPTQFVGAIIGKEGATIRNITKQTQSKIDVHRKENAGAAEKS..ITILS
xTFB3 1 PLRMLVPTQFVGAIIGKEGATIRNITKQTQSKIDVHRKENAGAAEKP..ITIHS
Vg1RBP/Vera 1 PLRMLVPTQFVGAIIGKEGATIRNITKQTQSKIDVHRKENAGAAEKP..ITIHS
hCRDBP 2 PLKILAHNNFVGRLLIGKEGRNLKKVEQDTETKITISSLQDLTLYNPERTITVKG
mCRDBP 2 PLKILAHNNFVGRLLIGKEGRNLKKVEQDTETKITISSLQDLTLYNPERTITVKG
chZBP1 2 PLKILAHNNFVGRLLIGKEGRNLKKVEQDTETKITISSLQDLTLYNPERTITVKG
hKOC 2 PLKILAHNNFVGRLLIGKEGRNLKKIEQD TDTKITISPLQDLTLYNPERTITVKG
xTFB3 2 PLKILAHNNFVGRLLIGKEGRNLKKIEQD TDTKITISPLQDLTLYNPERTITVKG
Vg1RBP/Vera 2 PLKILAHNNFVGRLLIGKEGRNLKKIEQD TDTKITISPLQDLTLYNPERTITVKG
hCRDBP 3 MVQVFIPAQAVGAIIGKKGQHIKQLSRFASASIKIAPPETPDSKVRM..VIITG
mCRDBP 3 MVQVFIPAQAVGAIIGKKGQHIKQLSRFASASIKIAPPETPDSKVRM..VVITG
chZBP1 3 TVHVFIPAQAVGAIIGKKGQHIKQLSRFASASIKIAPPETPDSKVRM..VVITG
hKOC 3 TVHQFIPALAVGAIIGKQGQHIKQLSRFAGASIKIAPAEAPDAKVRM..VIITG
xTFB3 3 TVHLFIPALAVGAIIGKQGQHIKQLSRFAGASIKIAPAEAGPDAKLRM..VIITG
Vg1RBP/Vera 3 TVHLFIPALAVGAIIGKQGQHIKQLSRFAGASIKIAPAEAGPDAKLRM..VIITG
hCRDBP 4 HIRVPASAA..GRVIGKGGKTVNELQNLTAAEVVVPRDQTPDENQVVI.VKIIG
mCRDBP 4 HIRVPASAA..GRVIGKGGKTVNELQNLTAAEVVVPRDQTPDENQVVI.VKIIG
chZBP1 4 HIRVPASAA..GRVIGKGGKTVNELQNLTAAEVVVPRDQTPDENQVVI.VKIIG
hKOC 4 HIRVPSFAA..GRVIGKGGKTVNELQNLTSSAEVVVVPRDQTPDENQVVI.VKITG
xTFB3 4 HIKVPSYAA..GRVIGKGGKTVNELQNLTSAEVVVPRDQTPDENQV..VKITG
Vg1RBP/Vera 4 HIKVPSYAA..GRVIGKGGKTVNELQNLTSAEVVVPRDQTPDENQV..VKITG
          * *          * * * * * * * *          * *          * * *

```

Figure 1.1 Alignment of KH RNA-binding domains of IMP-1 and related proteins. KH domain consensus sequence are shown in bold and by asterisks below the alignment. GenBank accession numbers are as follows: mCRDBP, AF061569; hCRDBP EST, AA196976/AA196977; chZBP1, AF026527; hKOC, U97188; xTFB3, AF042353; Vg1 RBP/Vera, AF064633 and AF055923, respectively. Adapted from Doyle et al, NAR 1998.

Other orthologous or paralogous members of the IGF2BP protein family include IMP2 (human), IMP3 (human), ZBP1 (chicken), and Vg1-RBP/Vera (*Xenopus*). The variety of names that have been attributed to the same protein illustrates the fact that investigators from various fields have identified distinct activities for the same molecule (Table 1.1).

Table 1.1 The VICKZ family of RNA Binding Proteins

Binding Protein	RNA	Function	Reference
VglRBP	Vgl	mRNA transport/translation	(7-9)
ZBP-1	β -actin	mRNA transport	(10-12)
CRD-BP	c-Myc	Inhibition of CRD-dependent mRNA decay	(13-17)
IMP-1	MDR1	Inhibition of CRD-dependent mRNA decay	(18)
IMP-1	BTRC	Inhibition of miR-dependent mRNA decay	(19,20)
IMP-1/3	CD44	Inhibition of mRNA decay	(21)
IMP-1	KRAS	Inhibition of mRNA decay	(22)

IMP1, CRD-BP, and ZBP1 only differ by 17 amino acids and are considered the same protein.

The *Xenopus* Vgl RNA-binding protein (VglRBP/Vera) localizes Vgl mRNA within the cell during *Xenopus* oogenesis (23). VglRBP recognizes the specific 3'UTR vegetal localization element (VLE) and localizes the mRNA to the vegetal cortex; therefore, *Xenopus* VglRBP is key in cellular developmental and differentiation (23). Importantly, IMP-1/CRD-BP/IGF2BP1 plays a critical role in mRNA decay (13,18,20,24,25), translation (13,26) and localization (27,28) and has been show to bind to a number of mRNA targets that are implicated in cancer (6). IMP-1 binds to the 5'-UTR of IGF-II mRNA, inhibiting the translation of the transcript and transgenic mice that overexpress IMP-1 have shown increases in IGF-II protein levels, which was accompanied by the induction of mammary tumors (17,29). IMP-1 binds to the 3'-UTR of H19 mRNA and the coding region stability determinant of c-Myc mRNA, promoting cell

proliferation and tumorigenesis (6). KOC RNA-binding protein, also known as IMP-3, exhibits an oncofetal pattern of expression where it is nearly absent from normal non-neoplastic cells, and found in melanomas, gastric adenocarcinoma, ovarian and pancreatic cancer (30-33). These results suggest that the IGF2BP protein family play extensive roles in the regulation of many genes, many that lead to the development of various cancers (6).

IMP-1 Structure and Action

Human Insulin Like Growth Factor 2 mRNA Binding Protein 1 (IGF2BP1/IMP-1) is a member of the highly conserved VICKZ RNA-binding protein family (5). IMP-1 is a 577 amino acid protein which contains two N-terminal RNA recognition motifs (RRM) followed by four C-terminal heterogeneous nuclear Ribonucleoproteins-K-homology (KH) domains (Fig. 1.2) (34-36).



Figure 1.2. Domain structure of IMP-1. The figure maps the known functional domains of IMP-1.

To determine the importance of structural domains of ZBP-1, the ortholog of IMP-1 in chickens, in binding β -actin mRNA, researchers performed GST pull-down assays using truncated versions of ZBP-1 (11). Farina and co-workers found that full length ZBP-1 was able to bind to the zipcode region of β -actin mRNA with a K_d of 1-10 nM. However, the truncated versions containing only the RRM domains or only the KH1-KH2 domain, were unable to bind the zipcode region of β -actin mRNA (11). This, in addition to other experiments supported the

conclusion that the KH3 and KH4 domains, but not the RRM domains nor KH1 and KH2 domains, are important in binding the β -actin mRNA zipcode region. A recent structural study showed that IMP-1 induces the RNA looping of target mRNA upon KH3 and KH4 domain recognition, suggesting the importance of the KH3 and KH4 domains in binding (12). Additionally, this study solved the crystal structure of the KH3-KH4 domain for IMP-1, and it was found that both the KH3 and KH4 domains adopted the $\beta_1\alpha_1\alpha_2\beta_2\beta_3\alpha_3$ orientation with the highly conserved flexible G-X-X-G linker connecting the α_1 and α_2 helices, suggesting the importance of KH3 and KH4 in binding IMP-1 target mRNAs (12).

IMP-1 traffics between the cytoplasm and nucleus via two nuclear export signals (NES), which are located in the KH2 and KH4 domains (37). It is hypothesized that IMP-1 binds to target mRNAs within the nucleus and that the subsequent IMP-1 containing messenger ribonucleoprotein (mRNP) complex is exported from the nucleus to distinct cytosol regions. For example, in motile cells, IMP-1 containing mRNPs localize β -actin mRNA to the cell periphery. IMP-1 mRNP granules have recently been purified from HEK-293 cells and these 100-300 nm particles contain 10-30 mRNA transcripts (38). Approximately 300 distinct mRNA transcripts were found in IMP-1 mRNPs in this cell line, representing approximately 3% of the mRNA transcriptome.

IMP-1 was initially identified for its ability to protect c-Myc mRNA from degradation (24,39). The mRNA of c-Myc is destabilized via rare codon usage at the start of the coding region stability determinant (CRD) (34,40), which induces translational stalling and subsequent cleavage of the transcript at the CRD. Other studies show that IMP-1 can directly protect c-Myc mRNA from degradation by a mammalian endoribonuclease (18). This data suggests IMP-1 may also function within polysomes to protect c-Myc mRNA from cleavage during times when

translation is stalled. Earlier studies indicated that that RNAi knockdown of IMP-1 caused a significant portion of c-Myc mRNA to shift to the polysome fraction where it was degraded due to low availability of tRNAs fitting the rare codon requirements of the CRD (13). This suggests IMP-1 may work in part by limiting the supply of mRNA available to the actively translating polysome fraction. While the precise mechanism by which IMP-1 stabilizes c-Myc mRNA remains obscure, several studies provide *in vivo* evidence that IMP-1 controls the half-life of c-Myc mRNA (13,17,41).

In addition to c-Myc, IMP-1 binds to other oncogenic mRNAs that promote tumorigenesis. IMP-1 binds to the coding region of β TrCP1 mRNA and over-expression of IMP-1 leads to stabilized β TrCP1 mRNA and elevated β TrCP1 protein levels, resulting in suppression of apoptosis in colorectal cancer cells (19). Also in colorectal cancer cells, IMP-1 binds to and stabilizes GLI1 mRNA leading to elevated GLI1 protein, transcriptional activation, and proliferation (42). IMP-1 has a high affinity for the coding region of multidrug resistance protein 1/ P-Glycoprotein (MDR1) mRNA (18). Consistent with the view that IMP-1 protects MDR1 mRNA from degradation, down-regulation of IMP-1 reduces MDR1 levels and re-sensitizes cancer cells to chemotherapy drugs (43). In addition to binding to the coding region of oncogenic transcripts, IMP-1 binds to the 3'-untranslated region (UTR) of mRNAs, a classical site for RNA-binding protein regulation. For example, IMP-1 binds to the coding region and 3'-UTR of K-Ras mRNA and its overexpression led to increases in c-Myc and K-Ras expression as well as to proliferation of colon cancer cells (22). The 3'-UTR of MITF mRNA is also a binding site for IMP-1 and this interaction is critical for protecting the MITF transcript from degradation by micro RNA 340 (miR-340), a mechanism believed to be important for cell proliferation in malignant melanomas (44,45). IMP-1 also binds with high affinity to sites in

the 3'-UTR of CD44 mRNA, and knockdown of IMP-1 reduces stability of CD44 mRNA, decreases CD44 protein, and reduces cellular adhesion and invadopodia (21). Importantly, these findings support the role of IMP-1 in mediating cancer cell metastasis and invasion. As summarized in Figure 1.3, IMP-1 is a master regulator stabilizing a number of mRNAs whose protein products have been implicated in cancer through their ability to promote cell proliferation, metastases and tumor-enabling inflammation (6).

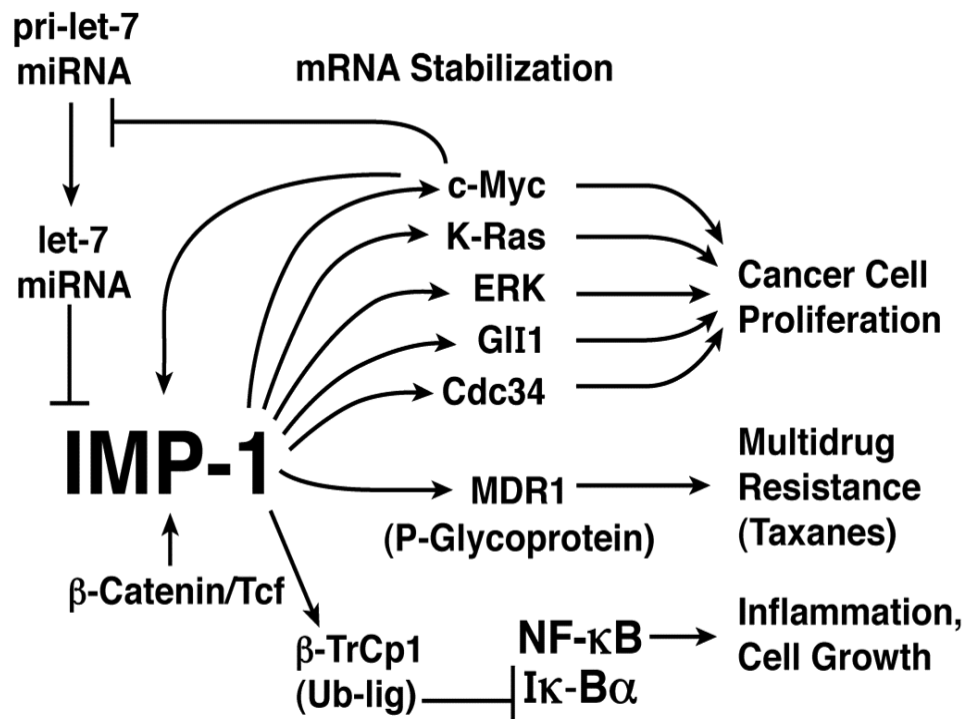


Figure 1.3. Schematic representation of IMP-1 action (from Mahapatra L., et al 2013).

Control of IMP-1 Expression

Despite its emerging role in cancer, there is surprisingly little known about how IMP-1 expression is regulated at the transcriptional level. In studies in HEK293 cells, IMP-1 transcription was proposed to be induced by β -catenin (CTNNB1) in a TCF-dependent manner.

In turn, CTNNB1-induced activation of IMP-1 expression was proposed to promote IMP-1-dependent stabilization of the BTRC and c-Myc mRNAs leading to elevated expression of both proteins (19). Post-transcriptional control of mRNA fate is a major regulatory mechanism by which gene expression is controlled. Studies from the Bartel lab found that differential lengths of the 3' end of the IMP-1 transcript play a critical role in determining IMP-1 expression (46). Consistent with various *in silico*-predicted poly-adenylation sites in the approximately 7-kb-long 3'-UTR of the transcript, at least three IMP-1 transcripts were observed in various tumor-derived cells and HEK293 cells, supporting the idea that IMP-1 expression is modulated by alternative polyadenylation (APA). Despite this exciting observation, the mechanism by which APA of IMP-1 is controlled has yet to be determined; however, it is probable that the 3'UTR shortening provides a potent escape route, preventing targeting by repressive microRNAs. This appears to be preferentially observed for transcripts encoding oncogenic factors which are targeted by tumor-suppressive microRNAs like the let-7 family, as demonstrated for IMP-1 (47). Post-transcriptional control of IMP-1 expression by microRNAs was suggested to modulate tumor cell fate. Downregulation of let-7 expression, frequently observed in aggressive tumor cells, was correlated with increased drug-resistance and an upregulation of IMP-1 (48). Increased expression of IMP-1 was proposed to enhance expression of multi-drug-resistance factor 1 (MDR1) by preventing MDR1 mRNA degradation via endonucleases, as had been previously observed for c-Myc (18). Additionally, it was demonstrated that IMP-1 promotes the expression of various bona fide let-7 targets including KRAS, Lin-28B and c-Myc (22).

It remains poorly understood how the transcription of IMP-1 is regulated and how it might be modulated by epigenetic mechanisms. In contrast, there is substantial evidence for a significant role of post-transcriptional mechanisms directing the control of IMP-1 expression.

The let-7-axis appears to emerge as a highly conserved regulatory mechanism that antagonizes the expression of IMP-1. This supports the view that IMP-1 enhances tumor cell aggressiveness, because the let-7 family of microRNAs is considered to exhibit a tumor suppressive role in most malignancies (49). Nonetheless, substantial effort is required to enhance our understanding of how the expression of IGF2BPs is modulated by the interplay of transcriptional and post-transcriptional networks. This will provide essential insights into how IMP-1 function is controlled during development and becomes dysregulated in diseases, such as cancer.

Importance of IMP-1 in Cancer

Consistent with its role in tumor growth and progression, IMP-1 expression is up-regulated by c-Myc (50) and β -catenin (19), and it is a major regulatory target of *let-7* microRNA (47). Reduced expression of *let-7* microRNA is one of the most common regulatory alterations in cancer. Overexpression of IMP-1 results in enhanced cell proliferation (15,51,52), suppression of apoptosis (22) and resistance to taxanes and other anticancer drugs (48,53). Expression of IMP-1 is associated with a poor prognosis in ovarian, lung, and colon cancer (15,32,54,55) (Figure 1.4).

IMP-1, through its capacity to bind to and stabilize mRNAs, either directly or indirectly increases expression and activity of key oncogenic proteins such as c-Myc, ERK, MDR1, and NF- κ B. We, and others, find that RNAi knockdown of IMP-1 in cell lines from several types of cancers reduces c-Myc levels, inhibits cell proliferation and triggers apoptosis (15,19,25). IMP-1 binds to MDR1 (multidrug resistance protein 1/P-glycoprotein) mRNA, stabilizing MDR1 mRNA, leading to overexpression of MDR1 and resistance to anticancer drugs (18,48,53). MDR1 carries out ATP-dependent pumping of xenobiotics and anticancer drugs out of cells. Overexpression of MDR1 is a common mechanism of resistance to anticancer drugs. RNAi knockdown of IMP-1, or expression of *let-7* miRNA, reduces the level of IMP-1, destabilizes

and down-regulates MDR1 and increases sensitivity of cancer cells to killing by therapeutically relevant concentrations of taxol, vinblastine and other anticancer drugs (48,53). IMP-1 binds to and stabilizes the mRNA encoding the ubiquitin ligase β -TRCP1 (20,51,56) leading to ubiquitylation and degradation of $\text{I}\kappa\text{-B}\alpha$, resulting in release and activation of NF- κB (20,51,53). Elevated NF- κB expression is common in cancer and tumor-promoting inflammation is an “enabling characteristic” in cancer (57). As summarized in Table 1.2, IMP-1/IGF2BP1/CRD-BP is expressed in diverse cancers.

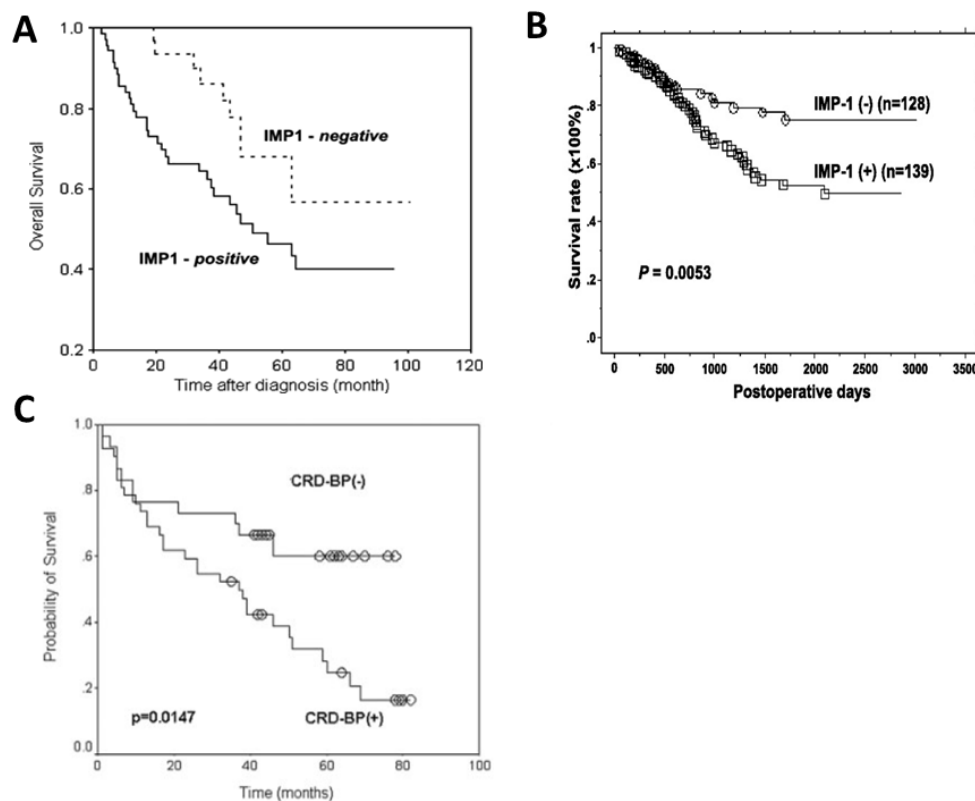


Figure 1.4. Kaplan Meier analysis of overall survival in patients with ovarian (A), lung (B) or colorectal cancer (C) that is IMP-1/CRD-BP positive or negative. Adapted from Kobel M et al, Oncogene 2007; Dimitriadis E et al., International Journal of Cancer 2007; Kato T et al, Clinical Cancer Research 2007.

Table 1.2. Expression of IMP-1 in human cancers

Cancer	Method	Incidence	References
Breast	RT-PCR	59% (69/118)	(58)
Ovarian	IHC	69% (73/106)	(15)
Melanoma	IHC	34% (13/38)	(51)
Non-small cell lung	RT-PCR	27% (4/11)	(25)
Pancreatic	Northern	33% (5/15)	(59)
Colorectal	RT-PCR	81% (17/21)	(60,61)
Hodgkin lymphoma	IHC	94% (101/108)	(62)

Adapted from Bell J., et al., Cell. Mol. Life Sci., 2013.

Current Limitations

One challenge in conducting studies on IMP-1 is the lack of specificity of currently available antibodies. Although we have achieved significant paralogue specificity for IMP-1, which allows for a largely unbiased analysis of IMP-1 expression in most cancer-derived cells, we currently cannot exclude slight paralogue cross-reactivity of monoclonal antibodies for IMP-3 at high protein concentrations (Figure 1.5).

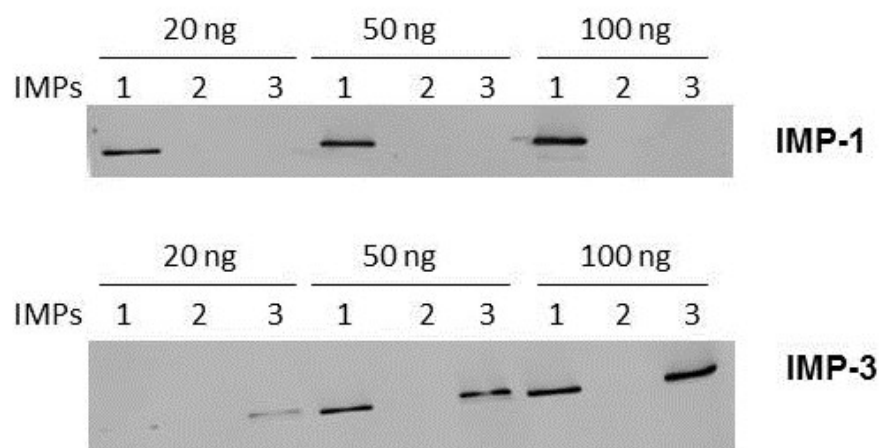


Figure 1.5. Specificity of IMP-1 and IMP-3 antibodies in detecting recombinant purified IGF2BPs. Indicated amounts of purified, recombinant IMP-1, IMP-2, or IMP-3 were purified and blots were probed with either IMP-1(Cell Signaling Technology D33A2) or IMP-3 (Abcam:Ab124959) antibody. There is no cross reactivity of the IMP-1 antibody and enhanced cross reactivity of the IMP-3 antibody with increasing amounts of protein loaded. Western blot provided by Dr. Chengjian Mao.

Despite this limitation, we have shown the specificity of our tools, by performing RNAi knockdown of IMP-1 and assessing the levels of IGF2BP paralogs both by Western blot and qRTPCR. The similarity in paralogue kDa size and amino acid sequence similarity makes differentiation of paralogs difficult by Western blot, therefore confidence in antibodies and siRNAs is critical. Additionally, because much of the IMP research is in the context of cancer using immunohistochemistry, it is essential to generate and use paralogue-specific antibodies in these experiments.

Thesis Synopsis

The work described herein primarily focuses on identification of novel small molecule inhibitors of IMP-1. IMP-1 is an important, but untargeted protein in human cancer. Because the oncofetal

mRNA-binding protein IMP-1 regulates the levels of diverse proteins important in cancer (Fig. 2), targeting this master regulator of oncogenic mRNA degradation with small molecules has great therapeutic potential (50,63). This approach combines the benefits of RNAi (degradation of target mRNAs) with improved biological stability and pharmacokinetics (63). Most currently used chemotherapeutics are quite toxic in part because they kill both cancer cells and rapidly-dividing non-malignant cells. IMP-1 is expressed at high levels in fetal cells and cancer cells and is nearly absent in most adult cells (64). Therefore, targeting IMP-1 selectively targets cancer cells, and holds great therapeutic promise.

In Chapter 2, we describe development and optimization of an *in vitro* method, fluorescence anisotropy microplate assay (FAMA), for use in high throughput screening (HTS). In a pilot study, we screened 17,600 small molecules using FAMA as proof of principle that we could identify inhibitors of IMP-1 binding to c-Myc RNA using this method. In Chapter 3, we expanded upon our initial findings that FAMA was robust and reproducible for HTS, and conducted a screen of approximately 150,000 small molecules and identified 2-[(5-bromo-2-thienyl)methylene]amino}benzamide (BTYNB) as our lead small molecule inhibitor. Based on the exciting results presented in Chapter 3, we believe that we have identified the first small molecule inhibitor of IMP-1 that not only works *in vitro*, but inhibits cell proliferation and colony formation in IMP-1 positive cancer cells. We have also shown that BTYNB treatment leads to decreased mRNA levels in a panel of IMP-1 targets. This result highlights BTYNB's use as both a potential therapeutic agent and as a molecular probe, enhancing our understanding of IMP-1's function in cancer cells. In addition to studying small molecule inhibitors of IMP-1, we were also interested in understanding whether or not there are novel molecular targets of IMP-1. In Chapter 4, we describe identification of Protein Kinase C alpha (PKC α) as a novel

molecular target of IMP-1. *In silico* analysis of IMP-1 RNAi knockdown in HEK 293T cells using publically available arrays (65) revealed PKC α mRNA as a likely molecular target of IMP-1. Knockdown of IMP-1 in HEK 293T cells resulted in a decrease in PKC α protein, while overexpression of IMP-1 in the same cell line resulted in an increase in PKC α mRNA. Compared to PKC α mRNA levels in cells treated with non-coding control siRNA, RNAi knockdown of IMP-1 in IGROV-1 and SK-MEL2 cells led to a decrease in PKC α mRNA. Similarly RNAi knockdown of IMP-1 lead to a decrease in PKC α protein levels in the same cell lines. One potential mechanism by which IMP-1 might increase PKC α levels is by binding to the IMP-1 binding sequence motif (UUUAY), which has previously been identified in *Drosophila* (66) and is found in the 3'-UTR of PKC α mRNA. Previous work found that IMP-1 stabilization of MITF mRNA interferes with microRNA 340-mediated degradation and that these sites were juxtaposed in the 3'UTR of the MITF transcript (44). Using miRWalk and other tools for predicting micro RNA (miR) sites in the mRNA 3'-UTR, miR-340 was the top miR for PKC α . This is consistent with the idea that PKC α mRNA is a molecular target for IMP-1. This thesis closes with conclusions from my work and describes some future directions that may arise from this body of research.

CHAPTER 2

High-Throughput Fluorescence Anisotropy Screen for Inhibitors of the Oncogenic mRNA-binding Protein, IMP-1

Notes and Acknowledgements:

This chapter is adapted from the following publication: Mahapatra L, Mao C, Andruska N, Zhang C, Shapiro DJ (2014) High-throughput fluorescence anisotropy screen for inhibitors of the oncogenic mRNA binding protein, IMP-1. *J Biomol Screen*. 19:427-436. The publication has been modified for this chapter and is reprinted with permission from the publisher. The original publication is available from <http://jbx.sagepub.com/> and using DOI: 10.1177/1087057113499633. This work was supported by the National Institute of Cancer (NCI) Award: 1 R21 CA173527-01 and the University of Illinois College of Medicine Hazel Craig Research Fellowship.

ABSTRACT

Cancer cell proliferation is regulated by oncogenes, such as c-Myc. An alternative approach to directly targeting individual oncogenes is to target IMP-1, an oncofetal protein that binds to and stabilizes mRNAs, leading to elevated expression of c-Myc and other oncogenes. Expression of IMP-1 is tightly correlated with a poor prognosis and reduced survival in ovarian, lung and colon cancer. Small molecule inhibitors of IMP-1 have not been reported. We established a fluorescence anisotropy/polarization microplate assay (FAMA) for analyzing binding of IMP-1 to a fluorescein-labeled 93 nucleotide c-Myc mRNA target (flMyc). This highly robust (Z' factor = 0.60) FAMA-based high throughput assay was used to screen 17,600 small molecules and lead to the successful identification of

inhibitors of IMP-1 binding to c-Myc. Our design strategically filters out toxic non-specific inhibitors using an early cell based assay in control cells lacking the target protein. Importantly, the first small molecule for IMP-1 identified by the *in vitro* high throughput screen selectively inhibited proliferation of IMP-1 positive cancer cells with very little or no effect on proliferation of IMP-1 negative cells.

INTRODUCTION

The oncofetal mRNA binding protein IMP-1/CRD-BP/IGF2BP1 is a multifunctional mRNA binding protein with important roles in mRNA degradation (1-3), translation (4), and localization (5). Overexpression of IMP-1 results in enhanced cell proliferation (6), suppression of apoptosis (7), and resistance to taxanes and other anticancer drugs (8, 9). Kaplan-Meier plots show that expression of IMP-1 is tightly correlated with a poor prognosis in ovarian, colon and lung cancer (10-12). Consistent with an important role in tumor growth and progression, IMP-1 expression is up-regulated by c-Myc (13) and β -catenin (14), and it is a major regulatory target of *let-7* microRNA (15). IMP-1, through its capacity to bind to and stabilize mRNAs, increases expression and activity of key oncogenes including c-Myc, K-Ras and ERK.

IMP-1 binds to a specific sequence that regulates the stability of c-Myc mRNA, stabilizing c-Myc mRNA, increasing levels of c-Myc mRNA and protein and increasing cell proliferation (12, 13). RNAi knockdown of IMP-1 in cell lines from several types of cancers reduces c-Myc levels, inhibits cell proliferation and triggers apoptosis (12, 14). Additionally, IMP-1 binds to MDR1 (multidrug resistance protein 1/P-glycoprotein) mRNA, stabilizing MDR1 mRNA, leading to overexpression of MDR1 and resistance to anticancer drugs (1, 8, 9). RNAi knockdown of IMP-1, or expression of *let-7* miRNA, reduces the level of IMP-1,

destabilizes and down-regulates MDR1 and increases sensitivity of cancer cells to killing by therapeutically relevant concentrations of taxol, vinblastine and other anticancer drugs (8, 9). Despite its emerging role in both tumor cell proliferation and multidrug resistance, small molecule modulators of IMP-1 have not been reported.

To develop a quantitative real-time assay for determining binding of IMP-1 to target RNAs, we designed a high throughput screening (HTS) and developed a fluorescence anisotropy microplate assay (FAMA). Using this assay, 17,600 test compounds were evaluated for their ability to inhibit binding of IMP-1 to a 93 nucleotide fluorescein-labeled c-Myc mRNA binding site (flmyc) (16). Because the 93 nucleotide c-Myc RNA binding site was too large to synthesize commercially, we developed simple methods for in vitro synthesis and fluorescein-labeling of the RNA.

Assays based on fluorescence anisotropy/polarization have emerged as alternatives to electrophoretic mobility shift assays (EMSA) that can be difficult to adapt for high throughput. These assays are based on changes in fluorescence polarization/anisotropy, which occurs on binding of a protein to a labeled RNA. When polarized light excites a fluorophore, such as the fluorescein-labeled c-Myc RNA (flmyc), the relatively small fl-RNA usually undergoes rotational diffusion more rapidly than the time required for light emission (**Fig. 2.1**). Therefore, the position of the fl-RNA at the time of light emission is largely randomized, resulting in depolarization of most of the emitted light. In contrast, when a protein, such as IMP-1 binds to the fl-RNA, the larger size and volume of the protein–fl-RNA complex causes rotation to be slower, increasing the likelihood that the protein–fl-RNA complex will be in the same plane at the time of light emission as it was at the time of excitation. Therefore, the emitted light remains highly polarized (**Fig. 2.1**). FAMA is ideal for HTS because it is a homogenous, rapid, and real-

time assay to assess binding in solution. Fluorescence polarization/anisotropy methods have recently been successfully utilized in HTS to identify small molecule inhibitors of biologically relevant RNA-protein interactions involved in diseases such as influenza and Rift Valley fever virus (17, 18).

In this study, we carried out an unusual purification that selects for biological activity of purified IMP-1, developed the flMyc RNA probe, and performed a pilot screen of 17,600 small molecules from a compound library in the University of Illinois High Throughput Screening Center. From the pilot screen, we identified 33 verified hits that inhibited binding of IMP-1 to flMyc and met fluorescence intensity cutoffs. Since our primary screen was set up to identify inhibition of IMP-1 binding to flmyc, it did not exclude toxic compounds. We first retested the hits for specificity by evaluating their ability to inhibit binding of the steroid hormone receptor, progesterone receptor (PR), to its fluorescein-labeled DNA binding site (fl-progesterone response element; fl-PRE). This specificity test was only moderately successful in filtering out compounds that subsequently proved toxic in IMP-1 negative cells. Although previous pilot screens often used orthogonal validation assays such as EMSA and filter binding, these methods may not fully recapitulate the complex milieu of living cells. Therefore, we assessed how effectively and selectively the hits inhibited a key activity of IMP-1; stimulation of cell proliferation. To establish a cell-based assay to filter the hits, we used RNAi knockdown of IMP-1 to confirm that IMP-1 expression was essential for proliferation of IMP-1 positive cells and that IMP-1 RNAi knockdown had no effect on proliferation of IMP-1 negative cells. The cell-based assay identified a substantial number of hits as toxic in the IMP-1 negative cells. This indicates that an early assay in cells that lack the target protein functions as a rapid filter to eliminate small molecules exhibiting non-specific binding and toxicity. Based on our findings a

two-step screening strategy in which an initial biochemical screen using purified protein identifies hits that target the desired protein-RNA interaction, followed by a cell-based assay to filter out non-specific and toxic hits. This approach allowed us to identify a lead as the first selective small molecule inhibitor of IMP-1.

MATERIALS AND METHODS

Unless otherwise stated, average \pm SEM is reported for experiments where SEM equals σ/\sqrt{n} , where σ represents the population standard deviation and n is the sample size.

Compound Libraries

The pilot screen chemical library used part of a library of commercially available small molecules from the Chembridge Microformat Library that is maintained in the University of Illinois High Throughput Screening Center. Compounds are stored at -20°C and arrayed in 384-well plates at concentrations of 1 or 10 mM in DMSO.

Protein Purification

IMP-1 was purified as described by Nielsen et al. (19), with minor modifications, mostly suggested by Dr. J. Christiansen. Untagged full-length IMP-1 in PET42a (Novagen) was expressed in a strain of BL21DE3pLysS expressing plasmid-encoded tRNAs for rare Arg, Ile and Leu codons (a generous gift of Dr. J. Christiansen). Following protein expression, cells were harvested, broken by sonication in 20 mM Tris-HCl, pH 7.8, 5 mM MgCl_2 , 100 mM KCl, 1 mM DTT and 1.4 $\mu\text{g/ml}$ aprotinin, Triton X-100 was added to 0.4%, and cell debris was removed by centrifugation at 8,000 RPM at 4°C for 10 min. The supernatant was made up to 10% in

glycerol, and layered on a sucrose cushion consisting of 1.1 M sucrose, 20 mM Tris-HCl, pH 7.8, 5 mM MgCl₂, 100 mM KCl, 1 mM DTT and 0.1% Triton X-100 and centrifuged for 2 hours at 4°C at 40,000 RPM. The resulting pellet contains IMP-1 bound to polysomal mRNA. The pellets were washed in 20 mM Tris-HCl, pH 7.8, 5 mM MgCl₂, 100 mM KCl, 1 mM DTT and 0.1% Triton X-100. IMP-1 was dissociated from polysomal mRNA by re-suspending the pellets in 20 mM Tris-HCl, pH 7.8, 5 mM MgCl₂, 650 mM KCl, 1 mM DTT and 0.1% Triton X-100. The suspension was centrifuged for 1 hour at 4°C at 40,000 RPM. The supernatant was adjusted to 200 mM KCl and 10% glycerol before it was applied to a 2 mL Heparin-Sepharose column (Amersham Biosciences) equilibrated in 20 mM Tris-HCl, pH 7.8, 5 mM MgCl₂, 200 mM KCl, 1 mM DTT, 0.1% Triton X-100 and 10% glycerol. After washing with the equilibration buffer, the protein was eluted by the same buffer containing 350 mM KCl. The indicated eluted fractions (E, elution) were resolved on a 10% SDS-PAGE gel and visualized by Coomassie blue staining. Purified IMP-1 from fractions E7 and E8 was near homogenous and was used in our studies.

Full-length FLAG-epitope tagged human PR-B (120 kDa) was purified from baculovirus-infected insect cells produced at 5L BioReactor scale in a facility at the University of Colorado Health Sciences Center facility (20) and was a generous gift of Prof. S. Nordeen.

Synthesis of Fluorescein-labeled c-Myc RNA Probe

The flMyc probe was produced essentially as we describe (87) with the minor modification of using the MEGAscript kit (Ambion) for *in vitro* transcription. Standard palindromic cPRE/GRE (5'-f-CTAGATTACCAGAACAATCTGTTCTTAC TCA-3') were synthesized as previously described (21). Briefly, sense strand oligonucleotide was synthesized with fluorescein (6-FAM)

at their 5' ends using phosphoramidite chemistry and PolyPak™ II (Glen Research) purified by the Biotechnology Center (University of Illinois Urbana Champaign). Oligonucleotide concentrations were calculated from A₂₆₀ and the labeled sense strands were annealed with equimolar amounts of unlabeled antisense strands.

Fluorescence Anisotropy Assays

The fluorescence anisotropy microplate assay (FAMA) buffer was modified from our earlier assay (16). Anisotropy change represents the difference between the anisotropy measured at each concentration of IMP-1 and the anisotropy value measured in the absence of IMP-1 (flmyc RNA alone). In competition experiments, unlabeled competitors were pre-mixed with the fluorescein-labeled RNA probe before IMP-1 was added. The anisotropy change for IMP-1 binding to flmyc-RNA with no competitor was set to 100%. Percent anisotropy change was calculated as follows: (anisotropy change (plus competitor)/ anisotropy change (no competitor))X100.

FAMA for High Throughput Screening was performed in 384-well low volume, flat bottom microplates (Greiner Bio-One). The optimum IMP-1 protein (10 nM) and flmyc RNA (1 nM) concentrations for the assay were chosen because they result in approximately 90% of maximal binding. Assays contained 20 mM Tris-HCl, pH 8.0, 150 mM KCl, 1 mM EDTA, 1 ng/μl tRNA, 1 ng/μl heparin, 0.4 U/μl RNasin, and 500 ng/μl RNase-free BSA. A sequential protocol was used to assess changes in anisotropy, intrinsic fluorescence of test compounds, the compounds' influence on the anisotropy signal of the probe alone, and the ability of compounds to inhibit binding of IMP-1 to flmyc. First, plates were loaded with 10 μl binding buffer containing fluorescein-labeled c-Myc RNA probe (2-fold in binding buffer) with a Matrix PlateMate Plus dispenser (Thermo Scientific) in every well. Then 100 nL of each test compound

from the 1 mM compound plates was transferred to each well of the test plates using the Matrix PlateMate Plus robotic pin transfer apparatus. Then fluorescence polarization/anisotropy (FP/FA) was determined using an Analyst HT Plate Reader (Molecular Devices). FITC FP 480 (excitation) and 535 (emission) filters were used. Then, 10 μ l of binding buffer and IMP-1 protein (final assay concentration 10 nM) was added to each well except control wells that contained received 10 μ l of binding buffer. FP/FA for each well was measured after 15 minutes, when the assay had reached equilibrium as determined from kinetic studies of the ON and OFF rate of IMP-1 binding to fIMyc. Thus, in the final assay compounds were tested at 5 μ M for their ability to inhibit binding of 10 nM of IMP-1 to 1 nM fIMyc RNA probe. Columns 23 and 24 on each plate contain DMSO and no test compounds and these wells served as screening controls.

For follow-on tests for specificity, fluorescein-labeled progesterone response element (fPRE) was diluted to 1 nM in a binding buffer containing 15 mM Tris-HCl, pH 7.9, 100 mM KCl, 1 mM dithiothreitol (DTT), 5% glycerol, 0.05% Nonidet™ P-40 (NP-40), 100 ng poly dI:dC (non-specific competitor), and 250 ng/ μ l BSA. The protocol for assessing change in anisotropy was similar to the one described above for the IMP-1:fIMyc experiments, except that compounds were tested at a final concentration of 10 μ M for their ability to inhibit binding of PR to the fPRE DNA probe. The concentration of PR used in the follow-on assay, 35 nM, is not saturating and is highly responsive to inhibition.

Data Analysis and Hit Scoring

To determine the robustness of our screening assay, the Z' factor for each plate was calculated as previously described (22). A Z' factor greater than 0.5 describes a robust assay suitable for high

throughput screening (22). The results from the pilot screen were further analyzed using a simple program we developed to evaluate and score different parameters and identify the most promising compounds from the HTS. Initially, compounds that altered the overall fluorescence intensity by >30% compared to control wells were considered as either enhancers or quenchers and were excluded from further analysis. The remaining compounds were evaluated for percent inhibition which was calculated relative to the assay plate control wells, where % inhibition = $(1 - ((mA_{Comp} - mA_{Min}) / (mA_{Max} - mA_{Min}))) \times 100$, where the assay minimum (mA_{Min}) is flMyc RNA alone and the assay maximum (mA_{Max}) is flmyc with IMP-1 protein. Although there is no universally accepted standard of what change in signal constitutes a “hit” suitable for further evaluation, some researchers consider that any small molecule that results in a change of more than three standard deviations from the mean is appropriate for further study. The average change in anisotropy for the compounds in the pilot HTS was $86.7 \text{ mA} \pm 6.7$. The S.D. is 7.7%, and $3 \times \text{S.D.}$ is $\sim 25\%$. We therefore carried out further analysis of small molecules that, when present at $5 \mu\text{M}$, altered the average change in anisotropy for binding of IMP-1 to flMyc by at least 25%. Compounds that met fluorescence intensity criteria and the percent inhibition cutoff were considered to be primary hits and were cherry-picked for follow-on assays.

Cell Culture and siRNA Transfection

IMP-1 positive IGROV-1 ovarian cancer cells and IMP-1 negative PC-3 prostate cancer cells were used in cell-based experiments. IGROV-1 cells were maintained in phenol-red free RPMI 1640 with 10% fetal bovine serum (FBS) and PC-3 cells were maintained in DMEM-F12 with 10% FBS. Cells were grown in monolayer and were maintained at 37°C with 5% CO_2 . IGROV-1 and PC-3 cells were plated in 96-well plates at a density of 1,000 cells/well and transfected

with an IMP-1 siRNA SMARTpool (Dharmacon) or a non-coding control siRNA using Dharmafect 1 transfection reagent (Dharmacon) according to the suppliers protocol. 5 days after transfection cell viability was determined using CellTiter 96 Aqueous One Solution Reagent (Promega). For both cell lines relative cell proliferation was calculated as previously described (23).

Testing Hits for Inhibition of Cell Proliferation

IGROV-1 and PC-3 cells were maintained and plated in 96-well plates as described above. Each cell line was plated in growth medium 24 hours before treatment. Treatment medium containing either 0.4% DMSO (vehicle) or inhibitor compounds at a final concentration of 20 μ M in DMSO. After 3 days, cell viability was determined using Promega CellTiter 96 Aqueous One Solution Reagent (MTS). For each compound percent inhibition of cell proliferation was calculated relative to assay plate DMSO controls, which were set to 0% inhibition. Small molecules were considered potential leads if percent inhibition of proliferation of the IMP-1 positive IGROV-1 cells was at least 3 fold higher than percent inhibition of the control IMP-1 negative PC-3 cells.

Western Blots

Cells were trypsinized, resuspended in their respective culture media, and plated into 6-well plates at 300,000 cells/well. Cells were harvested, washed in ice-cold phosphate-buffered saline (PBS), and whole-cell extracts were prepared in lysis buffer containing 1X radioimmunoprecipitation assay (RIPA) buffer (Millipore), 1 mM EGTA, 30 mM NaF, 2.5 mM sodium pyrophosphate, 1 mM sodium orthovanadate, 1mM β -glycerol phosphate, 1 mM

phenylmethyl-sulfonyl fluoride, and 1 tablet of protease inhibitor cocktail (Roche, Indianapolis, IN). Cells were collected, and debris was pelleted by centrifugation at 15,000 g for 10 minutes at 4°C. The supernatants were collected and stored at -20°C. Then, 20 µg total protein was loaded onto 10% (v/v) sodium dodecyl sulfate polyacrylamide gel electrophoresis (SDS-PAGE) gels, separated, and transferred to nitrocellulose (GE Healthcare). IMP-1 protein was detected using IMP-1 antibody (sc-21026, Santa Cruz, CA) and β-actin internal standard was detected using antibody A1978 (Sigma).

RESULTS

Validation of the High Throughput Screening Assay

We developed the fluorescence anisotropy microplate assay (FAMA) for analyzing the interaction of DNA and RNA binding proteins with their recognition sequences (16, 21). In demonstrating the utility of FAMA for analysis of RNA-protein interactions, we examined the ability of CRD-BP/IMP-1 expressed in *E. coli* and renatured from inclusion bodies to bind to a fluorescein-labeled c-Myc (flMyc) RNA binding site. Binding was low-affinity with an apparent K_D of several hundred nM (16). Christiansen, Nielsen and coworkers reported that epitope tagged IMP-1 binds poorly to RNAs (24) and developed an expression system for recombinant untagged IMP-1 using *E. coli* stably expressing several rare tRNAs and a purification protocol that selects for biologically active IMP-1(19). We expressed and purified IMP-1 using an update of this expression-purification system (**Fig.2. 2A**) and obtained purified untagged IMP-1 that was >90% homogeneous by SDS polyacrylamide gel electrophoresis (**Fig. 2.2B**).

To identify small molecule inhibitors that target IMP-1, we used modified binding conditions and a far more active IMP-1 preparation to update and improve our earlier assay for IMP-1 binding to flMyc (16). Purified untagged recombinant IMP-1 exhibited saturable high-affinity binding to the fluorescein-labeled 93 nucleotide (nt) c-Myc RNA site (starting at nt 1705), which contains the IMP-1 binding site. Under these binding conditions, the apparent K_d (the protein concentration at which 50% of the probe was bound) for IMP-1 binding to the flMyc was ~3 nM (**Fig. 2. 3A**). Based on the binding data, we selected 10 nM IMP-1 for screening. 10 nM IMP-1 yields approximately 90% of maximum binding to flMyc, resulting in a large anisotropy change (ΔmA) and a robust assay, while remaining highly responsive to inhibition by small molecules. In this assay, small molecules inhibitors will reduce the anisotropy change seen on binding of IMP-1 to flMyc (**Fig. 2.1**).

Binding of IMP-1 to the flMyc RNA is sequence and structure specific. Because IMP-1 binds unstructured single-stranded RNA, we tested the possibility that IMP-1 primarily interacts with the charged phosphate backbone. With the identification of an important role for polyphosphate in blood clotting (25), polyphosphate with a length similar to the flMyc RNA became available to us for testing. Even at 1,000 fold molar excess, polyphosphate does not compete for IMP-1 binding (**Fig. 2.3B**). Therefore, interaction with the charged phosphate backbone is not responsible for high-affinity binding of IMP-1 to RNAs. Binding of IMP-1 to flMyc was specific, as tRNA, even at 1,000 fold molar excess, had minimal ability to compete for binding (**Fig. 2.3B**). Addition of the unlabeled c-Myc RNA resulted in a concentration-dependent reduction in binding. A 2.5 fold molar excess of the unlabeled c-Myc RNA reduced binding of IMP-1 to flMyc by approximately 50% (**Fig. 2.3B**).

The performance of the optimized binding assay was evaluated for its stability. Under our assay conditions, binding of IMP-1 to flMyc is highly stable at room temperature and insensitive to changes in DMSO concentration. Using 10 nM IMP-1 and screening conditions, after 60 minutes at 25°C, activity was 97% of the initial activity (ΔmA at 60 min was 91.1 ± 1.3 vs. initial ΔmA of 94.1 ± 0.3 ; **Fig. 2.3C**). DMSO at the concentration to be used in the screen, and at twice that concentration, had no effect on binding of IMP-1 to flMyc (**Fig. 2.3D**). Thus, our assay had the requisite qualities for evaluation in a medium-scale pilot screen.

Pilot Screen for IMP-1 Inhibitors

To validate the assay and to identify small molecules that inhibit binding of IMP-1 protein to flMyc RNA, we carried out a pilot screen using 17,600 compounds (Plates 1-50) from the Chembridge Microformat Library. The performance of the optimized binding assay for use in HTS was evaluated for robustness by calculating the Z' factor for each of the 50 plates screened. The assay demonstrates robust performance with a mean Z' factor of 0.60 ± 0.06 (average \pm S.D.) and a signal to noise (S/N) of 12.4 (**Fig. 2.4A**). The average change in anisotropy for the compounds in the pilot screen was $86.7 \text{ mA} \pm 6.7$ (average \pm S.D.). The statistical parameters of the pilot screen are summarized in **Table 2. 1**.

For the primary screen, compounds exhibiting increases or decreases $>30\%$ in total fluorescence intensity compared to controls were considered as either enhancers or quenchers and were excluded from analysis. Similar cutoffs have been used on other FP/FA screens (26, 27). For the remaining compounds, we chose a cutoff of at least 25% inhibition (which is $\sim 3X$ S.D.) at a final compound concentration of 5 μM and identified 57 primary hits (hit rate 0.32%, 57/17600). **Figure 2.4B** is a scatterplot for the 17,600 compounds from the pilot screen.

To validate the 57 hits, we compared their ability to inhibit a control protein-nucleic acid interaction, binding of progesterone (PR), a steroid hormone receptor, to its DNA binding site, the fluorescein-labeled progesterone response element (flPRE) (**Fig 2.5A**) to their ability to inhibit IMP-1 binding to flMyc. Triplicate assays in small volume 384-well plates used the same method described for the primary screen. At 5 μ M, 33 compounds inhibited binding of IMP-1 to flMyc by >25% (**Fig 2.5B**). A substantial number of primary hits that did not pass the verification assay were close to the cutoff of 25% inhibition at 5 μ M. Our counter-screen for specificity used binding of PR to the flPRE in part because it exhibits a change in anisotropy whose magnitude is similar to that seen for the primary assay using IMP-1 and flMyc (**Fig. 2.5A**). Our aim was to quickly identify potential false positives that displayed high-affinity for non-specific nucleic acid sequence or binding proteins rather than for the IMP-1:cMyc interaction and to identify small molecules that display a high-affinity for DNA, such as ethidium bromide and other DNA intercalators. To provide a stringent test for specificity, we evaluated the ability of the verified hits to inhibit binding of PR to the flPRE at 10 μ M, twice the concentration used in the IMP-1 screen and verification assays. As shown in **Figure 2.5B**, only 3 of the 33 verified hits exhibited greater than 25% inhibition of PR:flPRE binding.

Evaluating Hits for Inhibition of Cell Proliferation

Elevated expression of IMP-1 in cancer cells is associated with increased cell proliferation, which likely stems from stabilizing c-Myc and other oncogene mRNAs. Evaluating the ability of verified hits that inhibit binding of IMP-1 to c-Myc to also inhibit effects of IMP-1 on cell proliferation provides a critical test of their effect on a key cancer-related function of IMP-1. To establish the cell proliferation assay, we carried out RNAi knockdown of IMP-1 in IMP-1

positive IGROV-1 ovarian cancer and in IMP-1 negative PC-3 prostate cancer cells (**Fig. 2.6**) in 96-well plates using a control non-coding (NC) siRNA and IMP-1 siRNA. After 5 days, MTS assays were performed and relative percent inhibition of cell proliferation was determined for each cell line (23). Compared to IGROV-1 cells transfected with the control siRNA, RNAi knockdown of IMP-1 caused an 80% decrease in IGROV-1 cell proliferation. In contrast, compared to transfection with the control siRNA, transfection of the IMP-1 negative PC-3 cells with IMP-1 siRNA had no effect on cell proliferation (**Fig. 2.6**).

We evaluated the effects of all the verified inhibitors from the *in vitro* pilot screen in cell proliferation assays in IMP-1 positive IGROV-1 cells and IMP-1 negative PC-3 cells. Our recent study identifying a small molecule inhibitor of androgen receptor confirms that PC-3 cells are a suitable toxicity control and are quite sensitive to small molecules exhibiting non-specific toxicity (28). Data is shown for a lead inhibitor and for representatives of the other classes of small molecules (**Fig. 2.7**). The lead small molecule inhibits proliferation of IMP-1 positive IGROV-1 cells, with very little or no effect on IMP-1 negative PC-3 cells (**Fig. 2.7**). Our lead small molecule inhibited binding of IMP-1 to fIMyc ($72 \pm 3.6\%$ inhibition at 5 μ M) and does not inhibit binding of PR to the fIPRE ($-31 \pm 3.2\%$ inhibition at 10 μ M). Thus, the lead compound demonstrated efficacy and selectivity both in *in vitro* assays using purified proteins and in cell-based assays. Additional evidence of the robust nature of our screen is shown by the fact that the lead inhibitor had a Z-score of -6.8 and was clearly differentiated from the other compounds on its HTS plate (**Fig. 2.8**).

DISCUSSION

Expression of IMP-1 is implicated in several human cancers. While Kaplan-Meier survival plots show a tight correlation between IMP-1 expression and survival ($p < 0.05$ for ovarian, lung and colon cancer), IMP-1 is also strongly implicated in melanomas (6, 8, 29) and other cancers. IMP-1 is an oncofetal protein expressed in fetal cells and cancer cells and nearly absent in most somatic cells (30, 31). Thus, IMP-1 is an excellent therapeutic target. Although a high-affinity binding site for IMP-1 that is implicated in regulation of c-Myc mRNA degradation was identified a number of years ago, small molecule biomodulators to probe the actions of IMP-1 and inhibit its activity in cancer cells have not been described. The substantial >90 nucleotide size of the high-affinity IMP-1 binding site in c-Myc mRNA, the lack of a clear consensus IMP-1 RNA binding site (32,33), and wide variations in the affinity of observed IMP-1 preparations for RNA (1,16,19) all complicate development of a high throughput screen. We show that purified IMP-1 binds with high-affinity and specificity to the c-Myc binding site. Even at a 1,000 fold molar excess, tRNA and polyphosphate had very little ability to compete with flMyc for IMP-1 binding (**Fig. 2.3B**). Thus, binding of IMP-1 to flMyc exhibited the requisite specificity for HTS.

Our primary screen used an *in vitro* assay for inhibition of binding of purified IMP-1 to flMyc rather than an assay for inhibition of cell proliferation for several reasons. In our hands, it is difficult to obtain the requisite reproducibility in cell-based assays for proliferation inhibitors in 384-well plates. More important, the *in vitro* assay using purified IMP-1 provides direct evidence that the primary hits actually inhibit the desired target—the IMP-1:flMyc interaction. Although recent studies show that IMP-1 stabilizes numerous mRNAs (32), we focused on identifying small molecule inhibitors of IMP-1 binding to c-Myc mRNA because the specific

sequence on c-Myc mRNA, the coding region determinant (starting at nt 1705), is the best defined and most extensively studied IMP-1 binding site. For other oncogene mRNAs stabilized by IMP-1, the IMP-1 binding sites are poorly defined (1, 3). We performed a pilot screen of 17,600 small molecules and identified 30 compounds that showed selective inhibition of IMP-1 binding to flMyc RNA and did not inhibit binding by the control DNA binding protein, PR to its DNA binding site, the PRE. We further evaluated the candidate compounds in physiologically relevant assays that are important to IMP-1's function by assessing cell proliferation in IMP-1 positive and negative control cells. By complementing *in vitro* assays to analyze specific inhibition of IMP-1:c-Myc binding with cell-based assays that evaluate an important biological endpoint in cancer cells, we identified a lead small molecule inhibitor of IMP-1.

Identifying inhibitors of RNA binding proteins is challenging (34, 35). Interestingly, we found that most of the compounds identified from our *in vitro* studies did not fail to work in intact cells; rather, they were toxic in a control cell line. This suggests that future high throughput screening campaigns to identify inhibitors of RNA-binding proteins may benefit from initial use of biochemical assays to identify specific inhibitors with early follow-on cell-based filtering assays to evaluate toxicity. This approach not only identifies specific inhibitors using *in vitro* binding, but characterizes a subset of those compounds exhibiting an important physiological function.

This work represents a promising start towards identification of small molecule inhibitors of IMP-1 and describes a path for HTS to identify additional small molecule IMP-1 biomodulators. The lead inhibitor we describe represents an important initial biomodulator for laboratory studies and further characterization; it is a candidate for structure-activity relationship studies and medicinal chemistry optimization to evaluate its ultimate therapeutic potential.

TABLES

Table 2. 1. Summary of Statistical Data from the Pilot Screen

Number of compounds screened	17,600
Total hits	57
Overall hit rate (%)	0.30
Percentage repeat	58
Number of compounds repeated	33
Mean Z'-factor	0.60 ± 0.06

FIGURES

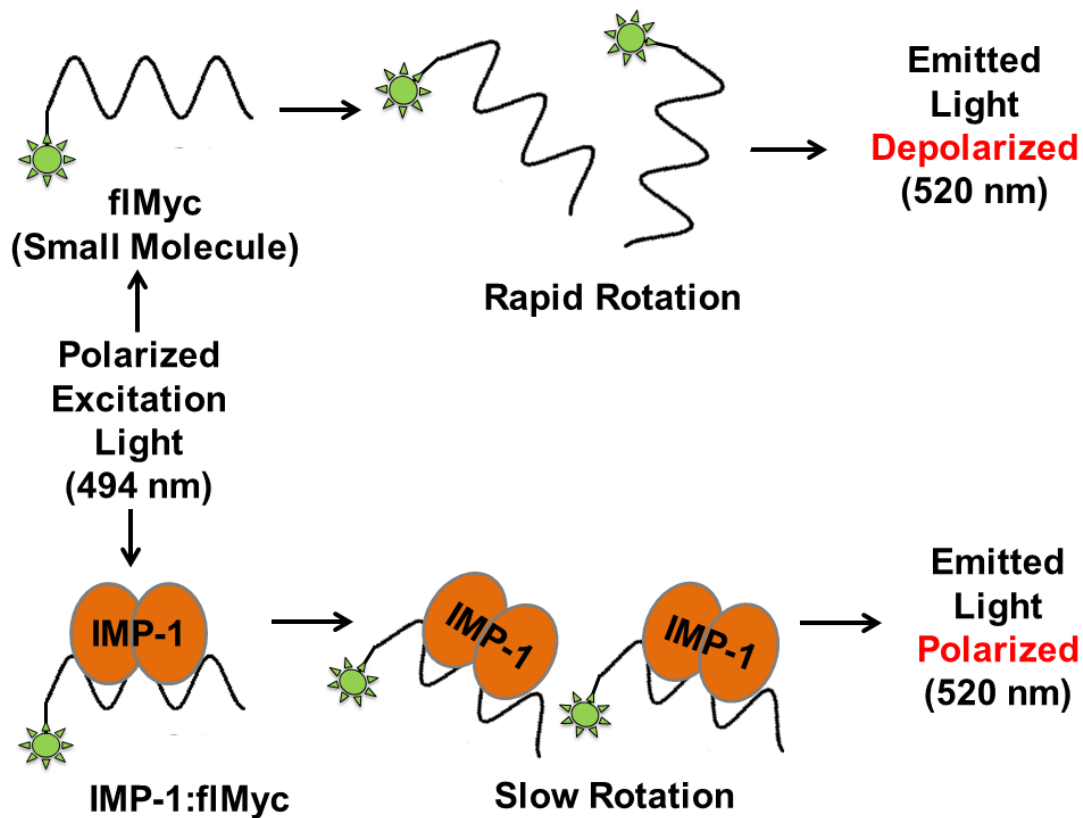


Figure 2.1. Schematic representation of Fluorescence Anisotropy Microplate Assay (FAMA) to evaluate binding of IMP-1 protein to flMyc RNA probe. After excitation with polarized light, flMyc rotates rapidly and the emitted light is largely depolarized. Binding of IMP-1 to the flMyc results in a much larger, less mobile complex. Therefore, the emitted light is more highly polarized.

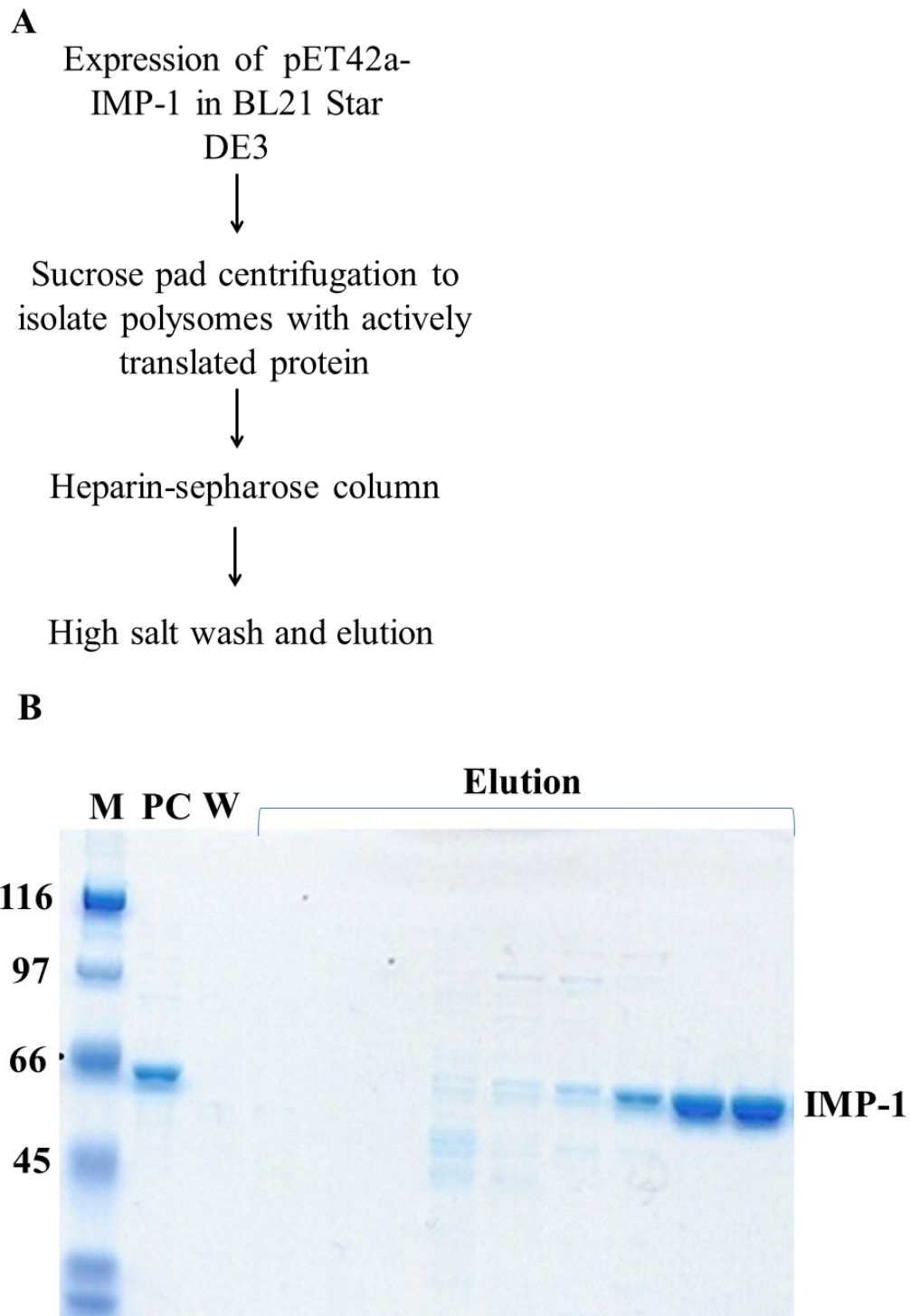


Figure 2.2. Purification of IMP-1. (A) Scheme of the protein expression and purification method used. (B) Purification of IMP-1 by affinity chromatography in Heparin-Sepharose column.

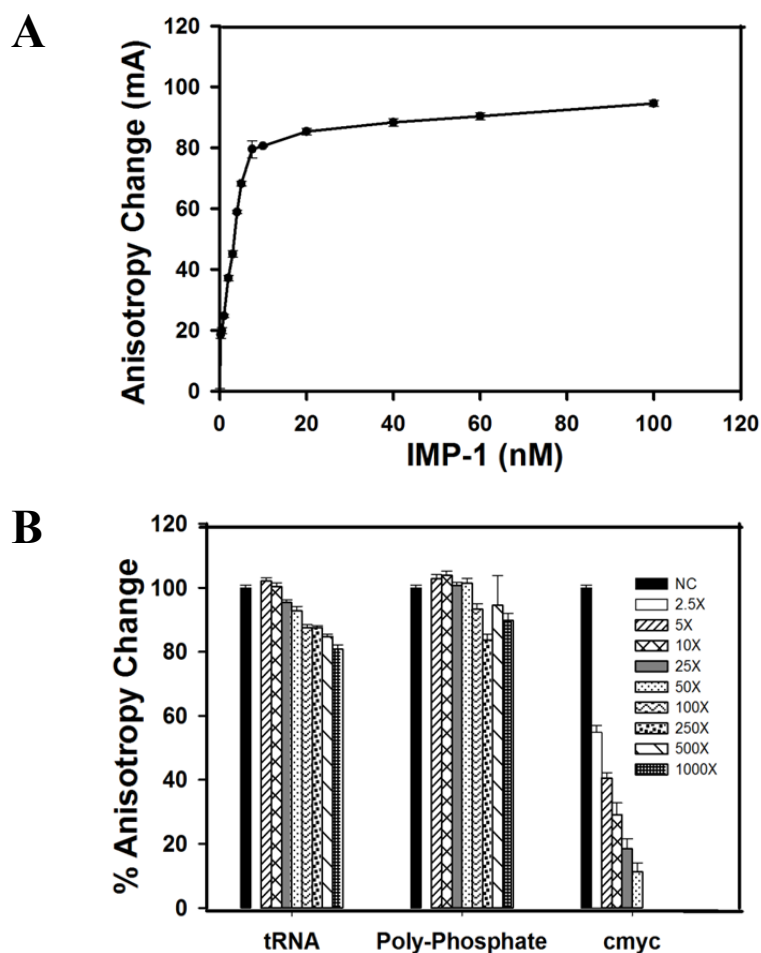
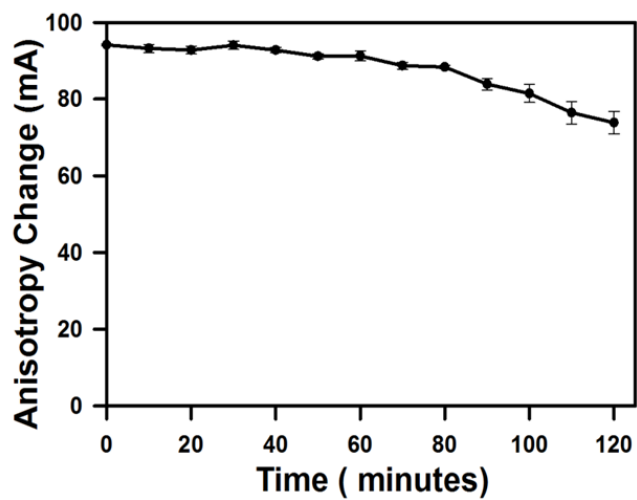


Figure 2.3. Specific, high affinity binding of IMP-1 to flmyc RNA. (A) Dose response studies of binding of IMP-1 to flmyc. 1nM of flmyc probe and indicated concentration of IMP-1 were incubated. Anisotropy change is the difference between flmyc + IMP-1 and flmyc alone. (B) Competition experiments to assess the specificity of IMP-1 binding to flmyc RNA. 10 nM IMP-1 protein was added to reactions containing 1 nM flmyc RNA, and the indicated molar excess of unlabeled specific c-Myc mRNA, or the non-specific competitors, tRNA, or polyphosphate. Anisotropy change minus competitor was set to 100%. (C) Stability of the IMP-1:flMyc complex at room temperature and at different DMSO concentrations. (D) Binding of IMP-1 to flmyc RNA is stable for 1 hour at room temperature. Measurements were made of the same wells over 120 minutes. DMSO at the concentration to be used in the screen (0.5%), and at twice that concentration (1%), had negligible effect on binding of IMP-1 to flMyc. The data in panels A-D represents the average \pm SEM (n=4).

C



D

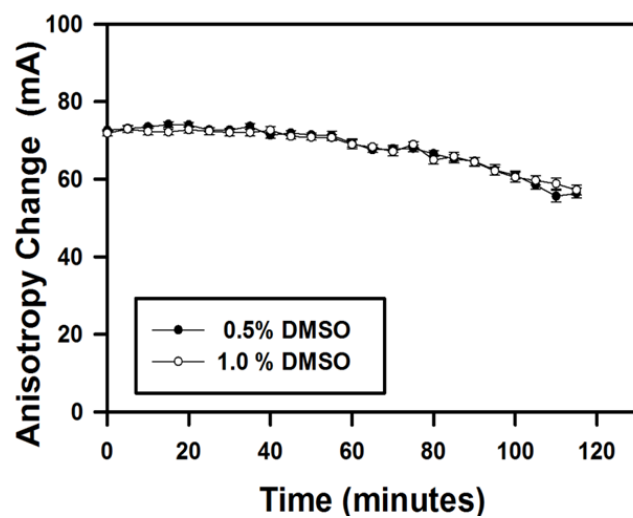


Figure 2.3 (continued)

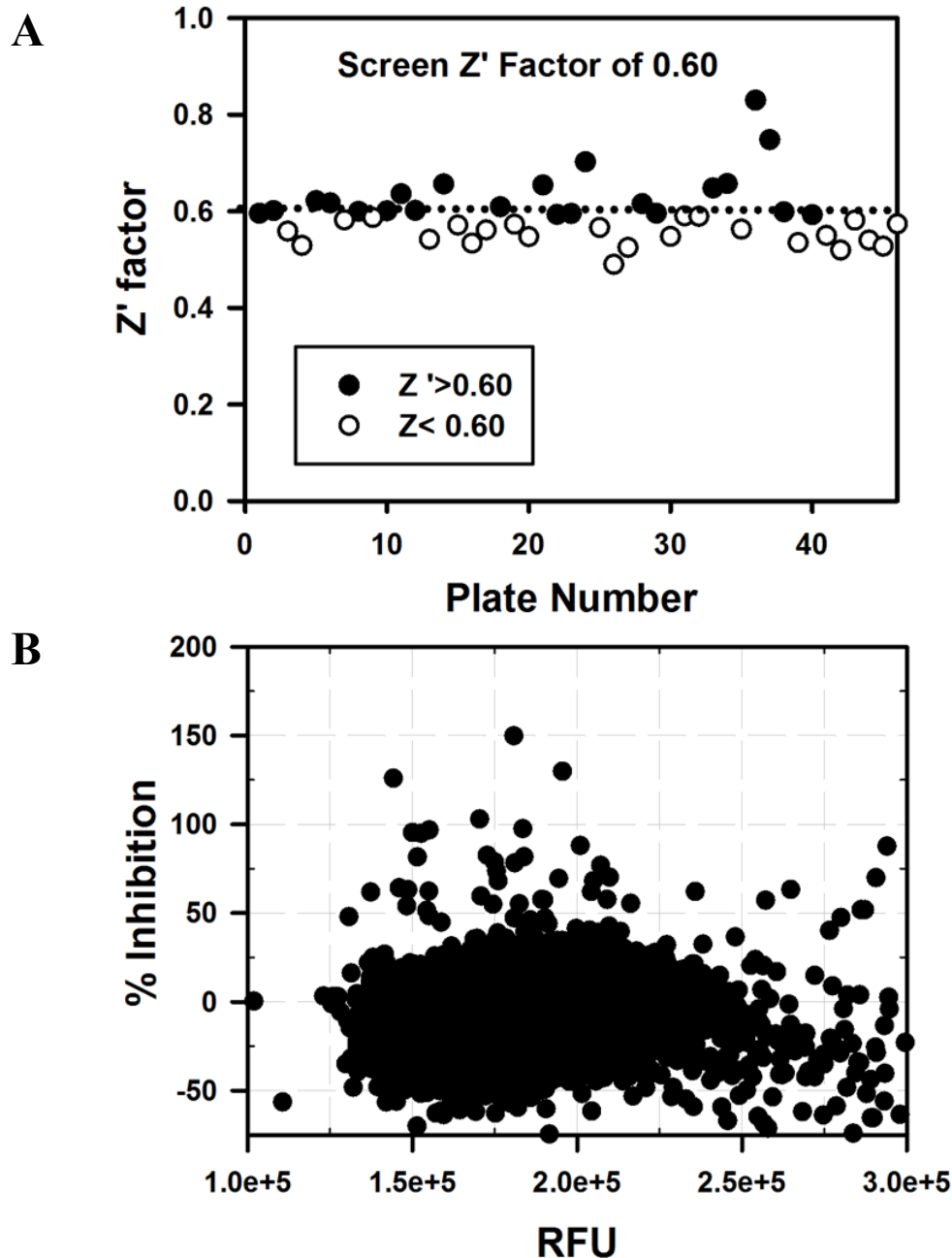


Figure 2.4. Assay validation and high throughput screening results. (A) Assessment of screen robustness for the 50 plates screened using the Z' factor. The dotted line demarcates a Z' factor of 0.6, the average Z' factor for the 50 plate pilot screen. (B) Scatterplot of 17,600 small molecules screened from 50 plates in pilot HTS. A percent inhibition >100% means the small molecule reduced the anisotropy to a level lower than was seen with fIMyc alone. RFU (relative fluorescence unit) represents the sum of the fluorescence intensities in the parallel and perpendicular channel for a given compound and % inhibition = $(1 - ((mA_{Comp} - mA_{Min}) / (mA_{Max} - mA_{Min}))) \times 100$. Data from HTS are single point assays.

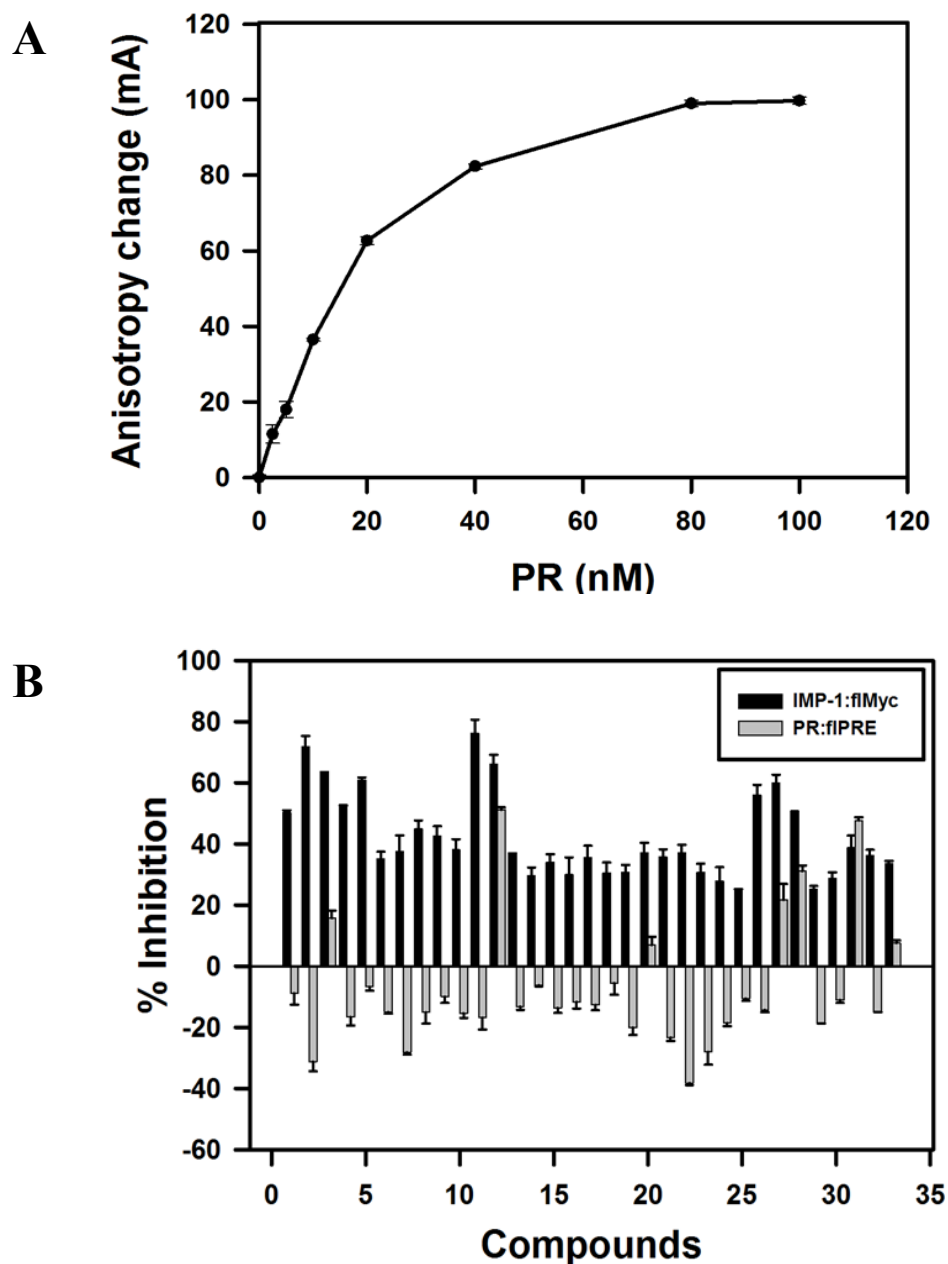


Figure 2.5. Evaluation of hits for potency and specificity. Hits from the primary screen were verified and evaluated for specificity in follow-on assays. **(A)** Binding of purified PR-b to flPRE DNA probe. Increasing amounts of PR were incubated with 1 nM flPRE-DNA probe. Compounds were evaluated for specificity by testing compounds for inhibition of binding of PR to flPRE. **(B)** Primary hits were tested at 5 μ M for the ability to inhibit binding of IMP-1 to flMyc RNA (black bars). Specificity of the verified hits was evaluated by testing their ability to inhibit binding of PR to flPRE at 10 μ M (grey bars). Compounds that did not pass the verification assay were not assayed for inhibition of PR binding to flPRE and only data from all the verified hits is shown. Surprisingly, a substantial percentage of verified hits slightly increased binding of PR to the flPRE. The data in panel A and B represents the average \pm SEM (n=4 (A); n=3 (B)).

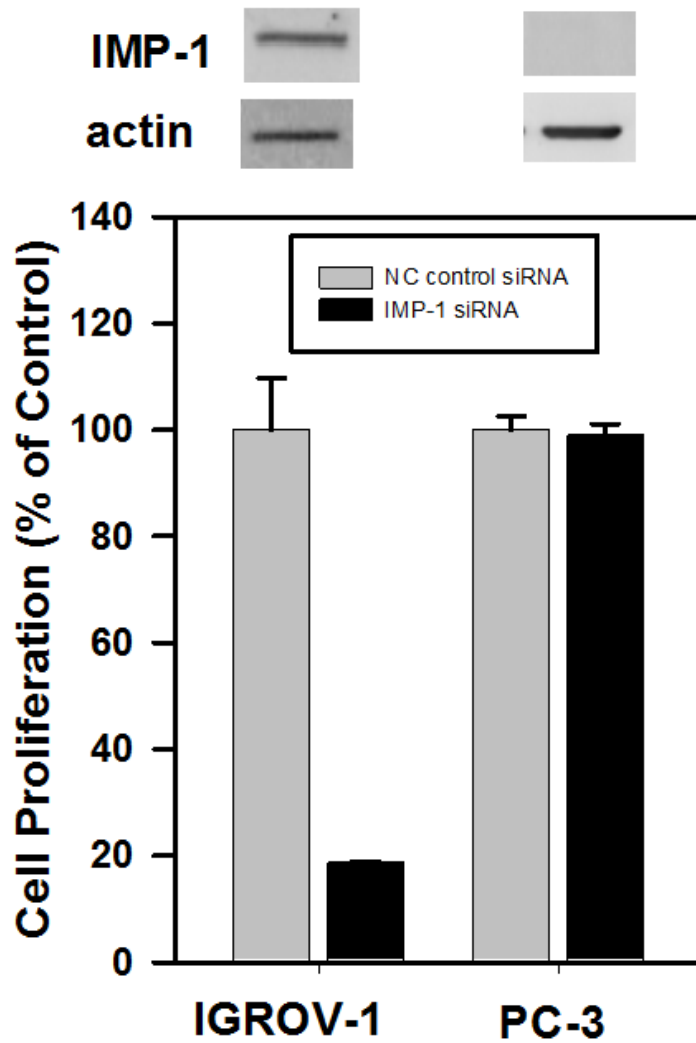


Figure 2.6. IMP-1 knockdown inhibits cell proliferation in IMP-1 positive cells. Top: Western blot of IMP-1 positive IGROV-1 ovarian cancer cells and IMP-1 negative PC-3 prostate cancer cells. For each cell line, cell number after transfection with the control non-coding siRNA was set to 100%. The data represents the average \pm SEM (n=5).

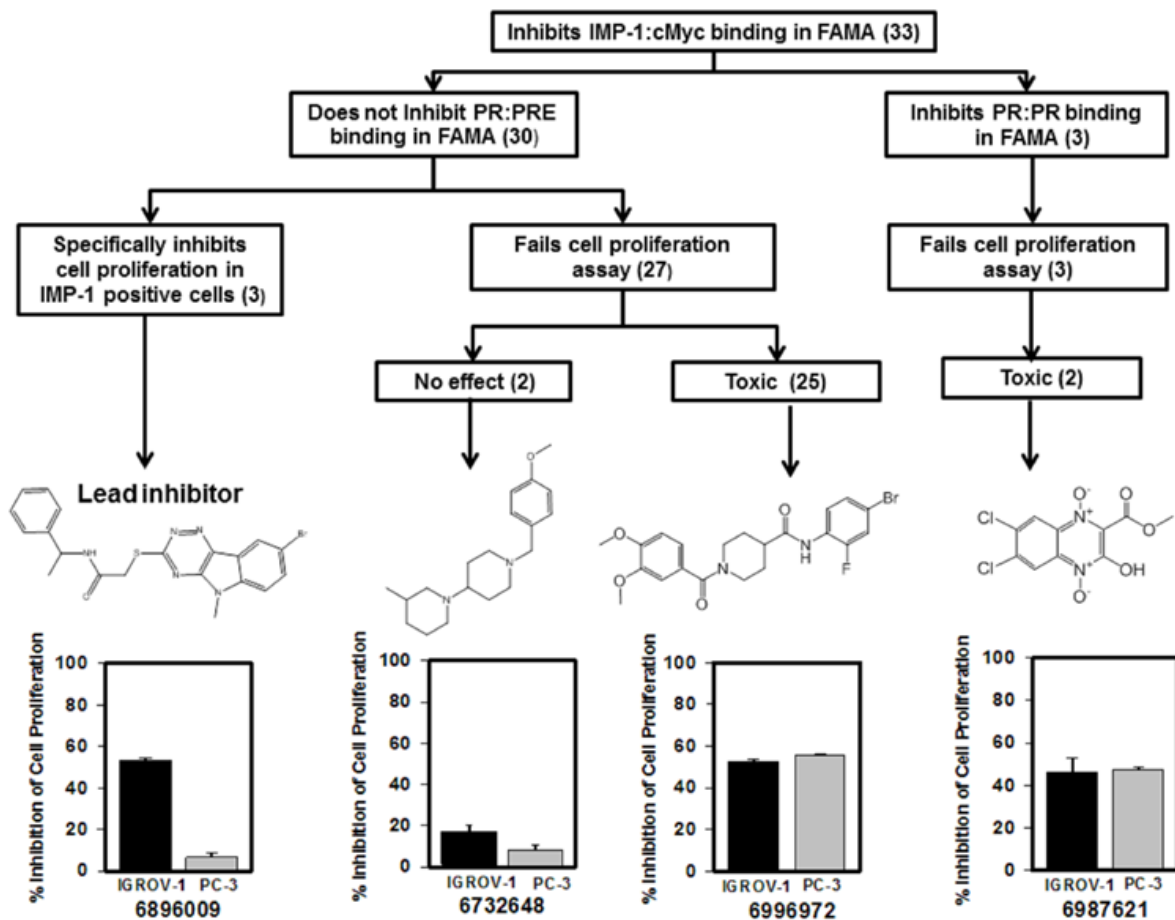


Figure 2.7. Scheme for categorizing representative compounds from the pilot screen. Compounds were categorized based on their properties in FAMA and cell proliferation studies. Cell proliferation data for representative compounds in each category is presented below their structures and the Chembridge number is shown. Compounds were assayed at 20 μ M in IMP-1 positive IGROV-1 cells and in IMP-1 negative PC-3 cells. The 4 categories (from left to right) are the lead IMP-1 inhibitor; a compound that passed the IMP-1 inhibition and PR inhibition assays, but did not inhibit proliferation of either cell line; a compound that passed the IMP-1 and PR assays and exhibits non-specific toxicity because it inhibits proliferation of both the IGROV-1 cells and the IMP-1 negative PC-3 cells; and a compound that failed the specificity test because it inhibited PR binding to the PRE and also was toxic to the PC-3 cells. Set to 100% was cell proliferation for each cell line treated with DMSO vehicle. The data represents the average \pm SEM (n=4).

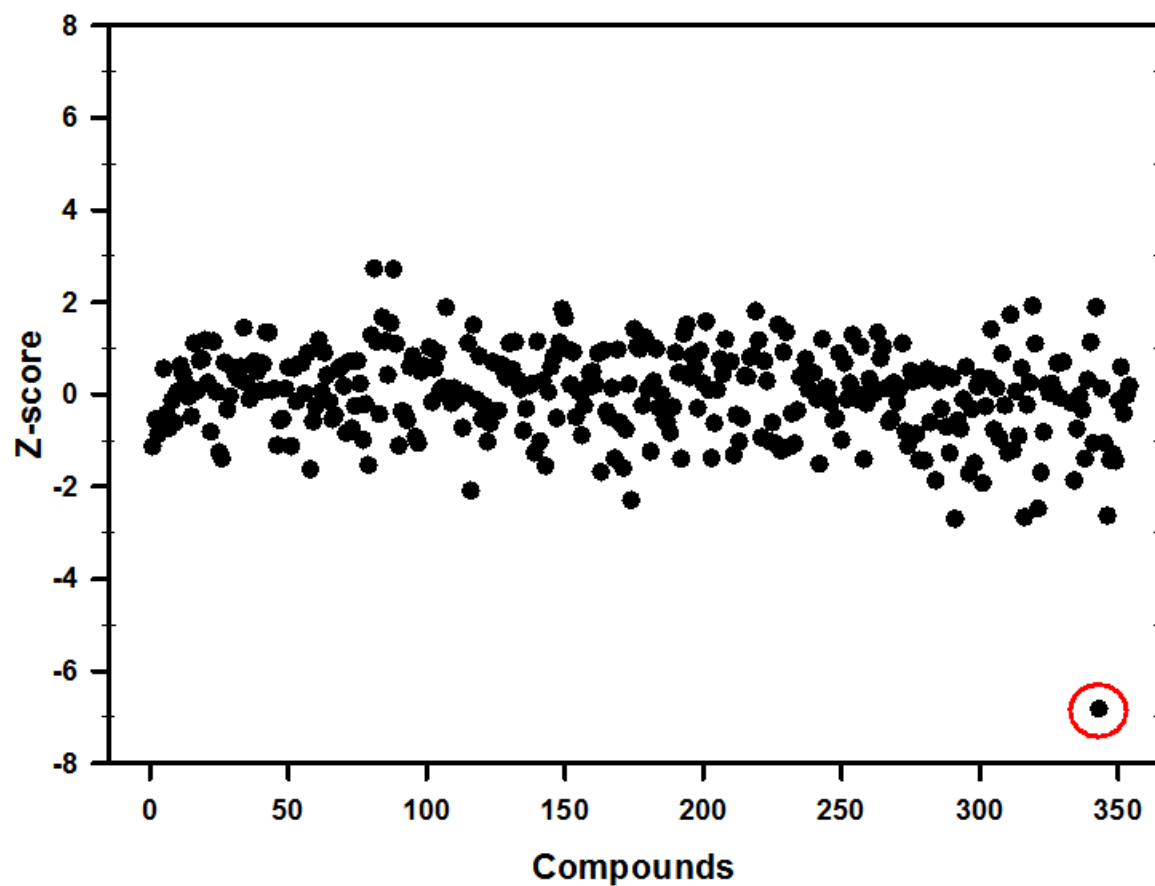


Figure 2. 8. Scatter plot of Z-scores from the plate containing the lead inhibitor. The lead inhibitor identified from the screen, 6896009 (black dot circled in red) had a Z-score of -6.82 and was clearly differentiated from the other compounds on the plate.

CHAPTER 3

A Small Molecule Inhibitor of the Oncogenic mRNA Binding Protein IMP-1/ IGF2BP1/CRD-BP Targets c-Myc mRNA and Inhibits Proliferation of Cancer Cells

Notes and Acknowledgements:

This chapter is adapted from the following manuscript: Mahapatra L, Mao C, Le J, Andruska ND, Shapiro DJ. A Small Molecule Inhibitor of the Oncogenic mRNA Binding Protein IMP-1/ IGF2BP1/CRD-BP Targets c-Myc mRNA and Inhibits Proliferation of Cancer Cells. Submitted for Review to the Journal of Biological Chemistry. We thank Dr. Chen Zhang of the University of Illinois Urbana Champaign High Throughput Screening Center for working with us to set up the assay. We also thank the members of our laboratory for critical reading and discussion of the manuscript. This work was supported by the National Institute of Cancer (NCI) Award: 1 R21 CA173527-01 and the University of Illinois College of Medicine Hazel Craig Research Fellowship.

ABSTRACT

Insulin-like growth factor 2 mRNA-binding protein 1 (IMP-1/IGF2BP-1/CRD-BP/ZBP1) binds to and stabilizes c-Myc and other mRNAs that are up-regulated in cancer. Although overexpression of IMP-1 is associated with a poor prognosis in most types of cancer, IMP-1 remains untargeted and c-Myc has been difficult to target. Using a fluorescence anisotropy microplate assay (FAMA) high-throughput screen of ~150,000 small molecules, we identified BTYNB as a novel, small molecule that specifically inhibits IMP-1 binding to its

recognition sequence in c-Myc mRNA. The potency of BTYNB in inhibiting binding of IMP-1 to c-Myc RNA *in vitro* correlated with its ability to specifically reduce the intracellular level of c-Myc mRNA. BTYNB destabilized c-Myc mRNA and strongly reduced the level of c-Myc protein. BTYNB also reduced the levels of other IMP-1 target mRNAs. Consistent with BTYNB acting in cells through IMP-1, overexpression of IMP-1 reverses BTYNB inhibition of cell proliferation and BTYNB has no effect on proliferation of IMP-1 negative cells. BTYNB was as effective as RNAi knock-down of IMP-1 in inhibiting proliferation of IMP-1 containing cancer cells. Notably, BTYNB completely blocked growth of IMP-1 containing melanoma and ovarian cancer cells in anchorage-independent colony formation assays. BTYNB is the first small molecule that targets cancer-associated mRNAs by inhibiting binding of an mRNA stabilizing protein to its target mRNAs.

INTRODUCTION

Insulin-like growth factor II mRNA-binding protein 1 (IMP-1/IGF2BP1), also known as the c-Myc coding region determinant-binding protein (CRD-BP) and zipcode binding protein 1 (ZBP1) binds to diverse cancer-associated mRNA targets. IMP-1 binding to mRNAs increases their stability and can also influence translation and mRNA localization (11,14,26,66). IMP-1 likely stabilizes target mRNAs by shielding them from degradation by endoribonucleases (14,18,39) and microRNAs (20).

Several lines of evidence support the important role of IMP-1 in cancer. IMP-1 binding stabilizes mRNAs that play critical roles in cell growth, proliferation, migration and inflammation (15,21,22,51). IMP-1 expression is up-regulated by c-Myc, β -catenin and hypoxia

(19, 50, 52) and it is a major regulatory target of *let-7* microRNA (47, 48). In cell culture, overexpression of IMP-1 results in enhanced cell proliferation (41, 51), suppression of apoptosis (22), resistance to taxanes and other anticancer drugs (48, 53) and increased inflammation (20). Moreover, transgenic mice that overexpress IMP-1 develop mammary tumors and colorectal cancer (61, 67). IMP-1 is expressed in fetal cells, is expressed at extremely low (68) or undetectable levels in normal cells (69, 70) and is frequently re-expressed in cancer cells. High levels of IMP-1 expression are associated with tumor recurrence and a poor prognosis in ovarian cancer, melanoma, breast (58), colon (22, 55, 60), lung (25,54), and other cancers (6).

Although IMP-1 upregulates the expression of mRNAs important in cancer, including c-Myc, CDC34, β TRCP-1 and MDR1 (18, 19, 50), a conserved IMP-1 recognition sequence has not been identified. Instead of a classical long conserved binding sequence, IMP-1 exhibits high affinity binding to weakly conserved, extended, relatively unstructured G-poor regions containing short interaction motifs (12, 65, 71). Therefore, many IMP-1 target mRNAs are likely still unidentified (11, 38, 65). The best-studied and most widely accepted IMP-1 target is the oncogene c-Myc. IMP-1 binds to the coding region stability determinant in c-Myc mRNA, protecting c-Myc mRNA from endonucleolytic degradation (16, 18, 40). In ovarian, lung, melanoma and other cells, RNAi knockdown of IMP-1 reduces c-Myc mRNA levels (13, 15, 43, 48, 51, 52) and overexpression of IMP-1 increases c-Myc levels (22, 43, 48, 52).

Given its dramatically elevated expression in cancer cells and its role in diverse cancers, targeting IMP-1 with small molecule biomodulators is an attractive strategy for probing IMP-1 in cancer and ultimately for improving therapy (6). Also, since c-Myc has proven difficult to target directly, reducing c-Myc levels by decreasing c-Myc mRNA stability by inhibiting the IMP-1—c-Myc mRNA interaction represents a novel therapeutic strategy. However, mRNA binding

proteins that play a role in cancer have proven challenging to target and small molecule biomodulators of IMP-1 and other cancer-related mRNA stabilizing proteins have not been reported. More broadly, despite their roles in diverse cell processes, with a few exceptions largely centered on proteins important in protein synthesis (72, 73), eukaryotic mRNA binding proteins have rarely been targeted with small molecule biomodulators.

To identify small molecule biomodulators of IMP-1, we developed a high throughput fluorescence anisotropy/ polarization microplate assay (FAMA) (71). We screened ~150,000 small molecules and here report a small molecule 2-{[(5-bromo-2-thienyl)methylene]amino} benzamide (BTYNB) that inhibits IMP-1 binding to a specific high affinity binding site in the coding region stability determinant of c-Myc mRNA. We show that BTYNB, identified from an *in vitro* screen, functions in cells to reduce intracellular levels of c-Myc mRNA and protein, and also reduces levels of other IMP-1 target mRNAs. Importantly, BTYNB inhibits cell proliferation and anchorage independent growth of IMP-1 positive cancer cells with no effect on IMP-1 negative cells, making it a candidate for further therapeutic evaluation. To our knowledge, BTYNB is the first small molecule inhibitor of a mammalian mRNA stabilizing protein.

MATERIALS AND METHODS

Proteins

Human IMP-1 and FLAG-PR-B were expressed and purified as we described previously (71,74).

Oligonucleotides

The flMyc probe was produced as previously described (71) and the palindromic cPRE/GRE (5'-f-CTAGATTACAGAACAATCTGTTCTTACTCA-3') was synthesized as previously described (75).

Chemical Libraries

The libraries screened were the ChemBridge Micro-FormatTM small molecule library obtained from ChemBridgeTM containing ~150,000 small molecules, the Marvel library developed at the University of Illinois by K. Putt and Hergenrother (76) containing ~9,700 small molecules, and the NCI Diversity Set from NIH with ~1,990 small molecules. Columns 23 and 24 on each plate of the screening library contain DMSO and no test compounds and these wells served as screening controls.

Plasmids

Vectors for purifying IMP-1 and synthesizing c-Myc RNA probe have been previously described (71). pET42a-IMP-1 codes for untagged full-length IMP-1, which was then expressed in a strain of BL21DE3pLysS expressing plasmid-encoded tRNAs for rare Arg, Ile and Leu codons (a generous gift of Dr. J. Christiansen). pBS.cMyc contains the c-Myc mRNA coding region instability determinant (nucleotides 1705–1792) and this region was amplified using the following primers: 5'-CAGAGATGCATAATACGACTCACTATAGGGAGATGAATAA-GCTGTAATATCAC-3' (the T7 promoter sequence is underlined) and 5'-CCTAAAATTGAAT-TGTTTACA-ATAG-3'. pCMV-IMP-1 codes for full length human IMP-1 and pTZ18U is a carrier DNA used to normalize the total amount of DNA transiently transfected.

High Throughput Screening Using FAMA

The fluorescence anisotropy microplate assay for analyzing binding of IMP-1 to the fluorescein-labeled c-Myc RNA was performed as described (71). Assays were carried out at room temperature in black wall 384-well microplates (Greiner Bio-One, NC) using a sequential method with a final volume of 20 μ l containing 20 mM Tris-HCl, pH 8.0, 150 mM KCl, 1 mM EDTA, 1 ng/ μ l tRNA, 1 ng/ μ l heparin, 0.4 U/ μ l RNasin, and 500 ng/ μ l RNase-free BSA. A sequential protocol was used to assess changes in anisotropy, intrinsic fluorescence of candidate compounds, the compounds' influence on the anisotropy signal of the probe alone, and the ability of compounds to inhibit binding of IMP-1 to flMyc. For high throughput screening, a master mix containing the flMyc probe was prepared at 4 °C. The master mix was divided into two parts. IMP-1 was added to one part to 10 nM in the final assays. First, using a Matrix PlateMate Plus dispenser (Thermo Scientific, MA), plates were loaded with 10 μ l binding buffer containing fluorescein-labeled c-Myc RNA probe (2-fold in binding buffer) in every well. Then 100 nl of each test compound from the 1 mM compound plates was transferred to each well of the test plates using the Matrix PlateMate Plus robotic pin transfer apparatus. Then fluorescence polarization/ anisotropy (FP/FA) was determined using an Analyst HT Plate Reader (Molecular Devices, CA). FITC FP 480 (excitation) and 535 (emission) filters were used. Then, 10 μ l of binding buffer and IMP-1 protein (final assay concentration 10 nM) was added to each well except control wells that contained received 10 μ l of binding buffer. FP/FA for each well was measured after 15 minutes, when the assay had reached equilibrium as determined from kinetic studies of the ON and OFF rate of IMP-1 binding to flMyc. Thus, in the final assay, compounds were tested at 5 μ M for their ability to inhibit binding of 10 nM IMP-1 to 1 nM flMyc RNA probe. "Hits" from the primary screen were analyzed and scored as previously described (71).

Dose-response curves for selected compounds were carried out as described for the HTS screen except that each well contained the indicated concentration of test compound. To assess for compound specificity, PR assays were carried out in a buffer containing 15 mM Tris-HCl, pH 7.9, 100 mM KCl, 1 mM dithiothreitol (DTT), 5% glycerol, 0.05% Nonidet™ P-40 (NP-40), 100 ng poly dI:dC (non-specific competitor), and 250 ng/μl BSA. Fluorescein-labeled progesterone response element (fPRE) was diluted to a final concentration of 1 nM in this binding buffer. The concentration of PR chosen for use in the follow-on assay is not saturating and is highly responsive to inhibition.

Cell Culture

Unless otherwise indicated, cells were maintained at 37 °C in 5% CO₂ in growth medium containing 1% penicillin and streptomycin and fetal bovine serum (FBS) (Atlanta Biological, Atlanta, GA). IMP-1 positive IGROV-1, ES-2, SK-MEL2, and HEK 293T cells and IMP-1 negative BG-1/MCF-7 and T47DKBLuc cells were used in cell-based experiments. Cells were maintained in the following culture media. IGROV-1, SK-MEL-2, and T47DKBLuc: RPMI-1640, supplemented with 10% FBS; ES-2: McCoy's 5A, supplemented with 10% FBS; BG-1/MCF-7: MEM supplemented with 5% FBS; HEK 293T: DMEM-F12 supplemented with 10% FBS.

MTS Cell Proliferation Assays

Cells were harvested and plated in 96-well plates at a density of 1,000 cells/well. The medium was replaced with treatment medium the following day, and plates were incubated at 37°C in 5%

CO₂ for 3 days. 20 µl of CellTiter 96 Aqueous One Solution Reagent (Promega, WI) was added to each well and the cells were incubated at 37° C in 5% CO₂ for 1 hour. A490 was then measured to assess cell viability. For each cell line, cell number was calculated from a standard curve of the number of cells plated versus A490 (77).

RNAi Knockdown

IGROV-1, ES-2, SK-MEL, BG-1, and T47DKBluc cells were plated in 96-well plates at a density of 1,000 cells/well and transfected with an IMP-1 siRNA SMARTpool (Dharmacon, CO) or a non-coding control (NC) siRNA using Dharmafect transfection reagent (Dharmacon, CO) or Lipofectamine 2000 (Invitrogen) according to the suppliers' protocol. 5 days after transfection cell viability was determined using CellTiter 96 Aqueous One Solution Reagent (Promega, WI). For both cell lines relative cell proliferation was calculated as previously described (77).

Transient Transfection

HEK 293T cells were plated 1,000 cells/well in 96-well plates in 10% FBS and transfected the following day. On the day of transfection, the medium was changed to Opti-MEM. DNA and Lipofectamine2000 (Invitrogen, CA) were diluted in Opti-MEM and incubated together for 20 min before adding to the well. A total of 100 ng of DNA was transfected into cells in each well at a DNA:Lipofectamine2000 ratio of 1:3. 24 h after transfection, inhibitor to a final concentration of 10 µM or DMSO control were added to the cells and incubated for 48 h. Cells were lysed in 100 µl of passive lysis buffer (Promega, WI), and luciferase activity was determined using Dual-Luciferase Reporter Assay (Promega, WI).

Soft Agar Colony Formation Assays

To assay anchorage-independent cell growth in soft agar, 1%, and 0.7% Select Agar (Invitrogen, CA) was prepared in water and warmed at 40°C before use. 1.5 ml of 0.5% bottom agar diluted in medium was added to each well of a 6-well cell culture plate and allowed to solidify at room temperature. Top agar was prepared by dilution in warm medium containing the various treatments. SK-MEL2 cells were resuspended in 1.5 ml of 0.35% top agar at 10,000 cells/well and ES-2 cells were resuspended in 1.5 ml of 0.35% top agar at 8,000 cells/well. For each cell line, cells were plated in 3 wells for each condition. The plates were kept at room temperature for 30 min until the top agar solidified, then 0.5 ml of medium containing the respective treatments was added on top of the agar. Culture medium on top of the agar was changed every 3–4 days. Colonies were visible by 1 week and counted at day 21 using a dissecting microscope. Photographs of colonies were taken using a Zeiss AxioImager2 imaging system at 10× magnification.

Western Blots

SK-MEL2 cells were plated at 200,000 cells/well in 6-well plates in RPMI-1640 containing 10% FBS. Medium was replaced the next day with fresh medium containing the indicated treatments. Whole cell extracts were prepared after 72 hour treatment in 1× radioimmune precipitation assay (RIPA) buffer (Millipore, CA) containing protease inhibitor mixture (Roche Applied Science, IN). Extract (20 µg of protein/lane) was run on 10% SDS-PAGE gels and transferred to nitrocellulose membranes. c-Myc antibody (Cell Signaling Technology, MA) was used at a

1:1000 dilution. The blot was stripped for 25 min and re-probed using a 1:10,000 dilution of β -actin monoclonal antibody (Sigma, MO).

Quantitative RT-PCR and mRNA Decay Analyses

SK-MEL2 cells plated at 300,000 cells/well in 6-well plates in RPMI-1640 containing 10% FBS. Medium was replaced the next day with fresh medium containing the indicated treatments. After 72 hours, RNA was extracted, and mRNA levels were measured by quantitative RT-PCR as described (78,79). For stability experiments SK-MEL2 cells were treated with either DMSO or 10 μ M BTYNB for 24 hours and treated with 5 μ M Actinomycin D (mRNA decay) and harvested at indicated time points. 36B4 mRNA level is used as the qRT-PCR internal standard. Primers used in qRT-PCR were: Myc forward primer (5'-CCGACGCGGGGACCCTATTC) and reverse primer (5'-AACGTTGAGGGGCATCGTCGC-3'); IMP-1 forward primer (5'-TGAACACCGAGAGTGAGACG-3') and reverse primer (5'-CTCATCGGGGATGTAGGAGA-3'); eEF2 forward primer (5'-GCACGTTCTGACTCTTCACTG) and reverse primer (5'-CTGGAGATCTGCCTGAAGGA); CALM1 forward primer (5'-CTCGCTCCCTCTGCTCTTC) and reverse primer (5'-AGGGAGAAGGCTTCCTTGAA); Collagen 5 α forward primer (5'-GCTGTGAAGTTGCAGTAAACCTTGAGGG) and reverse primer (5'-CATGGAAGAGATCTTGGGCT-CTCTCAA); β TRCP1 forward primer (5'-ACCAACATGGGCACATAAACT) and reverse primer (5'-TGGCATCCAGGTATGACAGAAT); 36B4 forward primer (5'-GTGTTCTGACAATGGCAGCAT) and reverse (5'-GACACCCTCCAGGAAGCGA). The fold change in expression of each gene was calculated using the $\Delta\Delta C_t$ method with 36B4 as the internal control.

Statistical Analysis

Results are expressed as the mean \pm S.E.M. of at least three independent experiments. Student's *t* test was used for comparison of the means between two groups. Significance was established when $p < 0.05$. The comparisons are described in the figure legends and are not shown in the body of the figures.

RESULTS

High Throughput Screen for Inhibitors of IMP-1

To identify small molecules that inhibit binding of IMP-1 to its binding site in the coding region stability determinant of c-Myc mRNA, we developed a high throughput fluorescence anisotropy micro-plate assay (FAMA) (71). The assay is based on the increase in fluorescence anisotropy/polarization when IMP-1 binds flMyc RNA. The IMP-1-flMyc complex is larger than flMyc RNA. Compared to flMyc, the IMP-1-flMyc complex will exhibit slower rotation, increasing the chance that the IMP-1-flMyc complex will be in the same plane at emission as it was at excitation, resulting in an increase in fluorescence anisotropy. A small molecule that blocks IMP-1 binding to flMyc will reverse the IMP-1-mediated increase in fluorescence anisotropy/polarization.

Screening was performed *in vitro*, using purified untagged IMP-1 and fluorescein-labeled c-Myc RNA in 384-well microplates. We screened small molecule libraries containing approximately 150,000 compounds and analyzed the results using screening software we developed and tested in a pilot study (71). We identified 981 compounds that reduced anisotropy of the IMP-1-flMyc complex by $>30\%$. After rescreening and eliminating compounds that no

longer reduced the anisotropy change by >30%, displayed intrinsic fluorescence, or reduced the signal of the free flMyc probe, 300 structurally diverse compounds were selected for further testing. Most of the small molecules excluded from further analysis either displayed intrinsic fluorescence, or reduced the signal by a little over 30% in the initial assay and slightly less than 30% on retesting. The robust nature of our screen is shown by the fact that the lead inhibitor had a Z-score of -10.2.

Validated hits were evaluated using FAMA for specificity and potency in dose response studies. Compounds that inhibited binding of IMP-1 to flMyc, with no effect in a control binding assay were further evaluated in cell-based assays for inhibition of cell proliferation, a critical readout for IMP-1 activity. Compounds that inhibited proliferation of IMP-1 positive cells with no effect on IMP-1 negative cells were considered leads for further evaluation. Figure 3.1 summarizes the sequence of assays used to identify the lead inhibitor of IMP-1 action.

BTYNB is a Structure-specific Small Molecule Inhibitor of IMP-1 Binding to c-Myc RNA

From the high throughput screen and initial follow-on studies we identified the lead small molecule 2-[(5-bromo-2-thienyl)methylene]amino}benzamide (BTYNB) (Fig. 3.2A). We evaluated the potency, efficacy and selectivity of BTYNB in dose-response studies. BTYNB inhibited binding of IMP-1 to flMyc ($50 \pm 4.7\%$ inhibition at 5 μM) and had negligible effects on binding of PR to flPRE at all concentrations tested, including 50 μM (Fig. 3.2B). A close structural relative of BTYNB, Compound 5226752, which shares 90% 3D similarity with BTYNB (Fig. 3.2A), had no effect on binding of IMP-1 to flMyc, or of PR to flPRE (Fig. 3.2C). To further probe the relationship between chemical structure and activity, we carried out a

limited study of structure activity relationships (SAR) and performed dose-response studies on 7 additional structural relatives of BTYNB. Only one of the 7 compounds (Compound 531848) inhibited binding of IMP-1 to flMyc (**Fig. 3.3**) and its potency was poor (**Fig. 3.3F**). Thus, BTYNB is a structure selective inhibitor of binding of IMP-1 to flMyc.

BTYNB Reduces the Level of IMP-1 Protein

Although *in vitro* assays, such as FAMA have the advantage of being homogenous and reproducible and are ideal for producing quantitative information on macromolecular interactions, FAMA does not fully recapitulate the complex environment of living cells. To test the effect of IMP-1 in intact cells, we initially used Western blot analysis to assess the IMP-1 status of 31 cell lines from diverse tissues. Consistent with most data from tumor immunohistochemistry and microarrays, which support a role for IMP-1 in nearly all types of cancer except prostate cancer and estrogen receptor α (ER α) positive breast cancer, IMP-1 was widely distributed but was nearly undetectable in prostate cancer cell lines and in ER α positive breast cancer cell lines.

To evaluate the effect of IMP-1 in cell lines from tumors that have proven difficult to target therapeutically and contain diverse levels of IMP-1, we selected IGROV-1 ovarian cancer cells, and SK-MEL2 melanoma cells as containing high and low levels of IMP-1, respectively and BG-1 and T47DKBluc breast cancer cells as IMP-1 negative cells containing undetectable levels of IMP-1 (**Fig. 3.4**).

In vitro assays, such as FAMA cannot assess potential effects of small molecules on intracellular levels of their targets. To test whether BTYNB influences intracellular levels of

IMP-1, we evaluated the effect of increasing concentrations of BTYNB on levels of IMP-1 protein in IGROV-1 and SK-MEL2 cells. BTYNB treatment resulted in a dose-dependent decline in IMP-1 levels in IGROV-1 (**Fig. 3.5A**) and SK-MEL2 cells (**Fig. 3.5B**). IMP-1 levels were clearly reduced at 10 μ M BTYNB, a concentration that inhibited binding of IMP-1 to flMyc by ~80% (**Fig. 3.2B**).

BTYNB Reduces the Levels of Cancer-related IMP-1 mRNA Targets

Knockdown of IMP-1/IGF2BP1/CRD-BP reduces levels of IMP-1 protein and this is thought to destabilize IMP-1 target mRNAs, reducing levels of cancer-related mRNAs important in cell proliferation, migration, cancer enabling inflammation and metabolic regulation (6). In contrast to c-Myc, for which a well-characterized IMP-1 binding site has been identified (16, 24, 41, 80), specific interactions regions remain unknown for most cancer-related IMP-1 targets. Moreover, IMP-1 binding sites display limited sequence conservation. It was therefore unclear whether IMP-1 would display broad ability to influence levels of IMP-1 target mRNAs or would be restricted to effectiveness on c-Myc mRNA. We tested the effect of BTYNB on levels of several IMP-1 mRNA targets. These mRNAs were chosen because IMP-1 depletion was shown to reduce their levels and because they promote a diverse range of oncogenic activities. Target mRNAs implicated in tumor cell proliferation (CDC34, CALM1 [calmodulin]), migration (CDC34, Col5A [Collagen V, α 1]), and tumor enabling inflammation (β TRCP1) were tested (19-22, 65). IGROV-1 and SK-MEL2 cells were maintained in 10 μ M BTYNB for 3 days and levels of CDC34, CALM1, β TRCP1 and Col5A mRNAs were quantitated by qRT-PCR. Although the IGROV-1 cells contain several fold higher levels of IMP-1 than the SK-MEL2 cells (**Fig. 3.4**),

and might therefore be less effective in inhibiting binding of IMP-1 to its mRNA targets, BTYNB had similar effects on levels of CDC34, CALM1 and Col5A mRNAs in the two cell lines. There was a statistically significant reduction in the level of CDC34, CALM1 and Col5A mRNA to approximately 30-70% of the levels in vehicle-treated controls (**Fig. 3.6**). In contrast, the level of β TRCP1 mRNA declined dramatically in SK-MEL2 cells, but was only reduced modestly in the IGROV-1 cells (**Fig. 3.6**). These data demonstrate that BTYNB reduces the levels of a diverse set of cancer-related IMP-1 mRNA targets.

BTYNB Reduces Levels of Eukaryotic Elongation Factor 2a and Inhibits Global Protein Synthesis

Recent PAR-CLIP and RIP studies suggest more than 1,000 mRNAs as potential candidates for IMP-1 binding, with eukaryotic elongation factor 2 (eEF2) as a top predicted target (65). eEF2 is a gene that plays an essential role in protein synthesis. The ability of cancer cells to rapidly proliferate is dependent on basal translation rates and thus on eEF2 (81). Furthermore, eEF2 is an important link between metabolic regulation in cancer and protein synthesis (82). eEF2 is overexpressed in many cancers, including lung, colorectal, pancreatic, and breast and is an important molecular target in these cancers (83,84). Therefore, we examined the effect of BTYNB on eEF2 mRNA and protein in more detail. We compared the effect of BTYNB with siRNA knockdown of IMP-1.

We treated IGROV-1 and SK-MEL2 cells with 10 μ M BTYNB for 72 hours and observed a ~2.5-fold decrease in eEF2 mRNA (**Fig. 3.7A, 3.7B**) and observed a decrease in eEF2 protein (**Fig. 3.7C**). To test whether the decline in eEF2 mRNA and protein reduced

protein synthesis, we measured the effect of BTYNB on incorporation of ^{35}S methionine into protein. Consistent with its ability to reduce the level of eEF2, a rate-limiting protein in protein synthesis, BTYNB treatment elicited a significant decrease in protein synthesis (**Fig. 3.7D**). Consistent with earlier work suggesting eEF2 is a likely IMP-1 target, RNAi knockdown of IMP-1 in IMP-1 positive IGROV-1 ovarian cancer cells (**Fig. 3.7E**) resulted in a ~7-fold decrease in eEF2 mRNA levels (**Fig. 3.7F**) and a smaller, but clearly detectable, decrease in eEF2 protein (**Fig. 3.7G**).

BTYNB Increases Degradation of c-Myc mRNA, Decreasing Expression of c-Myc mRNA and Protein

Given that c-Myc is the best established and most extensively studied target of IMP-1, we tested whether BTYNB inhibits a known activity of IMP-1, the ability to regulate c-Myc mRNA stability (13,16,24). Binding of IMP-1 to the c-Myc coding region stability determinant protects c-Myc RNA against degradation, stabilizing c-Myc RNA, increasing the levels of c-Myc RNA, protein and enhancing cell proliferation (14,15,50). In order to address the mechanism of action of BTYNB, we evaluated whether treatment with BTYNB increases c-Myc mRNA degradation, leading to a decrease in c-Myc mRNA and protein. To investigate the effect of BTYNB on the degradation of c-Myc mRNA, we employed the widely used technique of blocking new mRNA synthesis using Actinomycin D and following the decay of c-Myc mRNA. SK-MEL2 melanoma cells were pre-treated with DMSO vehicle, or with 10 μM BTYNB, mRNA synthesis was inhibited by addition of Actinomycin D and total RNA was isolated at the indicated times. The relative level of c-Myc mRNA at each time point was determined in three independent

experiments by normalizing to an internal control and setting the input amount of c-Myc mRNA to 100%. Consistent with the data showing BTYNB-mediated increased degradation of c-Myc mRNA (**Fig. 3.8A**), BTYNB treatment reduced the level of c-Myc mRNA by ~3 fold (**Fig. 3.8B**). BTYNB was as effective as RNAi knockdown in reducing the level of c-Myc mRNA (**Fig. 3.8C**). Likely because c-Myc protein is rapidly degraded and the level of c-Myc protein rapidly reflects the level of c-Myc mRNA, BTYNB elicited a robust decline in the level of c-Myc protein (**Fig. 3.8D**).

BTYNB Inhibits Proliferation of IMP-1 Positive Cancer Cells with no Effect in IMP-1 Negative Cells

Since overexpression of IMP-1 is associated with more aggressive tumors and a poor outcome in diverse cancers (15,54,55), and IMP-1 knockdown inhibits cell proliferation (15,48,51,52), and BTYNB influences levels of several oncogenes important in tumor cell proliferation, including c-Myc, CDC34 and eEF2, we evaluated the ability of BTYNB to inhibit proliferation of IMP-1 positive cancer cells. Because of their stem-like character and very high level of IMP-1 (**Fig. 3.4**), we included ES-2 ovarian cancer cells in the proliferation studies. Initially we assessed the effect of RNAi knockdown of IMP-1 on proliferation of IMP-1 positive and IMP-1 negative cells. Compared to a noncoding control (NC) siRNA, RNAi knockdown of IMP-1 reduced proliferation of IGROV-1, ES-2 and SK-MEL2 cells by ~7, 6 and 4 fold, respectively (**Fig. 3.9A-C**). In contrast, RNAi knockdown of IMP-1 did not inhibit proliferation of the IMP-1 negative BG-1 and T47DKBluc cells (**Fig. 3.9D-E**). Since IMP-1 knockdown did not inhibit cell proliferation and full-length IMP-1 was undetectable in these cells, (**Fig. 4**), we used BG-1 and

T47DKBluc cells as control IMP-1 negative cell lines. We hypothesized that if BTYNB was disrupting IMP-1 activity in the cells, treatment of the IMP-1 containing cells with BTYNB should result in a decrease in cell proliferation that was similar to what we observe with RNAi knockdown of IMP-1. In dose response studies, BTYNB elicited a robust dose-dependent inhibition of cell proliferation in IMP-1 positive cells (**Fig. 3.10A-C**), with IC₅₀s of 2.3 μ M, 3.6 μ M, and 4.5 μ M in ES-2, IGROV-1, and SK-MEL2 cells, respectively. Consistent with BTYNB acting by inhibiting binding of IMP-1 to target mRNAs, the dose-response curve for inhibition of cell proliferation (**Fig. 3.10A-C**) is similar to the dose-response curve for *in vitro* inhibition of binding of IMP-1 to fMyc (**Fig.3.2B**). At 10 μ M BTYNB, compared to the vehicle-treated controls, proliferation of IGROV-1, ES-2 and SK-MEL2 cells was reduced by 8.4, 4.8 and 9.6 fold, respectively. These data show that, at the reasonable dose of 10 μ M, BTYNB is as effective as RNAi knockdown in inhibiting proliferation of IMP-1 containing cancer cells.

To test BTYNB for general cell toxicity, IMP-1 negative cells were tested in dose response studies and there was no dose-dependent effect on cell proliferation at all concentrations tested, including 50 μ M (**Fig. 3.10D-E**).

BTYNB is a Structure-specific Inhibitor of IMP-1 Positive Cancer Cell Proliferation

Having established that BTYNB only works in IMP-1 positive cells, we next tested whether the structure specificity seen in the *in vitro* binding assay using purified IMP-1 and fMyc (**Fig. 3.2**) was also observed in intact cells. We therefore evaluated the effect of the close structural relative of BTYNB, Compound 5226752, (structures in **Fig. 3.2**) on proliferation of the same 5 lines of IMP-1 positive and IMP-1 negative cells tested in Fig. 10 with BTYNB. Consistent with our *in*

vitro finding that Compound 5226752 did not inhibit binding of IMP-1 to flMyc (**Fig. 3. 2B**), at all concentrations tested, Compound 5226752 did not inhibit proliferation of IMP-1 positive and IMP-1 negative cells (**Fig. 3.11**).

As a further test for off-target effects of BTYNB, we assessed whether BTYNB could inhibit estrogen mediated gene expression. We used IMP-1 negative T47DKBluc cells. T47DKBluc cells contain estrogen receptor α (ER α) and respond to addition of the estrogen, 17 β -estradiol (E₂) by activating expression of a stably transfected estrogen response element (ERE) luciferase reporter gene (78). Consistent with the absence of its IMP-1 target, BTYNB had no effect on expression of the ERE-luciferase gene (**Fig. 3.11**). Compound 522672 does not inhibit cell proliferation and BTYNB has no effect on cell proliferation or gene expression in IMP-1 negative cells (**Fig. 3.10D-F, Fig. 3.11**). Taken together these data indicate that BTYNB is a structure selective small molecule biomodulator with strong selectivity for IMP-1.

Overexpression of IMP-1 in HEK 293T Cells Reverses BTYNB Inhibition of Cell Proliferation

The lack of effect of IMP-1 knockdown or BTYNB in IMP-1 negative cells and the similar dose-response curves for BTYNB inhibition of IMP-1 binding to flMyc and for inhibition of cell proliferation support BTYNB action through IMP-1. We postulated that if BTYNB inhibits cell proliferation by reducing binding of IMP-1 to pro-proliferation mRNA targets, then overexpression of IMP-1 might reverse the effect of BTYNB on cell proliferation. We used HEK 293T cells because transfection of HEK 293T cells is unusually efficient, allowing assays of the effect of transient transfection on the entire cell population. As shown in **Figure 3.12A**, compared to control 293T cells, IMP-1 levels increased in 293T cells transfected with 100 ng of

CMV-IMP-1. Consistent with its effect in other IMP-1 positive cell lines, when HEK 293T cells were treated with 10 μ M BTYNB alone, or treated with BTYNB and transfected with a control plasmid, there was a significant decrease in cell proliferation compared to the cells treated with the vehicle control (**Fig. 3.12B, C**). Transfection with an IMP-1 expression plasmid abolished BTYNB inhibition of cell proliferation (**Fig. 3.12D**). These results support the view that BTYNB acts through IMP-1.

BTYNB Blocks Anchorage-independent Growth of IMP-1 Positive Cancer Cells

Anchorage-independent growth is a hallmark of cancer cells. Growth in soft agar is often used to evaluate anchorage independence of human ovarian and melanoma cancer cells. Because IGROV-1 cell did not form colonies efficiently under our conditions, we tested the ability of BTYNB to inhibit colony formation of SK-MEL2 and ES-2 cells grown in soft agar. As shown in **Figure 3.13**, SK-MEL2 and ES-2 cells supplemented with medium containing DMSO vehicle formed large colonies (>0.5 mm) after 21 or 14 days, respectively (**Fig 3.13A, 3.13C**). The growth of these cells into colonies was completely inhibited by 10 μ M BTYNB (**Fig 3.13B, 3.13D**). When colonies from all the wells of each treatment condition were counted, the DMSO-treated control SK-MEL2 and ES-2 wells contained 83 and 102 colonies/well >0.5 mm in diameter, respectively (**Fig. 3.13E, 3.13F**). Notably, there were no colonies >0.5 mm in diameter in the BTYNB-treated wells (**Fig 3.13 E, 3.13 F**) and on average 8 and 13 small colonies/well less than 0.5 mm in diameter for SK-MEL2 and ES-2 cells, respectively. Thus, BTYNB potently inhibits anchorage-independent growth of ovarian and melanoma cancer cells.

DISCUSSION

Our development of the first selective small molecule IMP-1 biomodulator is significant on several levels. Despite their ubiquitous roles in diverse cell processes, small molecule biomodulators of mammalian mRNA binding proteins have rarely been described. Thus, BTYNB serves as a prototype for this class of molecule. IMP-1's role in cancer, and the cancer related proteins and microRNAs (miRNAs) that control IMP-1 expression, make targeting IMP-1 especially attractive. IMP-1 is induced by the oncogene c-Myc and IMP-1 increases the level of c-Myc mRNA and protein by stabilizing c-Myc mRNA (16, 39, 80). This sets up a tumor promoting feed forward regulatory loop in which c-Myc induces IMP-1 and IMP-1 increases c-Myc protein levels, enabling c-Myc to further induce IMP-1. Breaking this oncogenic feed-forward regulatory loop ($\text{c-Myc} \rightarrow \text{IMP-1} \uparrow \rightarrow \text{c-Myc} \uparrow$) using c-Myc inhibitors is challenging. Despite considerable effort, its important role in mediating cell proliferation in both normal and cancerous cells (85, 86), has made c-Myc difficult to target. Targeting IMP-1 with small molecule inhibitors presents an alternative method for targeting c-Myc and breaking the $\text{c-Myc} \rightarrow \text{IMP-1} \uparrow \rightarrow \text{c-Myc} \uparrow$ feed forward regulatory loop.

Reduced expression of *let-7* family miRNAs is one of the most common regulatory alterations in human cancer (49). IMP-1 is a major regulatory target of let-7 miRNA and disruption of let-7 increases IMP-1 levels (47, 48). Since let-7 miRNAs are suppressors, targeting downregulation of *let-7* miRNAs in human cancer is challenging. Small molecule inhibitors that target IMP-1 are an attractive alternative because IMP-1 is strongly upregulated by loss of let-7 miRNAs and transmits and expands the loss of let-7 signal by binding to and stabilizing mRNAs encoding c-Myc and other cancer-related mRNAs.

The potential of BTYNB as a molecular probe for investigation of complex regulatory interactions is illustrated by the interplay between c-Myc, IMP-1 and let-7 miRNAs. Let-7 can reduce c-Myc mRNA levels by directly binding to the c-Myc mRNA 3'-UTR, or indirectly by reducing the level of IMP-1 leading to destabilization of c-Myc mRNA. BTYNB, by targeting part of this regulatory network by destabilizing c-Myc mRNA through inhibition of IMP-1, is an important new tool for investigation of this and other regulatory networks in cancer.

When we initiated our efforts to identify a small molecule inhibitor of IMP-1, we envisioned targeting cancer through a synthetic lethality screen. IMP-1/IGF2BP1/ CRD-BP was thought to be an oncofetal protein, expressed in embryonic cells, nearly absent in adult cells and re-expressed in many cancers. In an important very recent report, an N-terminal deletion of CRD-BP/IGF2BP1/IMP-1 was identified in adult tissues (68). Although the protein is missing 2 RNA binding domains, it appears to be functional (68). While the significance of the variant form of IMP-1/IGF2BP1/ CRD-BP and its relation to the full-length form remain to be elucidated in detail, these data indicate that extremely low levels of IMP-1 are present in normal cells. The variant protein is present at extremely low levels in normal cells and there is a 100-1,000 fold increase in IMP-1 levels in cancer cells relative to most normal adult cells. Development of BTYNB remains a successful application of a synthetic lethality screen to cancer cells.

RNAi knockdown of IMP-1 showed that IMP-1 plays an important role in cell proliferation and that loss of IMP-1 reduces levels of c-Myc mRNA (15, 19, 21). Moreover, the proliferation phenotype of cancer cells in which IMP-1 or c-Myc have been knocked down is similar, suggesting that c-Myc is an important IMP-1 target (50). Based in part on data from an endonuclease protection assay, a high affinity binding site for recombinant IMP-1 was identified

in the coding region instability determinant of c-Myc RNA (16). For our high throughput screen we used recombinant DNA technology and enzymatic coupling to synthesize a 93 nucleotide fluorescein-labeled RNA probe containing the c-Myc mRNA coding region instability determinant that binds IMP-1 and purified untagged IMP-1 (71, 87). BTYNB was clearly the most potent and selective compound to emerge from our screen of ~150,000 compounds.

mRNAs that interact with IMP-1 lack a strong conserved IMP-1 binding site. It was therefore unclear whether a small molecule identified as an inhibitor of binding of IMP-1 to its c-Myc mRNA binding site would only reduce the level of intracellular c-Myc mRNA, or would be active on a wide range of IMP-1 targets. Because the sites at which IMP-1 binds to most of its known mRNA targets have not been characterized in detail, we could not evaluate BTYNB specificity using *in vitro* assays and small mRNA fragments from known IMP-1 targets. We therefore investigated the ability of BTYNB to down-regulate diverse mRNA targets in cancer cells. BTYNB was effective against a range of mRNA targets. Interestingly, despite the presence of a several fold higher level of IMP-1 in the IGROV-1 cells compared to the SK-MEL2 cells, BTYNB elicited a similar reduction in the levels of CDC34, CALM1 and Col5A mRNAs in the two cell lines (**Fig. 6**). However, β TRCP1 mRNA levels were reduced much more dramatically in the SK-MEL2 cells than in the IGROV-1 cells. IMP-1 appears to stabilize target mRNAs largely by steric hindrance and interference with binding of nucleases and miRNAs (18, 20). Although the precise mechanism by which CDC34, CALM1, Col5A and eEF2 mRNAs are stabilized by IMP-1 is unknown, Spiegelman and coworkers have convincingly shown that IMP-1 stabilizes β TRCP1 mRNA by interfering with binding of miR-183 to sites in the 3'-UTR. Whether the increased effectiveness of BTYNB in downregulating β TRCP1 in SK-MEL2 cells

reflects the lower level of IMP-1 in these cells, or is related to the miR-183 degradation system is unclear.

The effectiveness of BTYNB in diverse IMP-1 positive cancer cell lines is likely related to its ability to down-regulate a broad range of cancer-related IMP-1 targets including, c-Myc, CDC34, β TRCP1, CALM1, Col5A and eEF2 mRNAs. This enables BTYNB to inhibit anchorage dependent and anchorage independent cancer cell proliferation and global protein synthesis. Whether the ability of BTYNB to inhibit total protein synthesis is exclusively related to down-regulation of the rate limiting elongation factor, eEF2, or is due to some combination of BTYNB inhibition of cell proliferation resulting in a reduced requirement for new protein synthesis and eEF2 down-regulation is unclear.

Our data supports the view that the intracellular actions of BTYNB are based on its ability to inhibit IMP-1. BTYNB exhibits similar dose response curves for inhibition of binding of IMP-1 to flMyc *in vitro* and for inhibition of cell proliferation. BTYNB inhibits proliferation of IMP-1 positive cells in which IMP-1 knockdown similarly inhibits cell proliferation and has no effect in IMP-1 negative cells in which IMP-1 siRNA has no effect. Overexpression of IMP-1 abolishes BTYNB inhibition of cell proliferation. We also found that the BTNYB derivative, Compound 5226752, did not inhibit binding of IMP-1 to flMyc *in vitro* and did not downregulate IMP-1 mRNA targets c-Myc, Col5A, eEF2, CALM1, and β TRCP1 in IMP-1 positive cells. Similarly, BTYNB did not down-regulate c-Myc, Col5A, eEF2, CALM1, and β TRCP1 mRNAs in IMP-1 negative BG-1 cells (data not shown).

Here we describe a broadly applicable HTS system for identifying small molecules that inhibit interaction of RNA-binding proteins with their RNA recognition sequences, demonstrate

that a small molecule identified using this simple *in vitro* assay with isolated components destabilizes c-Myc mRNA in cells, leading to decreases in steady state c-Myc mRNA and protein levels. Moreover, the small molecule identified using this system is broadly effective against diverse targets of the mRNA binding protein. BTYNB's selectivity and low toxicity, effectiveness against diverse cancer-related IMP-1 mRNA targets, and ability to abolish anchorage independent growth of IMP-1 containing cancer cells make it a strong candidate for further therapeutic testing and development.

FIGURES

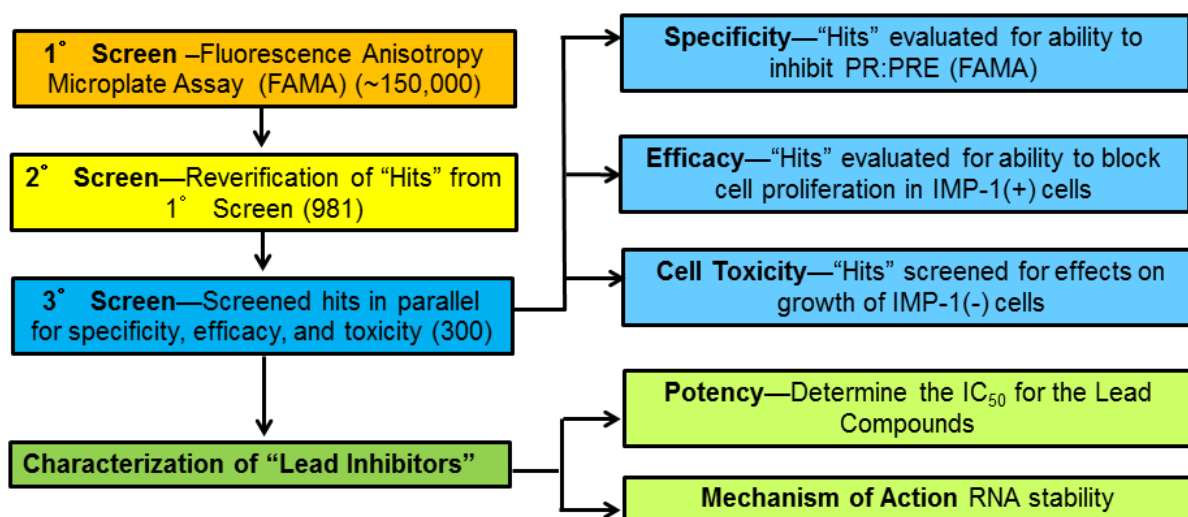


Figure 3.1. Scheme for identification and characterization of small molecule inhibitors of IMP-1. Our strategy for identification of small molecule IMP-1 inhibitors included the following assays. *In vitro* FAMA assays using purified IMP-1 and progesterone receptor (PR) and fluorescein-labeled c-Myc RNA and progesterone response element (PRE) to carry out the high throughput screen, verify the hits, and to further characterize the verified hits for potency, efficacy, and specificity. Cell growth assays for evaluating the ability of the lead small molecule candidates to inhibit proliferation of IMP-1 positive cells and testing for specificity and off-target toxicity in IMP-1-negative cancer cells. Dose-response studies of lead inhibitors to determine potency for inhibiting cell proliferation and early studies of mechanism of action.

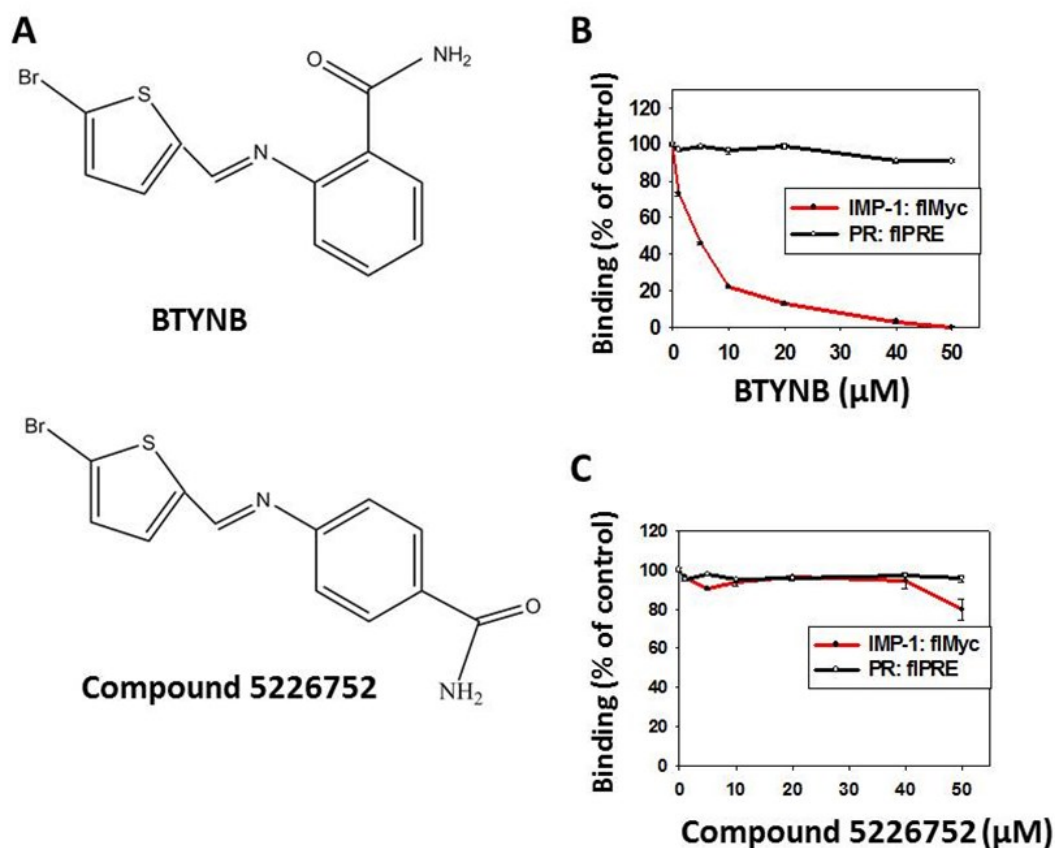


Figure 3.2. Dose-response studies show BTYNB is a sequence and structure selective inhibitor of IMP-1 binding to flMyc. (A) Shown are structures of 2-[(5-bromo-2-thienyl)methylene] amino}benzamide (BTYNB) and Compound 5226752, a close structural relative of BTYNB. Dose-response studies of the effect of BTYNB (B) and Compound 5226752 (C) on binding of IMP-1 to flMyc and flPRE. 1 nM flMyc and 10 nM IMP-1 or 1 nM flPRE and 30 nM PR-b and the indicated concentration of BTYNB (B) or Compound 5226752 (C), were incubated and mA measured. No inhibitor control was set to 100%. (n=5, average \pm S.E.M. Some error bars are smaller than the symbols).

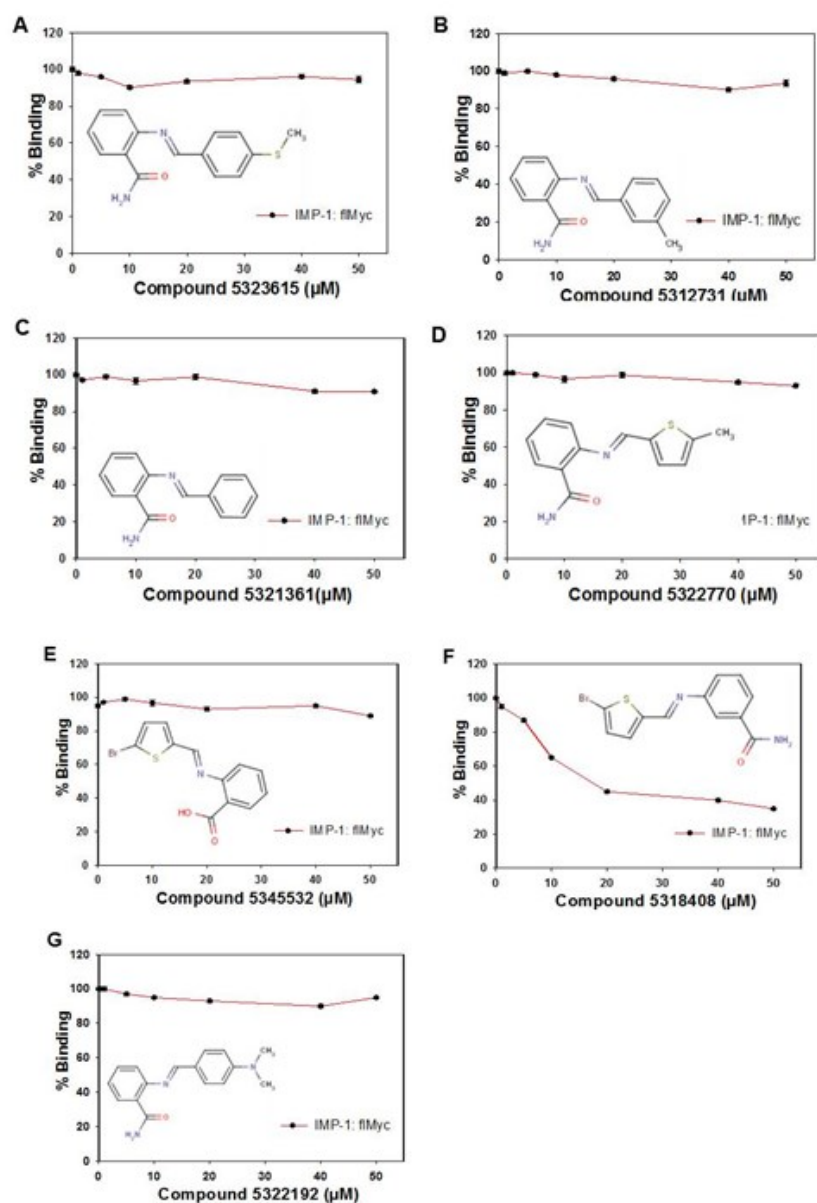


Figure 3.3. Structural relatives of BTYNB have little or no ability to inhibit binding of IMP-1 to flMyc. (A-G) Shown are structures of structural derivatives of BTYNB and dose response studies evaluating the ability of the compounds to inhibit binding of IMP-1 to flMyc. 1 nM flMyc and 10 nM IMP-1 and the indicated concentration of compound were incubated and mA measured. No inhibitor control was set to 100%. (n=5, average \pm S.E.M).

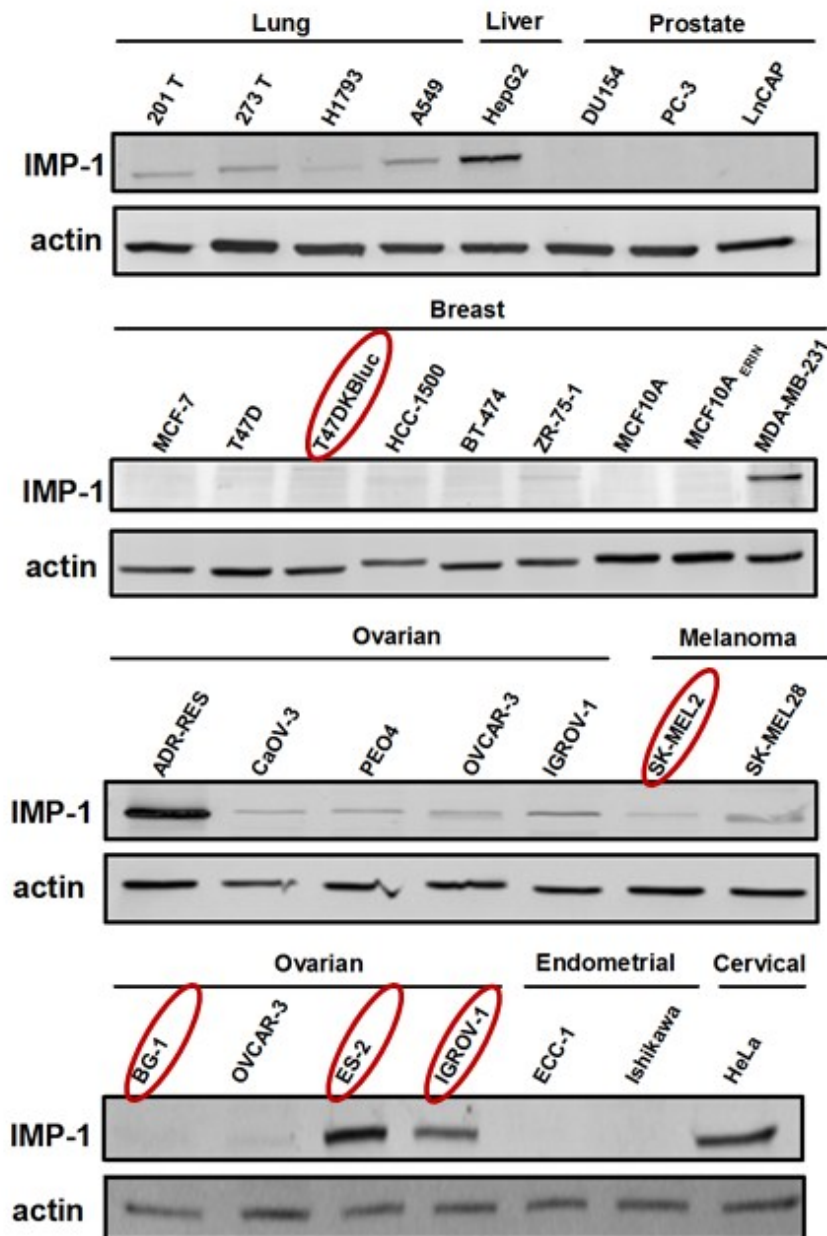


Figure 3.4. IMP-1/IGF2BP1/CRD-BP protein expression in 31 cancer cell lines. For Western blots, 20 μ g of protein lysate was loaded in each well and probed with IMP-1 antibody as described in “Materials and Methods”. Actin was used as a loading control.

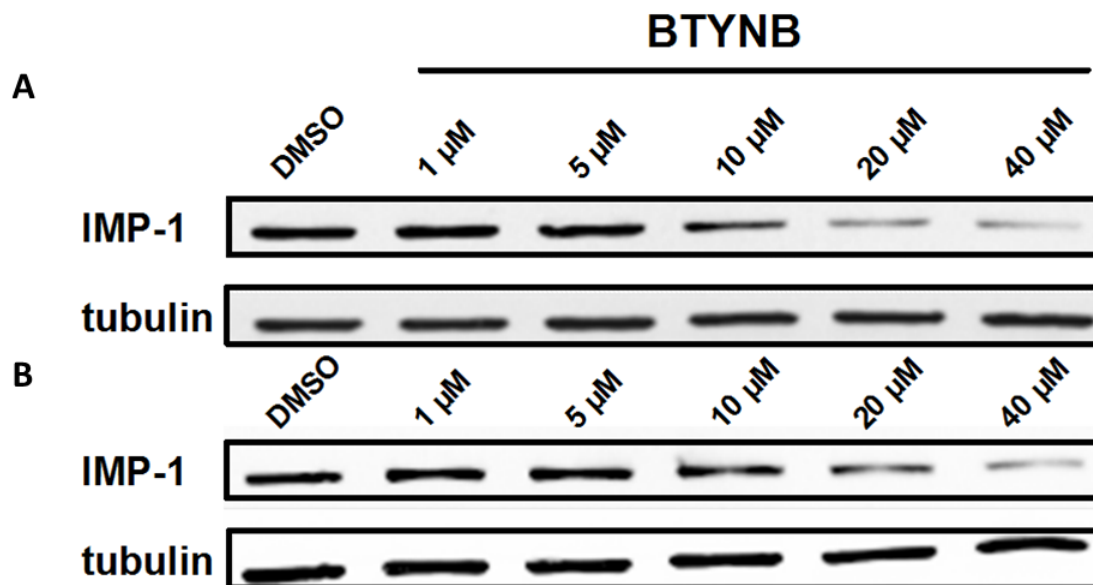


Figure 3.5. BTYNB decreases IMP-1 levels. IMP-1 positive cell lines, (A) IGROV-1 and (B) SK-MEL2 cells were maintained as described in “Materials and Methods” and were treated with the indicated concentration of BTYNB for 72 hours, harvested, and analyzed by Western blot using 20 μ g of protein/lane with tubulin as the internal standard.

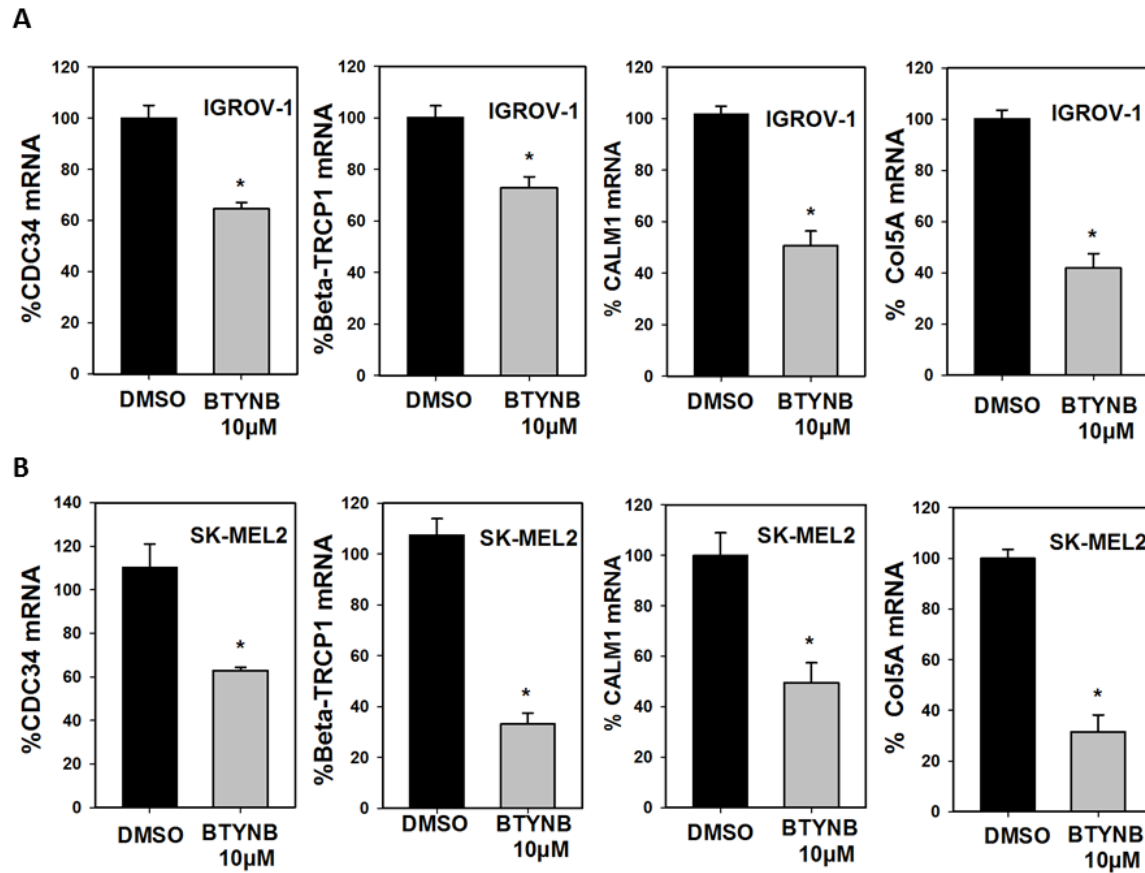


Figure 3.6. BTYNB decreases expression of IMP-1 mRNA targets. IMP-1 positive (A) IGROV-1 and (B) SK-MEL2 cells were maintained as described under “Materials and Methods” and were treated with either DMSO vehicle control or 10 µM of BTYNB for 72 hours, harvested, and mRNA levels quantitated by qRT-PCR. 36B4 was used as the internal standard. Data represents the mean \pm S.E.M. for three separate experiments. *P<0.05.

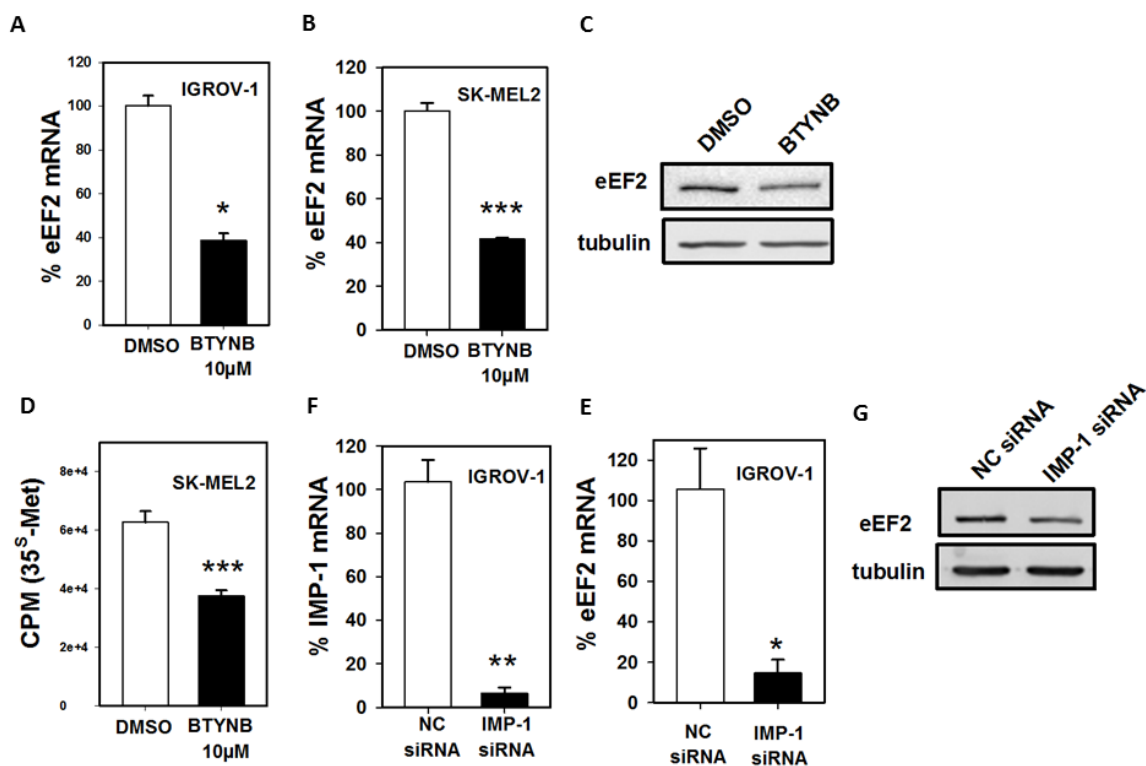


Figure 3.7. Knockdown of IMP-1 and treatment with BTYNB decrease expression of eEF2. Treatment with 10 μ M BTYNB for 72 hours leads to a decrease in eEF2 mRNA in IGROV-1 (A) and SK-MEL2 (B) cells. Treatment with 10 μ M BTYNB for 72 hours lead to a decrease in eEF2 protein in IGROV-1 cells (C). Treatment with 10 μ M BTYNB for 24 hours results in a decrease in protein synthesis in SK-MEL2 cells compared to cells treated with DMSO vehicle control (D). Knockdown of IMP-1 in IGROV-1 cells leads to a decrease in IMP-1 (E) and (F) eEF2 mRNAs compared to cells treated with a non-coding (NC) control siRNA for 72 hours. (G) RNAi knockdown of IMP-1 for 72 hours in IGROV-1 cells leads to a decrease in eEF2 protein. qRTPCR data represents the mean \pm S.E.M. for three separate experiments. The protein synthesis experiments shows the mean \pm S.E.M. (n=4) *P<0.05, **P<0.01, ***P<0.001.

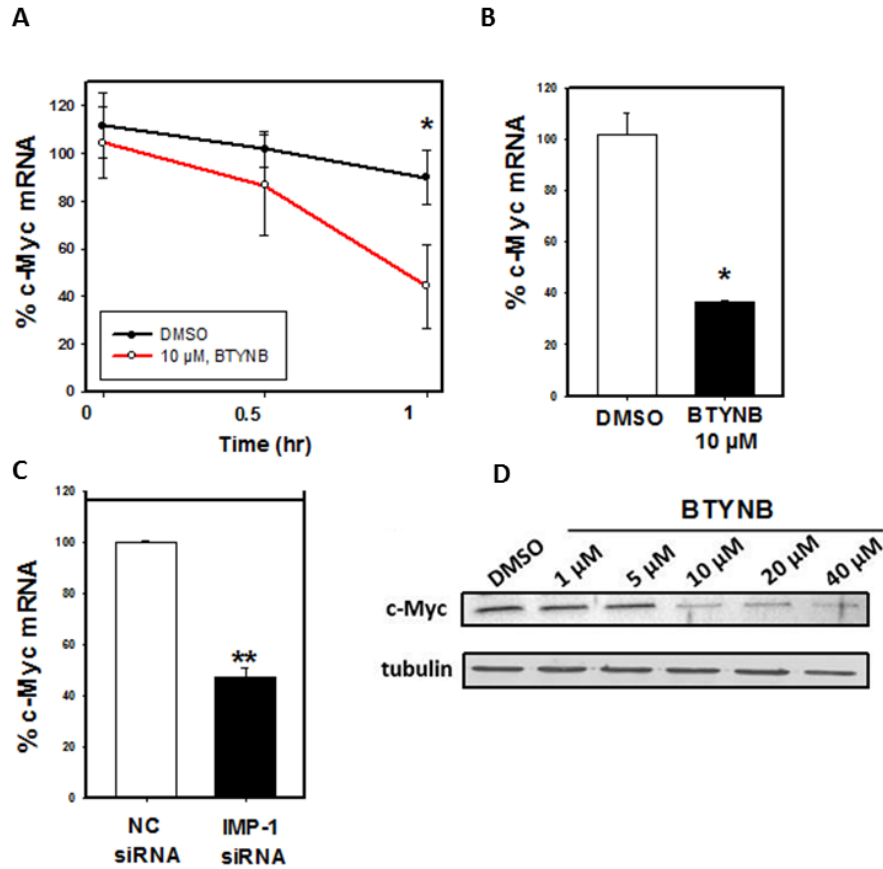


Figure 3.8. BTYNB decreases the stability of c-Myc mRNA, reducing expression of c-Myc mRNA and protein. (A) Decay of c-Myc mRNA was monitored in SK-MEL2 cells pre-treated with either DMSO or 10 μ M BTYNB and then treated with Actinomycin-D for the indicated times. c-Myc mRNA levels were determined by qRT-PCR using 36B4 as internal standard. The difference between 10 μ M BTYNB and the control (DMSO) was not significant ($p > 0.05$) at 30 minutes, while the difference between 10 μ M BTYNB and the control (DMSO) at 1 hour was significant ($p < 0.05$). (B) SK-MEL2 cells were incubated with either DMSO or with 10 μ M BTYNB for 72 hours and c-Myc mRNA was quantitated using qRT-PCR (C) c-Myc mRNA levels are reduced in SK-MEL2 cells treated for 72 hours with IMP-1 siRNA compared to Non-coding (NC) control. (D) Western blots showing a dose-response study of the effect of BTYNB on levels of c-Myc protein. Tubulin was used as a loading control. (A-C) ($n=3$, avg \pm S.E.M.).

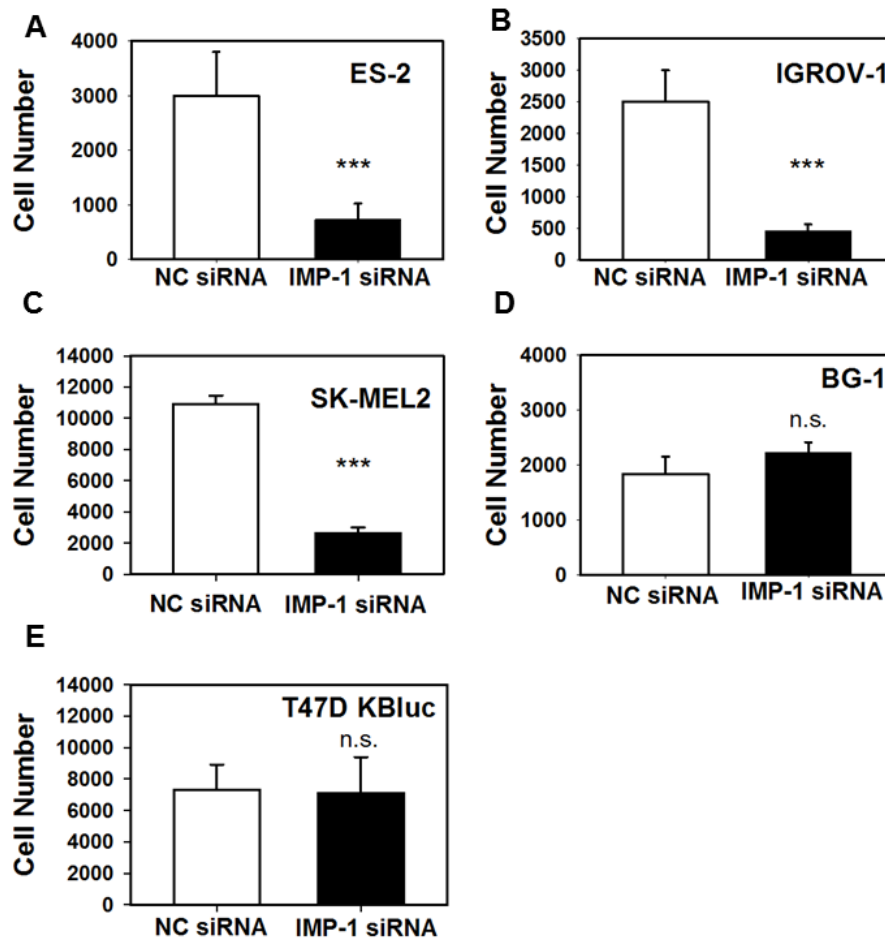


Figure 3.9. IMP-1 knockdown blocks proliferation of IMP-1 positive cells with no effect in IMP-1 negative cells. 1,000 ES-2 (A), IGROV-1 (B), SK-MEL2 (C), BG-1 (D) or T47DKBluc (E) cells were initially plated. Cells were then transfected with either noncoding (NC) control or IMP-1 siRNA and cell number was determined by MTS assay 5 days later. In all experiments, cell numbers were calculated from standard curves of cell number versus absorbance for each cell line and results are reported as the mean \pm S.E.M. (n=5) n.s.=not significant, * P <0.05, ** P <0.01, *** P <0.001.

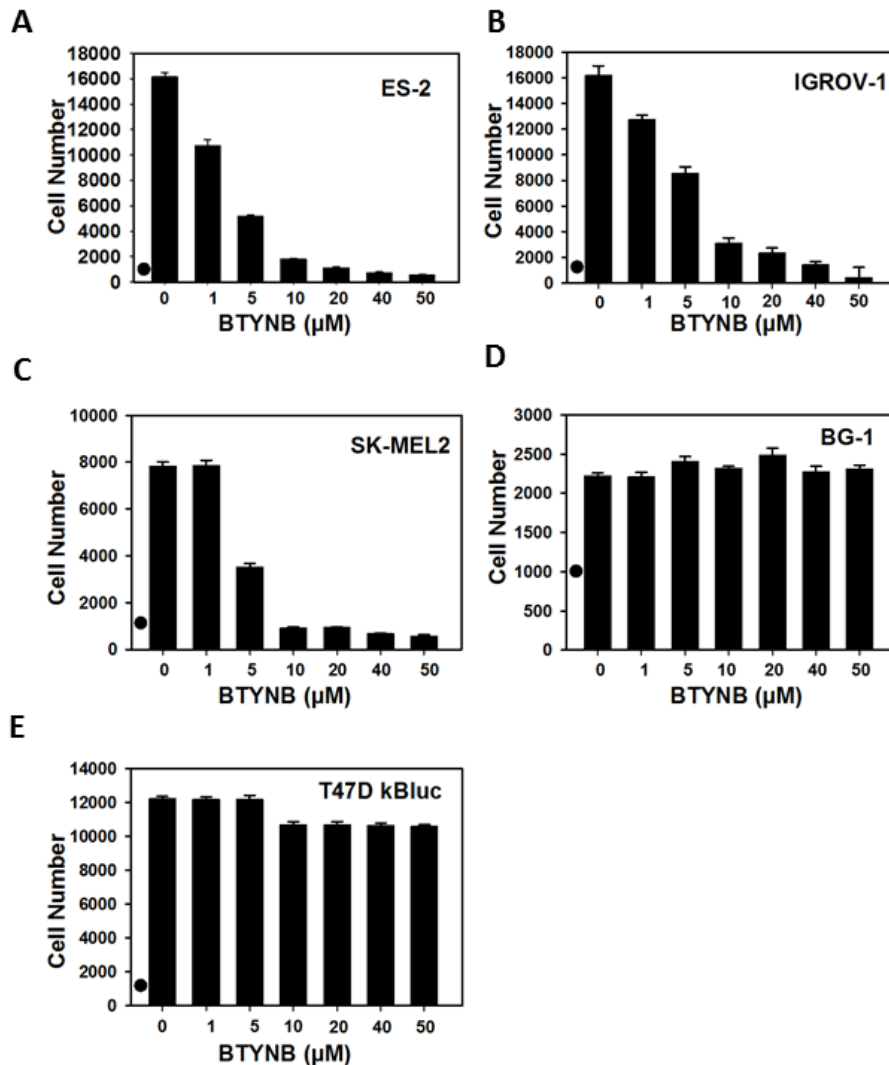


Figure 3.10. BTYNB is a dose-dependent inhibitor of IMP-1 positive cancer cell proliferation. 1,000 IMP-1 positive ES-2 (A), IGROV-1 (B), SK-MEL2 (C), or 1,000 IMP-1 negative BG-1 (D) or T47DKBluc (E) cells were plated and treated with the indicated concentration of BTYNB. The dot represents the cell number (1,000 cells) at day 0. Cell number was assayed using MTS 3 days later ($n=6$, $\text{avg} \pm \text{S.E.M.}$). IC_{50} values were obtained by curve-fitting using SigmaPlot.

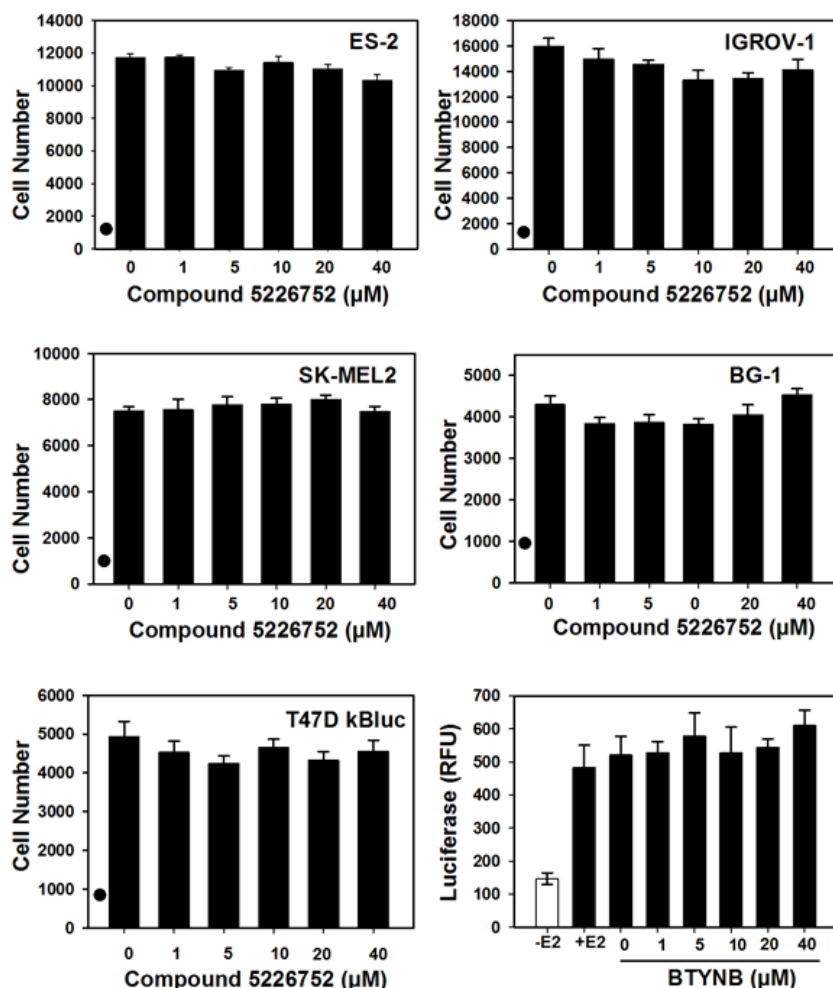


Figure 3.11. Compound 5226752, a structural relative of BTYNB, does not inhibit proliferation of IMP-1 positive or IMP-1 negative cells. 1,000 ES-2 (A), IGROV-1 (B), SK-MEL2 (C), BG-1 (D) or T47DKBluc (E) cells were initially plated and treated with the indicated concentrations of compound 5226752. Cell number was assayed using MTS 3 days later ($n=6$, $\text{avg} \pm \text{S.E.M.}$). (F) BTYNB does not inhibit E_2 - $\text{ER}\alpha$ mediated gene expression. To deplete endogenous estrogens, T47DKBluc cells that are stably transfected with an ERE luciferase reporter, were maintained in medium containing 10% charcoal-dextran (CD) treated FBS for 4 days. Cells were then maintained for 24 hours in medium without estrogen (white bar) or treated with estrogen (E_2) and the indicated concentration of BTYNB (black bars). Cells were lysed and assayed for luciferase activity as we described (88). Results are reported as the mean \pm S.E.M. ($n=6$).

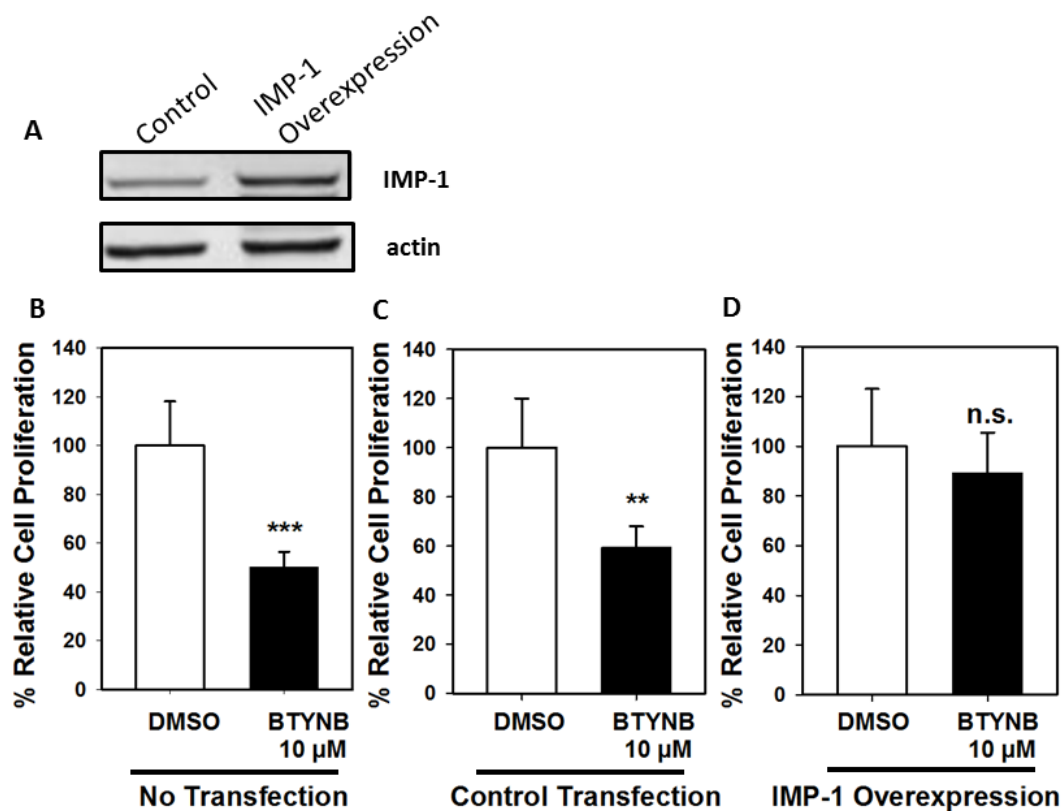


Figure 3.12. Overexpression of IMP-1 reverses BTYNB inhibition of cell proliferation. HEK 293T cells were transiently transfected without IMP-1 expression plasmid (Control) or with 100 ng of CMV-IMP-1 expression plasmid (IMP-1 overexpression). Western blot analysis demonstrates increased IMP-1 protein in the cells transfected with CMV-IMP-1 (A). 1,000 HEK 293T cells were initially plated and either not transfected (B), transfected with a control plasmid (C), or transfected with the CMV-IMP-1 (IMP-1 overexpression) (D). Cells were then treated with DMSO or 10 μ M of BTYNB for 48 hours and assayed using MTS. The difference between 10 μ M BTYNB and the control (DMSO) was significant in HEK 293T that were either not transfected or transfected with a control plasmid. Cells that were transfected with an IMP-1 overexpression plasmid and treated with 10 μ M BTYNB and the control (DMSO) did not exhibit significant BTYNB inhibition of cell proliferation. Results are reported as the mean \pm S.E.M. (n=3) n.s.=not significant, * P <0.05, ** P <0.01, *** P <0.001.

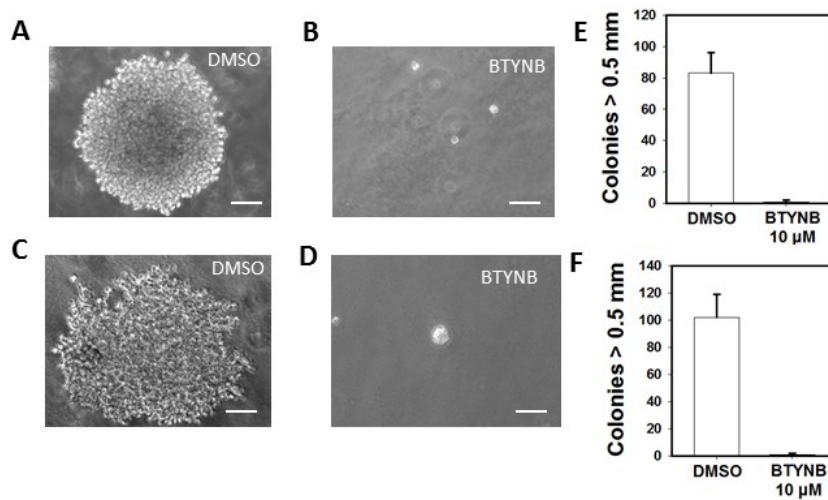


Figure 3.13. BTYNB inhibits anchorage-independent growth of IMP-1 positive cells in soft agar. 10,000 SK-MEL2 were plated into top agar containing DMSO (vehicle) (A) or 10 μ M BTYNB (B). 8,000 ES-2 cells were plated into top agar containing DMSO (vehicle) (C) or 10 μ M BTYNB (D). After 21 or 14 days for SK-MEL2 or ES-2 cells, respectively, colonies were counted and photographed at 10X magnification. The white scale bar in the photographs represents 10 μ m. The bar graphs represent the average of the total number of colonies counted in each well of the treatments for SK-MEL2 (E) or ES-2 (F) cells. The photographs are representative of the entire plate and of triplicate experiments.

CHAPTER 4

IMP-1 Regulates Protein Kinase C alpha mRNA and protein Levels

ABSTRACT

PKC α (protein kinase C alpha, PRKCA) is an important protein involved in multiple signaling pathways in cancer, and Insulin Like Growth Factor 2 mRNA Binding Protein 1 (IGF2BP1/IMP-1) has also been shown to participate in carcinogenesis. However, whether there is an interplay between PKC α and IMP-1 was unclear.. In this report we aimed to identify whether PKC α is a novel molecular target of IMP-1 and to study the likely biological impact of such an interaction. Using bioinformatics analysis, we predicted PKC α mRNA levels were regulated by IMP-1 knockdown. We experimentally validated IMP-1 as a direct regulator of PKC α mRNA levels. We also demonstrated that the targeting of PKC α by IMP-1 knockdown played a critical role in regulating downstream ERK signaling in cancer cells. Consistent with IMP-1 stabilizing PKC α mRNA resulting in increased levels of PKC α mRNA and protein, transient overexpression of IMP-1 increase the level of PKC α protein. In summary, this study identifies IMP-1 as a novel protein that regulates PKC α and illustrates that the downregulation of PKC α by IMP-1 knockdown modulates ERK signaling, an important biological processes in cancer cells.

INTRODUCTION

Protein kinase C alpha (PKC α) is a serine/threonine kinase that plays a key role in several signal transduction pathways, including those involved in apoptosis, cell proliferation and

migration (89-92). The PKC family contains related isoforms with different cofactor requirements, tissue and subcellular distribution, and substrate specificity (93). Based on their structural and functional characteristics, this protein family can be further classified into three subfamilies: conventional or classic PKC isozymes (cPKCs; α , β I, β II, and γ), novel or non-classic PKC isozymes (nPKCs; δ , ϵ , η , and θ), and atypical PKC isozymes (aPKCs; ζ , ι , and λ). PKC α is known to play a role in cellular proliferation, apoptosis and the migration in many types of cancer including melanoma, breast, ovarian, and lung cancer (92, 94-96), making this protein an important therapeutic target in cancer (97).

microRNAs (miRNAs) are small ~22-nucleotide non-coding RNAs that are an important class of gene regulators that are present in both plant and animal genomes (98, 99). Mature miRNAs incorporated into the RNA-induced silencing complex (RISC) regulate target mRNAs via complementary base pairing in the 3'UTR, 5'UTR, and protein coding regions (20). Binding of a miRNA-containing RISC to its target induces translational repression and/or mRNA degradation, thereby regulating target protein expression. Evidence demonstrates miRNAs are critically involved in cancer biology, playing both tumor suppressor and oncogenic roles (100-102). Although it is estimated that approximately 60% of all human mRNAs are subject to miRNA-dependent regulation (103, 104) and numerous studies demonstrate the importance of miRNA-dependent regulation in vitro and in vivo (98), the function of each individual miRNA remains to be elucidated, particularly as it pertains to the development and progression of human cancers.

Insulin-like growth factor II mRNA binding protein (IGF2BP1/IMP1), also known as zipcode-binding protein 1 (ZBP1), is a member of the VICKZ (Vg1RBP/Vera, IMP-1,2,3, CRD-BP, KOC and ZBP-1) family of RNA binding proteins (5). IMP1 and its orthologs modulate

cellular functions by mediating many aspects of RNA regulation, including intracellular RNA localization, stability, and translational control (10, 34, 39). As a largely oncofetal protein, IMP-1 binds to and stabilizes transcripts that are important in oncogenesis (18, 19, 60). Although IMP-1 has been reported to regulate the RNA stability of c-Myc (34), MDR1 (18), and β TRCP-1(19, 20), and other oncogenes, we were interested in identifying whether or not there are novel molecular targets of IMP-1. IMP-1 was also previously found to attenuate miRNA-dependent degradation of several mRNAs (20,44), including miR-340 mediated degradation of microphthalmia-associated transcription factor (MITF), a master regulator of melanocyte development and melanogenesis. Using miRWalk (105), miR-340 was the top miRNA predicted to bind to the 3'UTR of PKC α . These miR-340 binding sites also contained IMP-1 binding motifs (UUUAY) (44,66), suggesting a role for both IMP-1 and mir-340 in regulating PKC α levels. We also postulated that IMP1 regulates the post-translational fate of a variety of mRNA targets in IMP-1 positive cancer cell lines. Through inhibition of IMP1 expression, abnormal regulation of the associated mRNAs could result in changes in cell behavior and/or phenotype. In the present study, we used bioinformatic analysis of publically available microarrays and identified a panel of genes that were potentially regulated by IMP-1. We then performed RNAi knockdown of IMP-1 positive cells to test whether or not there was a decrease in levels of the mRNAs encoded by the panel of genes. From these studies, PKC α emerged as a novel molecular target of IMP-1. IMP-1 knockdown not only decreased the level of PKC α mRNA and protein, but also led to a decrease in protein levels of the downstream signaling molecules, ERK and p-ERK. Interestingly, when IMP-1 was overexpressed in HEK 293T cells, PKC α levels also increased, further supporting the idea that IMP-1 regulates PKC α mRNA. Finally, we used a miRNA inhibitor of miR-340 and observed an increase in PKC α protein levels, suggesting a role

for miR-340 in regulating PKC α . This work for the first time establishes the role of the oncofetal protein IMP-1 in regulating levels of PKC α , an important target in cancer.

MATERIALS AND METHODS

Cell Culture

Unless otherwise indicated, cells were maintained at 37 °C in 5% CO₂ in growth medium containing 1% penicillin and streptomycin and fetal bovine serum (FBS) (Atlanta Biological, Atlanta, GA). IMP-1 positive IGROV-1, SK-MEL2, and HEK 293T cells were used in cell-based experiments. Cells were maintained in the following culture media. IGROV-1, SK-MEL-2: RPMI-1640, supplemented with 10% FBS; HEK 293T: DMEM-F12 supplemented with 10% FBS.

Plasmids and Oligonucleotides

The IMP-1 mammalian expression plasmid was created as follows: The IMP-1 coding region was amplified by PCR with a pair of primers, 5'-CAGCTGGTACCATGAACAAGC TTT ACA TCG GCA AC and 5'-GTATTCTAGACCTCACTTCCTTCGTGCCTGGGCCTG. The PCR product was digested with Kpn I and Xba I, and then cloned into pCMV-hER α (106) to generate pCMV-IMP-1. The empty plasmid pTZ18U served as a negative control. Plasmids were transfected into HEK 293T cells using Lipofectamine 2000 (Invitrogen) according to the manufacturer's instructions. Locked nucleic acid (LNA) anti-sense oligonucleotides for miR-340 and a miR-control were purchased from Exiqon, Inc.

Transient Transfections

For siRNA transient transfection, IGROV-1 and SK-MEL2 cells plated at 300,000 cells/well in 6-well plates in RPMI-1640 containing 10% FBS. Medium was replaced the next day with fresh medium containing either a non-coding siRNA smartpool (Dharmacon) or IMP-1 specific siRNA smartpool. Lipofectamine 2000 or Dharmafect 1 transfection reagent was used for transient transfections. HEK 293T cells were maintained in DMEM/F12 containing 10% FBS and antibiotics. One day before transfection, 0.15 million cells were seeded into each well of a 24-well plate. 1 µg total DNA (carrier PTZ18U plasmid DNA was used to reach 1 µg) was transfected into each well of a 24-well plate. Transfection using Lipofectamine 2000 was as described by the supplier (Invitrogen). Transfections used a ratio of DNA to Lipofectamine 2000 of 1:3 with the cells in 0.5 ml Opti-MEM. 7-8 hours after transfection, the transfection medium was replaced with standard growth medium (DMEM/F12 plus 10% FBS and antibiotics). For transient transfections using the LNA miR inhibitors, IGROV-1 cells were seeded at a density of 100,000 cells/well in 12 well plates. The next day, after cells were allowed to adhere, LNA inhibitors were added to cells using Lipofectamine 2000 according to the manufacturer's instructions. The transfection complex was removed after 24 hours and replaced with complete medium. After another 72 hours, cells were harvested and protein was extracted and analyzed using Western blot.

Endogenous Gene Expression

IGROV-1 and SK-MEL2 cells were plated and transiently transfected as described above. After 72 hours, RNA was extracted, and purified using the Qiagen RNeasy kit. cDNA was

prepared from 1 µg of RNA with M-MuLV reverse transcriptase from New England Biolabs. Diluted cDNA was used to perform quantitative RT-PCR using SYBR Green (ABI Thermocycler). Primers for quantitative RT-PCR were: 36B4 forward primer (5'-GTGTTTCGACAATGGCAGCAT) and reverse (5'-GACACCCTCCAGGAAGCGA); IMP-1 forward primer (5'-TGAACACCGAGAGTGAGACG-3') and reverse primer (5'-CTCATCGGGGATGTAGGAGA-3'); PRKCA forward primer (5'-ATGTCACAGTACGAGATGCAAAA) and reverse (5'-GCTTTCATTCTTGGGATCAGGAA). The fold change in expression of each gene was calculated using the $\Delta\Delta C_t$ method with 36B4 as the internal control.

Whole Cell Extracts and Western Blots

Following treatment, cells were harvested, washed in ice-cold phosphate-buffered saline (PBS), and whole-cell extracts were prepared in lysis buffer containing 1X radioimmunoprecipitation assay (RIPA) buffer (Millipore), 1 mM EGTA, 30 mM NaF, 2.5 mM sodium pyrophosphate, 1 mM sodium orthovanadate, 1 mM β -glycerol phosphate, 1 mM phenylmethylsulfonyl fluoride, and 1 tablet of protease inhibitor cocktail (Roche, Indianapolis, IN). Cells were collected, and debris was pelleted by centrifugation at 15,000 g for 10 minutes at 4°C. The supernatants were collected and stored at -20°C. Then, 20 µg total protein was loaded onto 10% (v/v) sodium dodecyl sulfate polyacrylamide gel electrophoresis (SDS-PAGE) gels, separated, and transferred to nitrocellulose (GE Healthcare). IMP-1 protein was detected using IMP-1 antibody (sc-21026, Santa Cruz, CA), PKCa was detected using sc-208 (Santa Cruz) ERK was detected using 4695 (Cell Signaling Technology), p-ERK was detected using 4370 (Cell Signaling Technology) and α -tubulin, an internal standard was detected using antibody A1978 (Sigma).

Luciferase assays

IGROV-1 cells were plated in complete medium (10% FBS + RPMI) at a concentration of 20,000 cells/well in a 12 well plate. After cells were allowed to adhere overnight, cells were transiently transfected with either a control non coding siRNA SMARTpool or and IMP-1-specific siRNA SMARTpool as described above. The transfection complex was removed and replaced with complete medium for an additional day. The following day the cells were transiently transfected with a reporter containing 5 copies of an NF- κ B binding site driving expression of luciferase (NF- κ B)₅-Luc (generous gift provided by Dr. Lin Feng Chen). 48 hours later, cells were washed once in phosphate-buffered saline, and 150 μ l of 1 \times Passive Lysis Buffer (Promega, Madison, WI) was used to lyse the cells. Luciferase activity was determined using firefly luciferase reagent from Promega.

Statistical Analysis

Results are expressed as the mean \pm S.E.M. of at least three independent experiments. Significance was established when $p < 0.05$. Student's t test was used for comparison of the means between two groups.

RESULTS

Identification of Downregulated Transcripts in IMP-1-depleted HEK 293T Cells

In order to identify novel molecular targets of IMP-1, we performed *in silico* analysis using publically available microarrays (65) in which IMP-1 had been depleted. These studies had been initially conducted in the context of performing a transcriptome-wide analysis of proposed

binding sites for RNA-binding proteins including IMP-1. RNAi knockdown of IMP-1 in HEK 293T cells confirmed decreases in IMP-1 regulated genes, but also revealed potential novel IMP-1 regulated genes. We were particularly interested in genes that are known to play a role in cancer, specifically in the processes of cell proliferation and migration. A summary of lead candidates from the initial *in silico* analysis is presented in **Table 4.1**.

Knockdown of IMP-1 Leads to a Decrease in PKC alpha mRNA

Having established a set of potential novel IMP-1 regulated genes, we next wanted to see whether RNAi knockdown of IMP-1 in IMP-1 positive cancer cells could downregulate the expression of these genes. In particular, we were interested in further exploring whether or not there was a decrease in genes related to cell proliferation, given that this is an important physiological readout of IMP-1 activity. We observed a robust knockdown of IMP-1 in both IGROV-1 and SK-MEL2 cells (**Figure 4.1A, 4.1C**), and saw a decrease in PKC α mRNA (**Figure 4.1B, 4.1D**). Importantly, PKC α has been implicated in promoting proliferation in a variety of cancers, which is summarized in **Table 4.2**. Interestingly, we were not able to see a decrease in Cyclin D2, (CCND2), which may suggest that either Cyclin D2 is not a molecular target of IMP-1, or its targeting by IMP-1 may be cell-specific.

Knockdown of IMP-1 Leads to a Decrease in PKC α and ERK Protein

In cancer cells, PKC α is involved in cell proliferation, survival, invasion, migration, apoptosis, and anticancer drug resistance through interaction with several signal transduction pathways (93,

107). For example, during cancer cell proliferation and survival, PKC α stimulates survival or proliferation-associated signaling pathways, such as Ras/Raf/MEK/ERK (108, 109) or PI3K/Akt (110) pathways, but suppress the expression of cancer suppressor-associated or apoptotic signals such as the caspase cascade or Bax subfamily (111). Given that ERK signaling is a well-known, downstream readout for PKC α activity, we were curious whether knockdown of IMP-1 could reduce ERK signaling via PKC α . As shown in **Figure 4.2**, IMP-1 knockdown in IGROV-1 and SKMEL-2 cells led to a decrease in PKC α protein as well as basal ERK 1/2 and phosphorylated ERK 1/2 protein, suggesting the MAPK signaling pathway is altered upon IMP-1 depletion.

Knockdown of IMP-1 Decreases PKC α Protein and Overexpression of IMP-1 Increases PKC α Protein in HEK 293T Cells

As further confirmation of the results from the *in silico* microarray analysis where we observed a 4 fold decrease in IMP-1 mRNA in HEK 293T cells that were depleted of IMP-1, knockdown of IMP-1 lead to a decrease in IMP-1 protein in the same cell line (**Fig. 4.3A**). Knockdown of IMP-1 also lead to a decrease in PKC α protein (**Fig 4.3A**), which is consistent with the results we obtained for the IMP-1 positive cancer cell lines. Interestingly, when we performed a transient transfection using either a control plasmid or an IMP-1 expression plasmid, the HEK 293T cells in which IMP-1 was overexpressed also resulted in an increase in PKC α protein (**Fig. 4.3B**), supporting the view that IMP-1 regulates PKC α levels.

PKC α is Characterized as a Target for miR-340

MicroRNAs (miRs) inhibit gene expression by binding to the mRNA transcript of the target gene to induce its degradation. To identify miRs that target PKC α , and might have some interplay

with IMP-1 in regulating PKC α levels we used four cited algorithms, miRanda – mirSVR, miRDB, miRWalk, and Targetscan, and identified miR-340 as a top predicted microRNA (**Table 4.3**). Three putative binding sites of the microRNA in the 3'-UTR of PKC α , with the IMP-1 binding sites overlaid are shown in **Figure 4.4**. Given these *in silico* results, we then performed a transient transfection using a miR-340 antagonist and found that treatment with the mir-340 inhibitor lead to an increase in PKC α protein as shown in **Figure 4.5**, suggesting a role of miR-340 in regulating PKC α in cancer cells.

DISCUSSION

As the importance of IMP-1 in cancer is being elucidated, it is critical to fully understand the functions of this oncofetal RNA-binding protein related to the development and progression of the disease. IMP-1 has classically been recognized for its ability to regulate mRNAs by modulating their stability and translation (5). However, the effect of IMP-1 on each mRNA target is usually modest, making it challenging to explain the pathophysiological effects of IMP-1 through its regulation of a single target (6). Despite this, it is important to identify novel molecular targets of IMP-1 and relate these to cancer pathology in order expand our knowledge of the complex regulatory networks influenced by IMP-1. In this report, we demonstrate that IMP-1 regulates the level of PKC α in ovarian and melanoma cells, and has downstream effects on the RAS–RAF–MAPK pathway by altering ERK 1/2 levels. We also show that miR-340, which has been previously shown to work in conjunction with IMP-1 to regulate the microphthalmia-associated transcription factor (MITF), a master regulator of melanocyte development and melanogenesis, as regulating PKC α protein levels. Using miRWalk and other tools for predicted

micro RNA (miR) binding sites in the PKC α mRNA 3'-UTR (105), miR-340 was the top miR (**Table 3**). This lends additional support to the idea that PKC α is a molecular target for IMP-1. One potential mechanism by which IMP-1 might increase PKC α levels is by binding to the IMP-1 binding sequence motif (UUUAY), which has previously been identified in *Drosophila* (66) and is found in the 3'-UTR of PKC α mRNA (**Figure 4.4**). A future direction of this research will involve further exploring the interplay between IMP-1 and mir-340 in regulating PKC α levels.

In addition to enhancing cell proliferation, PKC α has been implicated in promoting inflammation and preventing apoptosis of cancer cells (112-114). Importantly, activation of PKC α has been linked to NF- κ B activation and induction of inhibitor of apoptosis (IAP) genes, including IAP1, IAP2, X-IAP, and survivin (115). We and others have shown that RNAi knockdown of IMP-1 leads to reduced expression of an NF- κ B luciferase reporter (19) (**Fig. 4.6**). Interestingly from *in silico* analysis we identified 4 potential NF- κ B binding sites in the IMP-1 promoter region (nt -2000—+1), suggesting that in addition to being activated downstream of PKC α , NF- κ B may directly act as a transcription factor for IMP-1. Taken together, this suggests that there may exist a pro-inflammatory, positive feedback regulatory loop in which IMP-1 increases NF- κ B activity and NF- κ B induces additional IMP-1.

Although our findings support previous research regarding the oncogenic activity of IMP-1 in cancer, our data also highlight PKC α as a novel molecular target of IMP-1 in cancer and explores the effect of IMP-1 knockdown on the RAS–RAF–MAPK signal transduction pathway in ovarian cancer and melanoma. Future studies that explore regulatory mechanisms relating IMP-1 and PKC α expression, including miRNA regulatory networks and NF- κ B activity will provide greater understanding of IMP-1 in cancer biology and may represent new avenues for therapeutic interventions to improve the prognosis of IMP-1 positive cancers.

TABLES

Table 4.1—Downregulated transcripts in IMP-1—depleted HEK 293T cells from microarray analysis

Gene	Function	Fold Change
JKAMP	Regulator of the duration of MAPK8 activity in response to various stress stimuli. Facilitates degradation of misfolded endoplasmic reticulum (ER) luminal proteins through the recruitment of components of the proteasome and endoplasmic reticulum-associated degradation (ERAD) system.	-3.91
PRKCA	Calcium-activated, phospholipid- and diacylglycerol (DAG)-dependent serine/ threonine-protein kinase that is involved in regulation of cell proliferation, apoptosis, differentiation, migration and adhesion, tumorigenesis by directly phosphorylating targets such as RAF1, BCL2, CSPG4, TNNT2/CTNT, or activating signaling cascade involving MAPK1/3 (ERK1/2) and RAP1GAP.	-2.35
CCND2	Member of the cyclin protein family that is involved in regulating cell cycle progression.	-2.18
NUDT21	Component of the cleavage factor Im (CFIm) complex that plays a key role in pre-mRNA 3'-processing.	-3.80

Table 4.2—PKC α and its roles in multiple types of cancer cells

Cancer	Role in Cancer	Reference
Breast cancer	Cell proliferation and metastasis, antiapoptosis, antiestrogen resistance	(116-118)
Ovarian cancer	Cell proliferation and invasion	(119,120)
Melanoma	Cell survival, invasion, and migration	(94,121)
Lung cancer	Cell proliferation, metastasis, and antiapoptosis	(92,122)
Liver cancer	Cell growth, invasion, and migration	(108,109)

Table 4.3—Predicted miRNA sites on PRKCA mRNA 3' UTR region produced by miRWalk and other programs

microRNA	miRanda	miRDB	miRWalk	RNA22	Targetscan
hsa-miR-340	X	X	X	X	X
hsa-miR-514	X	X	X		X
hsa-mir-370	X		X	X	X
hsa-miR-432	X		X	X	X
hsa-miR-205	X	X	X		X
hsa-miR-424	X		X	X	X
hsa-miR-1827	X		X	X	X

FIGURES

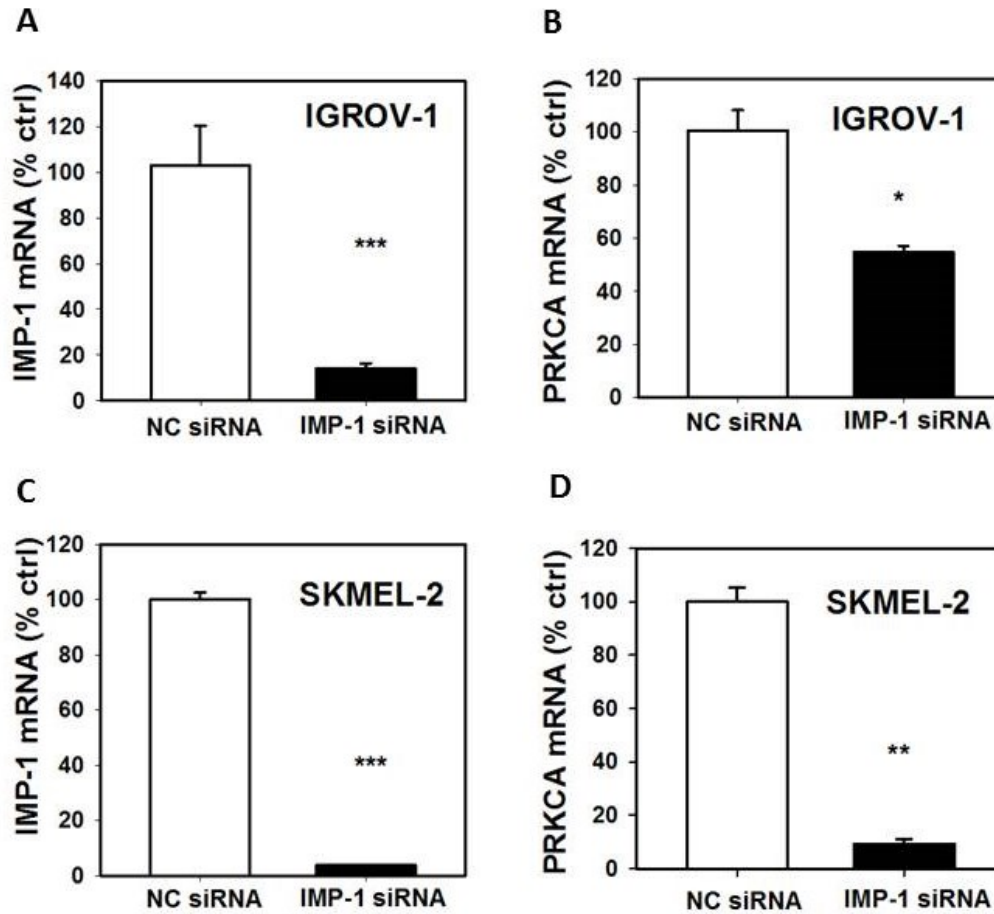


Figure 4.1. Knockdown of IMP-1 decreases PKC α mRNA. IGROV-1 and SKMEL-2 cells were treated with Noncoding Control (NC) or IMP-1 siRNA for 72 hours before RNA extraction. IMP-1 (A, C) and PKC α (B,D) mRNA was quantitated using quantitative RT-PCR and normalized to 36B4. Data represent the mean of three independent experiments \pm S.E.M.

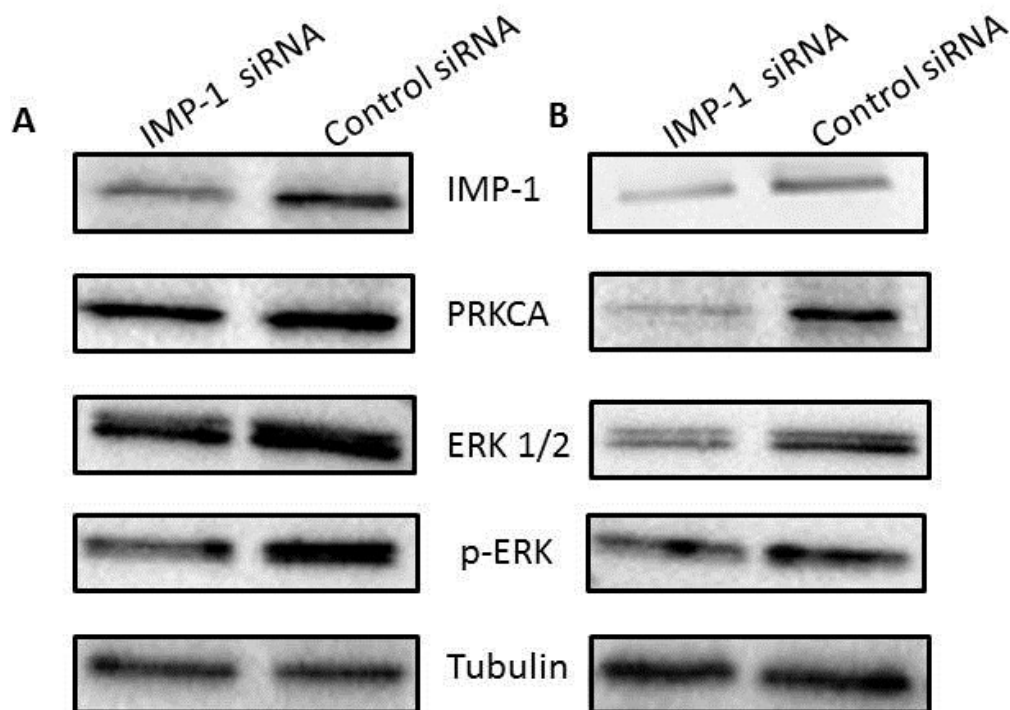


Figure 4.2. Knockdown of IMP-1 decreases PKC α and ERK protein. IGROV-1 (A) and SKMEL-2 (B) cells were treated with Noncoding Control (NC) or IMP-1 siRNA for 72 hours before the cells were harvested, protein was extracted, and equal amounts of protein were fractionated on 10% polyacrylamide gels and analyzed by Western blotting. Tubulin served as a loading control.

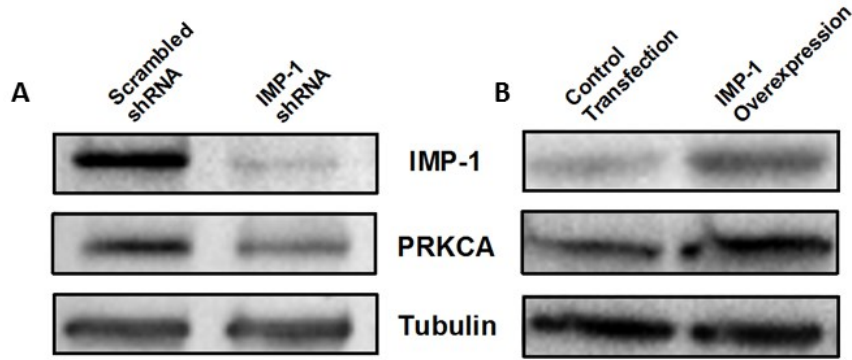


Figure 4.3. Knockdown of IMP-1 leads to a decrease in PKC α protein while overexpression of IMP-1 leads to an increase in PKC α protein in HEK 293T cells. HEK 293T cells were either treated with scramble shRNA or IMP-1 shRNA for 72 hours (A) or transfected with a control plasmid or an IMP-1 overexpression plasmid for 48 hours (B). In both A and B, 20 μ g of protein lysate was loaded and blots were probed for IMP-1, PKC α , and α -tubulin as a loading control.

Putative site 1

nt 3291

PRKCA 3'UTR—5'..AUGCAUCAUGCAAUGAAUUUUGCAUGUUUAUAAUAAACCU

Putative site 2

nt 3371

PRKCA 3'UTR—5'..AGUAUAAA GAGAGUAUUUAAAUUUUAUAAG ACACAAU

Putative site 3

nt 8111

PRKCA 3'UTR—5'..CAGAAAAUAGGUGUCAAGUCCACUUUAUAAGAACCUUUUU

Figure 4.4. Putative binding sites for miR-340 and IMP-1 in the 3'UTR of PKC α mRNA. 3 potential binding sites for miR-340 in the 3' UTR of PKC α mRNA are indicated with pink boxes and IMP-1 binding sites are overlaid in green.

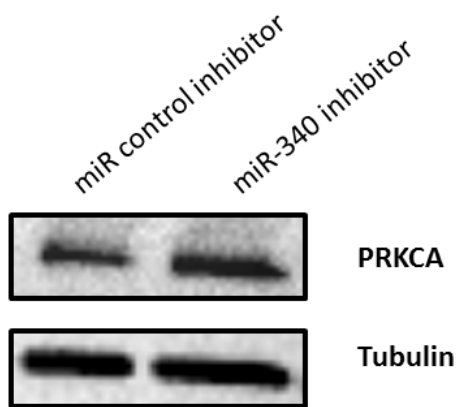


Figure 4.5. miR-340 regulates PKC α protein levels. IGROV-1 cells were plated in complete medium and then either transiently transfected with a control microRNA inhibitor or a miR-340 inhibitor. Cells were harvested and protein was harvested and analyzed using Western blot analysis. Tubulin served as a loading control.

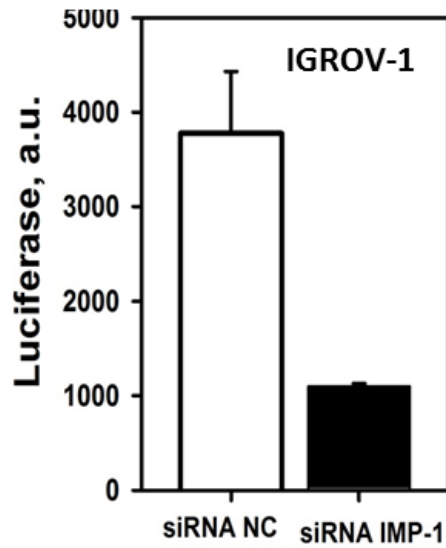


Figure 4.6. IMP-1 knock-down in IGROV-1 cells reduces NF- κ B luciferase activity. IGROV-1 cells were transfected as follows: Day 0: Control (NC) or IMP siRNA; Day 2: (NF- κ B)₅-luc; Day 4: Treatment with TNF α (10 ng/mL). Luciferase activity was assayed on day 5. (n= 3; avg \pm SEM). p<0.05.

CHAPTER 5

DISCUSSION

IGF2 mRNA-binding protein 1 (IGF2BP1/IMP-1) is a member of the RNA-binding IGF2BP protein family, which is also called the VICKZ proteins, which comprises three members in mammals (IMP-1/2/3) (5). Several studies have shown that IMP-1 controls the localization, translation and/or turnover of specific mRNAs such as c-Myc in the cytoplasm, and serves an essential function in modulating cell proliferation, and migration (6,15,27,52,123). The significance of IMP-1 action is emphasized by the fact that IMP-1 exhibits an oncofetal pattern of expression, meaning that it is expressed during development, largely turned off in non-neoplastic adult tissue, and often re-expressed in cancer. This RNA-binding protein is expressed in a diverse range of primary malignancies, including breast, ovarian, lung, skin, and colon cancer and in most other cancers. Moreover, IMP-1 expression correlates with increased metastasis and overall poor prognosis, suggesting that IMP-1 is a critical oncogenic factor.

Given its oncofetal pattern of expression, its role in a variety of cancers, and the fact that there are no known inhibitors of IMP-1, my research has focused on identifying and characterizing new small molecule inhibitors of IMP-1 action. These inhibitors could then serve as starting points for the development of therapeutically relevant drugs and additionally will be useful as probes to improve our understanding of IMP-1's oncogenic activities. As described in Chapter 2, we first performed a pilot screen to serve as proof of principle that our screening method was appropriate for identifying small molecule inhibitors of IMP-1. Further, as detailed in Chapter 3, we performed a high throughput screen to help us identify applicable chemical scaffolds. This document elaborates on screening methodologies and mechanistic studies

performed to better understand the ‘lead’ compound identified in our studies. In Chapter 4, we circle back to the role of IMP-1 in cancer etiology and report the identification of the well-known protein kinase, PKC α as a novel molecular target of IMP-1.

High throughput screening

High throughput screening (HTS) is an automated process that allows the researcher to quickly assay the biological or biochemical activity of a large number of drug-like compounds once the steps required for implementation are designed; however, it requires a fair amount of initial groundwork before assembly into a fully feasible high throughput screen. Although our laboratory has extensive experience with designing both *in vitro* biochemical and cell-based screens, the screen for IMP-1 inhibitors was the first to use a long, single stranded RNA probe, there was no template to follow. Every step in the screen was carefully planned and executed on a pilot scale before the actual screen. There were quite a few challenging hurdles before each segment of the screen was set up. For example, in order to test compounds in a high throughput screen for their ability to inhibit binding of IMP-1 to a 93 nucleotide fluorescein-labeled c-Myc RNA binding site (fIMyc), we had to synthesize milligram amounts of IMP-1 and the RNA probe. In order to obtain biologically active IMP-1, we modified a purification protocol that utilizes an expression system for recombinant untagged IMP-1 using *E. coli* stably expressing several rare tRNAs. The IMP-1 produced using this more labor intensive protocol was at least 100 fold more active than His-tagged IMP-1 we used in a study several years ago. Additionally, because the 93 nucleotide c-Myc RNA binding site was too large to synthesize commercially, we developed simple methods for *in vitro* synthesis and fluorescein-labeling of the RNA.

We carried out an initial pilot screen of 17,600 small molecules using *in vitro* fluorescence anisotropy microplate assay (FAMA). Our aim was to demonstrate that this method could be used to identify small molecules that interfere with IMP-1 binding to c-Myc mRNA. Although this biochemical approach raises fewer technical concerns compared to cell-based screening with regard to off-target effects, we still wanted to exclude from our analyses compounds with intrinsic fluorescence, which could be regarded as false positives. In order to address this, we developed a sequential protocol where we assessed changes in anisotropy, intrinsic fluorescence of test compounds, the compounds' influence on the anisotropy signal of the probe alone, and the ability of compounds to inhibit binding of IMP-1 to flMyc. The screen had a robust Z'-factor value of 0.6 which makes it a very reproducible assay and suitable for HTS.

Based on the results of the successful pilot screen we carried out a high throughput screen of ~ 150,000 small molecules from the University of Illinois High Throughput Screening Center. Using a similar set up as the pilot screen, we executed the primary high throughput screen. To increase the likelihood of identifying relatively potent medically relevant inhibitors, we screened using the relatively low concentration of 5 μ M of each compound. We developed and implemented a screening program to filter out hits and tier lead compounds based on characteristics such as potency and lack of intrinsic fluorescence. Since our primary screen was for inhibition of binding of IMP-1 to flMyc, it did not exclude compounds that non-specifically denature proteins or alter their structure. Therefore, we retested hits to test for specificity by evaluating their ability to inhibit binding of the steroid hormone receptor, progesterone receptor (PR), to its fluorescein-labeled DNA binding site (fl-progesterone response element; flPRE). We chose to retest hits for specificity using PR:fl-PRE FAMA, because this assay produces a similar

change in anisotropy as was observed for IMP-1 binding to c-Myc. Because the PR:flPRE assay looks at inhibition of binding of a DNA binding protein to a DNA response element, this may also shed insight as to whether or not the hits identified from the screen were specific to inhibiting an RNA binding protein—RNA interaction. In addition to the results from the PR:flPRE assays, we also had data for compounds identified for a previous FAMA screen that identified the estrogen receptor (ER) inhibitor TPSF. Although the ER inhibitor screen was carried out using a different final concentration of compound, this also shed insight as to whether or not inhibitors from our screen were also identified from those studies and therefore most likely broadly toxic compounds.

Although many *in vitro* screens typically use an orthogonal *in vitro* assay such as electrophoretic mobility shift assay (EMSA) to further validate lead inhibitors, the assays do not address a clear bottleneck in drug discovery—the ability of a compound to recapitulate effects observed in biochemical assays in the complex environment of cells. Therefore, we assessed how effectively and selectively the hits inhibited a key activity of IMP-1; stimulation of cell proliferation. One of the challenges of this project was to establish accurate cell-based assays for IMP-1. Unlike other systems such as estrogen receptor where there is an extensive and well-documented literature describing the presence or absence of ER in a particular cell line, IMP-1 is a relatively new molecular target in cancer biology and thus required initial groundwork to establish IMP-1 positive and negative cell lines for cell-based experiments. To establish a cell-based assay to filter the hits, we used RNAi knockdown of IMP-1 to confirm that IMP-1 expression was essential for proliferation of IMP-1 positive cells and that IMP-1 RNAi knockdown had no effect on proliferation of IMP-1 negative cells. The RNAi knockdown studies also helped verify that the antibodies we were using were specific for IMP-1. Using a

panel of IMP-1 positive and negative cells, we filtered compounds that inhibited proliferation of IMP-1 positive cells with little or no effect on IMP-1 negative cells. Among this subset of compounds, we identified 2-{[(5-bromo-2-thienyl) methylene] amino} benzamide (BTYNB) as our lead inhibitor.

An alternative to high throughput screening is to identify hits using rational design or virtual screening. Both approaches require significant structural information that has not been fully elucidated for IMP-1. Although the crystal structure for part of the chicken orthologue of IMP-1, ZBP-1, has been solved, it remains difficult to predict chemical scaffolds that could successfully inhibit IMP-1 function. Thus, rational design and virtual screen are not presently feasible and HTS is a reasonable approach for identifying novel inhibitors of IMP-1.

BTYNB—A promising new inhibitor of IMP-1 action

Following the primary *in vitro* high throughput screen and follow-on cell-based assays, we identified 2-{[(5-bromo-2-thienyl) methylene] amino} benzamide (BTYNB) as our lead inhibitor. BTYNB exhibited similar values for 50% inhibition of binding of IMP-1 to flMyc *in vitro* and for inhibition of proliferation of IMP-1 positive cancer cells. BTYNB inhibited anchorage-independent growth of IMP-1 positive cells in soft agar. Overexpression of IMP-1 reversed BTYNB's inhibition of cell proliferation, suggesting that the compound is acting through IMP-1. Treatment with BTYNB decreased IMP-1 target mRNAs, such as eEF2 and CDC34 in IMP-1 positive cells, but had no effect on these mRNAs in IMP-1 negative cells. We show that BTYNB decreased stability of c-Myc mRNA at 1 hour and that treatment with BTYNB decreases steady state c-Myc mRNA and protein at 72 hours. To our knowledge, this is the first small molecule inhibitor to decrease mRNA stability and the first small molecule

inhibitor of IMP-1, and important but previously untargeted protein in cancer. We aspire to advance this promising IMP-1 inhibitor through preclinical studies. Although discussed here, these long term goals are beyond the scope of this thesis.

Lead optimization of BTYNB using limited structure-activity relationships (SAR)

Eight commercially available structural analogues of BTYNB were evaluated as part of optimization studies. One small molecule was able to inhibit binding of IMP-1 to flmyc in FAMA by 30% when tested at 10 μ M; however, all of the other analogues of this chemical family did not inhibit binding. When tested for inhibition of cell proliferation, this small molecule inhibited proliferation of IMP-1 negative cells, and thus was considered potentially toxic. While limited, this structural data could serve as a guide for synthesis of BTYNB derivatives with improved potency and specificity. Promising compounds that emerge from optimization can be evaluated for specificity using FAMA and cell proliferation studies using multiple IMP-1 positive and negative cell lines. Ultimately, microarrays can test for off-target effects of BTYNB treatment.

Identification of PKC α as a novel molecular target of IMP-1

In Chapter 4, I demonstrate that PKC α expression levels are directly related to IMP-1 expression levels by either overexpressing or decreasing IMP-1 levels in HEK 293T and cancer cell lines. I also used Western blot analysis to demonstrate that IMP-1 depletion decreases PKC α and ERK protein levels, suggesting that IMP-1 regulates the RAS-RAF-MAPK signaling pathway. Taken together, this data strongly suggest that PKC α is a legitimate target of IMP-1. Interestingly, using tools such as Target Scan and miRWALK, we found that the 3'-UTR of PKC α mRNA

contains binding sites for both IMP-1 and miR-340. miR-340 and IMP-1 have previously been shown to compete for binding to the 3'-UTR of MITF mRNA (44), lending further credence to the view that PKC α is a molecular target of IMP-1. Using a miR-340 inhibitor, we observed an increase in PKC α protein levels, suggesting that PKC α is regulated by miR-340. This also highlights the possibility that miR-340 may be functioning in conjunction with IMP-1 to regulate PKC α levels and future studies may focus on elucidating this complex regulatory network.

Future studies to evaluate BTYNB in mouse xenograft models

The *in vivo* effectiveness of BTYNB, or the lead compound to emerge from optimization, must be determined in preclinical animal models in order to establish its potential for use in human therapy. This could be tested in IMP-1 positive ES-2 ovarian cancer and SK-MEL2 melanoma cell models because there is an unmet need for novel therapeutic agents in ovarian cancer and melanomas due to chemotherapy resistance, metastatic potential, and these cell lines exhibit stem cell-like properties. It has been widely proposed that residual stem cells repopulate tumors after therapy. Initial tumor studies involve generating ES-2 and SK-EML2 mouse xenografts with bioluminescent imaging to visualize both the primary tumor and potential metastases. Another future direction of this work will involve optimizing BTYNB by pharmacokinetics as well as determining the maximum tolerated dose and performing histopathologic assessment of tissues and organs from BTYNB-treated mice. The results from these studies will be the basis for future studies determining whether potency, specificity, and toxicity can be improved with medicinal chemistry.

The ultimate goal of this research is to develop BTYNB so that it is suitable for further optimization and establish it as a potential therapeutic for IMP-1 positive cancers, for which there are few targeted therapies.

CHAPTER 6

REFERENCES CITED

1. Mullen TE, and Marzluff, W. (2008) Degradation of histone mRNA requires oligouridylation followed by decapping and simultaneous degradation of the mRNA both 5' to 3' and 3' to 5'. *Genes Dev.* **22**, 50-65.
2. Hogan DJ, Riordan DP, Gerber AP, Herschlag D, and Brown, P. (2008) Diverse RNA-binding proteins interact with functionally related sets of RNAs, suggesting an extensive regulatory system. *PLoS Biol.* **6**, e255.
3. Ciafrè SA, and Galardi, S. (2013) microRNAs and RNA-binding proteins: a complex network of interactions and reciprocal regulations in cancer. *RNA Biol.* **10**, 935-942
4. Wurth L, and Gebauer, F. (2014) RNA-binding proteins, multifaceted translational regulators in cancer. *Biochim Biophys Acta.*
5. Yisraeli JK. (2005) VICKZ proteins: a multi-talented family or regulatory RNA-binding proteins. *Biol Cell* **97**, 87–96.
6. Bell, J. L., Wachter, K., Muhleck, B., Pazaitis, N., Kohn, M., Lederer, M., and Huttelmaier, S. (2013) Insulin-like growth factor 2 mRNA-binding proteins (IGF2BPs): post-transcriptional drivers of cancer progression? *Cellular and molecular life sciences : CMLS* **70**, 2657-2675
7. Deshler JO, Highett MI, and Schnapp, B. (1997) Localization of Xenopus Vg1 mRNA by Vera protein and the endoplasmic reticulum. *Science* **276**, 1128–1131.
8. Elisha Z, Havin L, Ringel I, and Yisraeli, J. (1995) Vg1 RNA binding protein mediates the association of Vg1 RNA with microtubules in Xenopus oocytes. *EMBO J* **14**, 5109–5114
9. Schwartz SP, Aisenthal L, Elisha Z, Oberman F, and Yisraeli, J. (1992) A 69-kDa RNA-binding protein from Xenopus oocytes recognizes a common motif in two vegetally localized maternal mRNAs. *Proc Natl Acad Sci USA* **89**, 11895–11899
10. Huttelmaier S, Zenklusen D, Lederer M, Dichtenberg J, Lorenz M, Meng X, Bassell GJ, Condeelis J, and RSinger RH. (2005) Spatial regulation of beta-actin translation by Src-dependent phosphorylation of ZBP1. *Nature* **438**, 512–515.
11. Farina, K. L., Huttelmaier, S., Musunuru, K., Darnell, R., and Singer, R. H. (2003) Two ZBP1 KH domains facilitate beta-actin mRNA localization, granule formation, and cytoskeletal attachment. *The Journal of cell biology* **160**, 77-87

12. Chao, J. A., Patskovsky, Y., Patel, V., Levy, M., Almo, S. C., and Singer, R. H. (2010) ZBP1 recognition of beta-actin zipcode induces RNA looping. *Genes & development* **24**, 148-158
13. Weidensdorfer, D., Stohr, N., Baude, A., Lederer, M., Kohn, M., Schierhorn, A., Buchmeier, S., Wahle, E., and Huttelmaier, S. (2009) Control of c-myc mRNA stability by IGF2BP1-associated cytoplasmic RNPs. *RNA* **15**, 104-115
14. Lemm, I., and Ross, J. (2002) Regulation of c-myc mRNA decay by translational pausing in a coding region instability determinant. *Molecular and cellular biology* **22**, 3959-3969
15. Kobel, M., Weidensdorfer, D., Reinke, C., Lederer, M., Schmitt, W. D., Zeng, K., Thomssen, C., Hauptmann, S., and Huttelmaier, S. (2007) Expression of the RNA-binding protein IMP1 correlates with poor prognosis in ovarian carcinoma. *Oncogene* **26**, 7584-7589
16. Bernstein, P. L., Herrick, D. J., Prokipcak, R. D., and Ross, J. (1992) Control of c-myc mRNA half-life in vitro by a protein capable of binding to a coding region stability determinant. *Genes & development* **6**, 642-654
17. Ioannidis P, Mahaira LG, Perez SA, Gritzapis AD, Sotiropoulou PA, Kavalakis GJ, Antsaklis AI, Baxevanis CN, and Papamichail, M. (2005) CRD-BP/IMP1 expression characterizes cord blood CD34+ stem cells and affects c-myc and IGF-II expression in MCF-7 cancer cells. *The Journal of biological chemistry* **280**, 20086–20093.
18. Sparanese, D., and Lee, C. H. (2007) CRD-BP shields c-myc and MDR-1 RNA from endonucleolytic attack by a mammalian endoribonuclease. *Nucleic Acids Res* **35**, 1209-1221
19. Noubissi, F. K., Elcheva, I., Bhatia, N., Shakoori, A., Ougolkov, A., Liu, J., Minamoto, T., Ross, J., Fuchs, S. Y., and Spiegelman, V. S. (2006) CRD-BP mediates stabilization of betaTrCP1 and c-myc mRNA in response to beta-catenin signalling. *Nature* **441**, 898-901
20. Elcheva, I., Goswami, S., Noubissi, F. K., and Spiegelman, V. S. (2009) CRD-BP protects the coding region of betaTrCP1 mRNA from miR-183-mediated degradation. *Molecular cell* **35**, 240-246
21. Vikesaa, J., Hansen, T. V., Jonson, L., Borup, R., Wewer, U. M., Christiansen, J., and Nielsen, F. C. (2006) RNA-binding IMPs promote cell adhesion and invadopodia formation. *EMBO J* **25**, 1456-1468
22. Mongroo PS, Noubissi FK, Cuatrecasas M, Kalabis J, King CE, Johnstone CN, Bowser MJ, Castells A, Spiegelman VS, and Rustgi, A. (2011) IMP-1 displays cross-talk with K-Ras and modulates colon cancer cell survival through the novel proapoptotic protein CYFIP2. *Cancer research* **71**, 2172-2182.

23. Git A, and Standart, N. (2002) The KH domains of Xenopus Vg1RBP mediate RNA binding and self-association. *RNA* **8**, 1319-1333.
24. Brewer, G., and Ross, J. (1989) Regulation of c-myc mRNA stability in vitro by a labile destabilizer with an essential nucleic acid component. *Molecular and cellular biology* **9**, 1996-2006
25. Ioannidis, P., Kottaridi, C., Dimitriadis, E., Courtis, N., Mahaira, L., Talieri, M., Giannopoulos, A., Iliadis, K., Papaioannou, D., Nasioulas, G., and Trangas, T. (2004) Expression of the RNA-binding protein CRD-BP in brain and non-small cell lung tumors. *Cancer letters* **209**, 245-250
26. Weinlich, S., Huttelmaier, S., Schierhorn, A., Behrens, S. E., Ostareck-Lederer, A., and Ostareck, D. H. (2009) IGF2BP1 enhances HCV IRES-mediated translation initiation via the 3'UTR. *RNA* **15**, 1528-1542
27. Stohr N, Kohn M, Lederer M, Glass M, Reinke C, Singer RH, and Huttelmaier, S. (2012) IGF2BP1 promotes cell migration by regulating MK5 and PTEN signaling. *Genes & development* **26**, 176-189.
28. Patel VL, Mitra S, Harris R, Buxbaum AR, Lionnet T, Brenowitz M, Girvin M, Levy M, Almo SC, Singer, R., and Chao, J. (2012) Spatial arrangement of an RNA zipcode identifies mRNAs under post-transcriptional control. *Genes & development* **26**, 43-53.
29. Liao B, Hu Y, Herrick DJ, and Brewer, G. (2005) The RNA-binding protein IMP-3 is a translational activator of insulin-like growth factor II leader-3 mRNA during proliferation of human K562 leukemia cells. *J Biol Chem.* **280**, 18517-18524.
30. Sheen YS, Liao YH, Lin MH, Chu CY, Ho BY, Hsieh MC, Chen PC, Cha ST, Jeng YM, Chang CC, Chiu HC, Jee SH, Kuo ML, and Chu, C. (2015) IMP-3 promotes migration and invasion of melanoma cells by modulating the expression of HMGA2 and predicts poor prognosis in melanoma. *J Invest Dermatol* **135**, 1065-1073.
31. Okada K, Fujiwara Y, Nakamura Y, Takiguchi S, Nakajima K, Miyata H, Yamasaki M, Kurokawa Y, Takahashi T, Mori M, and Doki, Y. (2012) Oncofetal protein, IMP-3, a potential marker for prediction of postoperative peritoneal dissemination in gastric adenocarcinoma. *J Surg Oncol* **105**, 780-785.
32. Gu L, Shigemasa K, and Ohama, K. (2004) Increased expression of IGF II mRNA-binding protein 1 mRNA is associated with an advanced clinical stage and poor prognosis in patients with ovarian cancer. *Int J Oncol.* **24**, 671-678.
33. Liu H, Shi J, Anandan V, Wang HL, Diehl D, Blansfield J, Gerhard G, and Lin, F. (2012) Reevaluation and identification of the best immunohistochemical panel (pVHL, Maspin, S100P, IMP-3) for ductal adenocarcinoma of the pancreas. *Arch Pathol Lab Med.* **136**, 601-609.

34. Doyle GAR, Betz NA, Leeds PL, Fleisig AJ, Prokipcak RD, and Ross J. (1998) The c-myc coding region determinant-binding protein: a member of a family of KH domain RNA-binding proteins. *Nucleic Acid Res* **26**, 5036–5044.
35. Nielsen J, Kristensen MA, Willemoës M, Nielsen FC, and Christiansen, J. (2004) Sequential dimerization of human zipcode-binding protein IMP1 on RNA: a cooperative mechanism providing RNP stability. *Nucleic Acids Res.* **32**, 4368-4376.
36. Barnes M, van Rensburg G, Li WM, Mehmood K, Mackedenski S, Chan CM, King DT, Miller AL, and Lee, C. (2015) Molecular Insights into the Coding Region Determinant-binding Protein-RNA Interaction through Site-directed Mutagenesis in the Heterogeneous Nuclear Ribonucleoprotein-K-homology Domains. *J Biol Chem.* **290**, 625-639.
37. Nielsen J, Adolph SK, Rajpert-De Meyts E, Lykke-Andersen J, Koch G, Christiansen J, and Nielsen, F. (2003) Nuclear transit of human zipcode-binding protein IMP1. *Biochem J.* **376**, 383-391.
38. Jonson, L., Vikesaa, J., Krogh, A., Nielsen, L. K., Hansen, T., Borup, R., Johnsen, A. H., Christiansen, J., and Nielsen, F. C. (2007) Molecular composition of IMP1 ribonucleoprotein granules. *Molecular & cellular proteomics : MCP* **6**, 798-811
39. Leeds P, Kren BT, Boylan JM, Betz NA, Steer CJ, Gruppuso PA, and Ross J. (1997) Developmental regulation of CRD-BP, an RNA-binding protein that stabilizes c-myc mRNA in vitro. *Oncogene* **14**, 1279–1286.
40. Prokipcak RD, Herrick DJ, and Ross, J. (1994) Purification and properties of a protein that binds to the C-terminal coding region of human c-myc mRNA. *The Journal of biological chemistry* **269**, 9261–9269.
41. Coulis, C. M., Lee, C., Nardone, V., and Prokipcak, R. D. (2000) Inhibition of c-myc expression in cells by targeting an RNA-protein interaction using antisense oligonucleotides. *Molecular pharmacology* **57**, 485-494
42. Noubissi FK, Goswami S, Sanek NA, Kawakami K, Minamoto T, Moser A, Grinblat Y, and Spiegelman, V. (2009) Wnt signaling stimulates transcriptional outcome of the hedgehog pathway by stabilizing GLI1 mRNA. *Cancer research* **69**, 8572–8578.
43. Boyerinas B, Park SM, Murmann AE, Gwin K, Montag AG, Zillardt MR, Hua YJ, Lengyel E, and Peter, M. (2012) Let-7 modulates acquired resistance of ovarian cancer to Taxanes via IMP-1-mediated stabilization of multidrug resistance 1. *International journal of cancer. Journal international du cancer* **130**, 1787-1797.
44. Goswami S, Tarapore RS, Poenitzsch Strong AM, Teslaa JJ, Grinblat Y, Setaluri V, and Spiegelman VS. (2015) MicroRNA-340-mediated degradation of microphthalmia-associated transcription factor mRNA is inhibited by the coding region determinant-binding protein. *J Biol Chem.* **290**, 384-395.

45. Poenitzsch Strong AM, Setaluri V, and Spiegelman, V. (2014) MicroRNA-340 as a modulator of RAS-RAF-MAPK signaling in melanoma. *Arch Biochem Biophys.* , 118-124.
46. Mayr C, and Bartel, D. (2009) Widespread shortening of 3'UTRs by alternative cleavage and polyadenylation activates oncogenes in cancer cells. *Cell* **138**, 673–684.
47. Boyerinas, B., Park, S. M., Shomron, N., Hedegaard, M. M., Vinther, J., Andersen, J. S., Feig, C., Xu, J., Burge, C. B., and Peter, M. E. (2008) Identification of let-7-regulated oncofetal genes. *Cancer research* **68**, 2587-2591
48. Boyerinas, B., Park, S. M., Murmann, A. E., Gwin, K., Montag, A. G., Zillhardt, M., Hua, Y. J., Lengyel, E., and Peter, M. E. (2012) Let-7 modulates acquired resistance of ovarian cancer to Taxanes via IMP-1-mediated stabilization of multidrug resistance 1. *International journal of cancer. Journal international du cancer* **130**, 1787-1797
49. Boyerinas, B., Park, S. M., Hau, A., Murmann, A. E., and Peter, M. E. (2010) The role of let-7 in cell differentiation and cancer. *Endocr Relat Cancer* **17**, F19-36
50. Noubissi, F. K., Nikiforov, M. A., Colburn, N., and Spiegelman, V. S. (2010) Transcriptional Regulation of CRD-BP by c-myc: Implications for c-myc Functions. *Genes & cancer* **1**, 1074-1082
51. Elcheva, I., Tarapore, R. S., Bhatia, N., and Spiegelman, V. S. (2008) Overexpression of mRNA-binding protein CRD-BP in malignant melanomas. *Oncogene* **27**, 5069-5074
52. Craig, E. A., Weber, J. D., and Spiegelman, V. S. (2012) Involvement of the mRNA binding protein CRD-BP in the regulation of metastatic melanoma cell proliferation and invasion by hypoxia. *Journal of cell science* **125**, 5950-5954
53. Craig, E. A., and Spiegelman, V. S. (2012) Inhibition of coding region determinant binding protein sensitizes melanoma cells to chemotherapeutic agents. *Pigment cell & melanoma research* **25**, 83-87
54. Kato T, Hayama S, Yamabuki T, Ishikawa N, Miyamoto M, Ito T, Tsuchiya E, Kondo S, Nakamura Y, and Daigo, Y. (2007) Increased expression of insulin-like growth factor-II messenger RNA-binding protein 1 is associated with tumor progression in patients with lung cancer. *Clinical Cancer Research* **13**, 434-442.
55. Dimitriadis, E., Trangas, T., Milatos, S., Foukas, P. G., Gioulbasanis, I., Courtis, N., Nielsen, F. C., Pandis, N., Dafni, U., Bardi, G., and Ioannidis, P. (2007) Expression of oncofetal RNA-binding protein CRD-BP/IMP1 predicts clinical outcome in colon cancer. *International journal of cancer. Journal international du cancer* **121**, 486-494
56. Lauscher JC, Grone J, Dullat S, Hotz B, Ritz JP, Steinhoff U, Buhr HJ, and Visekruna, A. (2010) Association between activation of atypical NF-kappaB1 p105 signaling pathway

- and nuclear beta-catenin accumulation in colorectal carcinoma. *Molecular carcinogenesis* **49**, 121-129.
57. Hanahan D, and Weinberg, R. (2011) Hallmarks of Cancer: The Next Generation. *Cell* **144**, 646-674.
 58. Ioannidis, P., Mahaira, L., Papadopoulou, A., Teixeira, M. R., Heim, S., Andersen, J. A., Evangelou, E., Dafni, U., Pandis, N., and Trangas, T. (2003) 8q24 Copy number gains and expression of the c-myc mRNA stabilizing protein CRD-BP in primary breast carcinomas. *International journal of cancer. Journal international du cancer* **104**, 54-59
 59. Müeller-Pillasch F, Lacher U, Wallrapp C, Micha A, Zimmerhackl F, Hameister H, Varga G, Friess H, Büchler M, Beger HG, Vila MR, Adler G, and Gress, T. (1997) Cloning of a gene highly overexpressed in cancer coding for a novel KH-domain containing protein. *Oncogene* **14**, 2729-2733.
 60. Ross, J., Lemm, I., and Berberet, B. (2001) Overexpression of an mRNA-binding protein in human colorectal cancer. *Oncogene* **20**, 6544-6550
 61. Hamilton, K. E., Noubissi, F. K., Katti, P. S., Hahn, C. M., Davey, S. R., Lundsmith, E. T., Klein-Szanto, A. J., Rhim, A. D., Spiegelman, V. S., and Rustgi, A. K. (2013) IMP1 promotes tumor growth, dissemination and a tumor-initiating cell phenotype in colorectal cancer cell xenografts. *Carcinogenesis* **34**, 2647-2654
 62. Natkunam Y, Vainer G, Chen J, Zhao S, Marinelli RJ, Hammer AS, Hamilton-Dutoit S, Pikarsky E, Amir G, Levy R, Yisraeli JK, and Lossos, I. (2007) Expression of the RNA-binding protein VICKZ in normal hematopoietic tissues and neoplasms. *Haematologica* **92**, 176–183.
 63. Thomas JR, and Hergenrother, P. (2008) Targeting RNA with Small Molecules. *Chem Rev.* **108**, 1171-1224.
 64. Ioannidis P, Mahaira L, Papadopoulou A, Teixeira MR, Heim S, Andersen JA, Evangelou E, Dafni U, Pandis N, and Trangas, T. (2003) CRD-BP: a c-Myc mRNA stabilizing protein with an oncofetal pattern of expression. *Anticancer research* **23**, 2179-2183.
 65. Hafner, M., Landthaler, M., Burger, L., Khorshid, M., Hausser, J., Berninger, P., Rothballer, A., Ascano, M., Jr., Jungkamp, A. C., Munschauer, M., Ulrich, A., Wardle, G. S., Dewell, S., Zavolan, M., and Tuschl, T. (2010) Transcriptome-wide identification of RNA-binding protein and microRNA target sites by PAR-CLIP. *Cell* **141**, 129-141
 66. Munro, T. P., Kwon, S., Schnapp, B. J., and St Johnston, D. (2006) A repeated IMP-binding motif controls oskar mRNA translation and anchoring independently of *Drosophila melanogaster* IMP. *The Journal of cell biology* **172**, 577-588

67. Tessier, C. R., Doyle, G. A., Clark, B. A., Pitot, H. C., and Ross, J. (2004) Mammary tumor induction in transgenic mice expressing an RNA-binding protein. *Cancer research* **64**, 209-214
68. Fakhraldeen, S. A., Clark, R. J., Roopra, A., Chin, E. N., Huang, W., Castorino, J., Wisinski, K. B., Kim, T., Spiegelman, V. S., and Alexander, C. M. (2015) Two Isoforms of the RNA Binding Protein, Coding Region Determinant-binding Protein (CRD-BP/IGF2BP1), Are Expressed in Breast Epithelium and Support Clonogenic Growth of Breast Tumor Cells. *The Journal of biological chemistry* **290**, 13386-13400
69. Nielsen, J., Christiansen, J., Lykke-Andersen, J., Johnsen, A. H., Wewer, U. M., and Nielsen, F. C. (1999) A family of insulin-like growth factor II mRNA-binding proteins represses translation in late development. *Molecular and cellular biology* **19**, 1262-1270
70. Hansen, T. V., Hammer, N. A., Nielsen, J., Madsen, M., Dalbaeck, C., Wewer, U. M., Christiansen, J., and Nielsen, F. C. (2004) Dwarfism and impaired gut development in insulin-like growth factor II mRNA-binding protein 1-deficient mice. *Molecular and cellular biology* **24**, 4448-4464
71. Mahapatra, L., Mao, C., Andruska, N., Zhang, C., and Shapiro, D. J. (2014) High-throughput fluorescence anisotropy screen for inhibitors of the oncogenic mRNA binding protein, IMP-1. *Journal of biomolecular screening* **19**, 427-436
72. Lan, L., Appelman, C., Smith, A. R., Yu, J., Larsen, S., Marquez, R. T., Liu, H., Wu, X., Gao, P., Roy, A., Anbanandam, A., Gowthaman, R., Karanicolas, J., De Guzman, R. N., Rogers, S., Aube, J., Ji, M., Cohen, R. S., Neufeld, K. L., and Xu, L. (2015) Natural product (-)-gossypol inhibits colon cancer cell growth by targeting RNA-binding protein Musashi-1. *Molecular oncology* **S1574-7891**, 00075-00077.
73. Chan, J., Khan, S. N., Harvey, I., Merrick, W., and Pelletier, J. (2004) Eukaryotic protein synthesis inhibitors identified by comparison of cytotoxicity profiles. *RNA* **10**, 528-543
74. Melvin, V. S., and Edwards, D. P. (2001) Expression and purification of recombinant human progesterone receptor in baculovirus and bacterial systems. *Methods Mol Biol* **176**, 39-54
75. Wang, S. Y., Ahn, B. S., Harris, R., Nordeen, S. K., and Shapiro, D. J. (2004) Fluorescence anisotropy microplate assay for analysis of steroid receptor-DNA interactions. *BioTechniques* **37**, 807-808, 810-807
76. Putt, K. S., and Hergenrother, P. J. (2004) A nonradiometric, high-throughput assay for poly(ADP-ribose) glycohydrolase (PARG): application to inhibitor identification and evaluation. *Analytical biochemistry* **333**, 256-264
77. Kretzer, N. M., Cherian, M. T., Mao, C., Aninye, I. O., Reynolds, P. D., Schiff, R., Hergenrother, P. J., Nordeen, S. K., Wilson, E. M., and Shapiro, D. J. (2010) A

- noncompetitive small molecule inhibitor of estrogen-regulated gene expression and breast cancer cell growth that enhances proteasome-dependent degradation of estrogen receptor $\{\alpha\}$. *The Journal of biological chemistry* **285**, 41863-41873
78. Mao, C., Patterson, N. M., Cherian, M. T., Aninye, I. O., Zhang, C., Montoya, J. B., Cheng, J., Putt, K. S., Hergenrother, P. J., Wilson, E. M., Nardulli, A. M., Nordeen, S. K., and Shapiro, D. J. (2008) A new small molecule inhibitor of estrogen receptor α binding to estrogen response elements blocks estrogen-dependent growth of cancer cells. *The Journal of biological chemistry* **283**, 12819-12830
 79. Jiang, X., Orr, B. A., Kranz, D. M., and Shapiro, D. J. (2006) Estrogen induction of the granzyme B inhibitor, proteinase inhibitor 9, protects cells against apoptosis mediated by cytotoxic T lymphocytes and natural killer cells. *Endocrinology* **147**, 1419-1426
 80. Ioannidis, P., Trangas, T., Dimitriadis, E., Samiotaki, M., Kyriazoglou, I., Tsiapalis, C. M., Kittas, C., Agnantis, N., Nielsen, F. C., Nielsen, J., Christiansen, J., and Pandis, N. (2001) C-MYC and IGF-II mRNA-binding protein (CRD-BP/IMP-1) in benign and malignant mesenchymal tumors. *International journal of cancer. Journal international du cancer* **94**, 480-484
 81. Hizli, A. A., Chi, Y., Swanger, J., Carter, J. H., Liao, Y., Welcker, M., Ryazanov, A. G., and Clurman, B. E. (2013) Phosphorylation of eukaryotic elongation factor 2 (eEF2) by cyclin A-cyclin-dependent kinase 2 regulates its inhibition by eEF2 kinase. *Molecular and cellular biology* **33**, 596-604
 82. Leprivier, G., Remke, M., Rotblat, B., Dubuc, A., Mateo, A. R., Kool, M., Agnihotri, S., El-Naggar, A., Yu, B., Somasekharan, S. P., Faubert, B., Bridon, G., Tognon, C. E., Mathers, J., Thomas, R., Li, A., Barokas, A., Kwok, B., Bowden, M., Smith, S., Wu, X., Korshunov, A., Hielscher, T., Northcott, P. A., Galpin, J. D., Ahern, C. A., Wang, Y., McCabe, M. G., Collins, V. P., Jones, R. G., Pollak, M., Delattre, O., Gleave, M. E., Jan, E., Pfister, S. M., Proud, C. G., Derry, W. B., Taylor, M. D., and Sorensen, P. H. (2013) The eEF2 kinase confers resistance to nutrient deprivation by blocking translation elongation. *Cell* **153**, 1064-1079
 83. Oji Y, Tatsumi N, Fukuda M, Nakatsuka S, Aoyagi S, Hirata E, Nanchi I, Fujiki F, Nakajima H, Yamamoto Y, Shibata S, Nakamura M, Hasegawa K, Takagi S, Fukuda I, Hoshikawa T, Murakami Y, Mori M, Inoue M, Naka T, Tomonaga T, Shimizu Y, Nakagawa M, Hasegawa J, Nezu R, Inohara H, Izumoto S, Nonomura N, Yoshimine T, Okumura M, Morii E, Maeda H, Nishida S, Hosen N, Tsuboi A, Oka Y, and H., S. (2014) The translation elongation factor eEF2 is a novel tumor-associated antigen overexpressed in various types of cancers. *Int J Oncol.* **5**, 1461-1469
 84. Nakamura, J., Aoyagi, S., Nanchi, I., Nakatsuka, S., Hirata, E., Shibata, S., Fukuda, M., Yamamoto, Y., Fukuda, I., Tatsumi, N., Ueda, T., Fujiki, F., Nomura, M., Nishida, S., Shirakata, T., Hosen, N., Tsuboi, A., Oka, Y., Nezu, R., Mori, M., Doki, Y., Aozasa, K., Sugiyama, H., and Oji, Y. (2009) Overexpression of eukaryotic elongation factor eEF2 in

- gastrointestinal cancers and its involvement in G2/M progression in the cell cycle. *Int J Oncol* **34**, 1181-1189
85. Fernandez, P. C., Frank, S. R., Wang, L., Schroeder, M., Liu, S., Greene, J., Cocito, A., and Amati, B. (2003) Genomic targets of the human c-Myc protein. *Genes & development* **17**, 1115-1129
 86. Lin, C. Y., Loven, J., Rahl, P. B., Paranal, R. M., Burge, C. B., Bradner, J. E., Lee, T. I., and Young, R. A. (2012) Transcriptional amplification in tumor cells with elevated c-Myc. *Cell* **151**, 56-67
 87. Mao, C., Flavin, K. G., Wang, S., Dodson, R., Ross, J., and Shapiro, D. J. (2006) Analysis of RNA-protein interactions by a microplate-based fluorescence anisotropy assay. *Analytical biochemistry* **350**, 222-232
 88. Andruska N, Zheng X, Yang X, WG, H., and DJ, S. (2014) Anticipatory estrogen activation of the unfolded protein response is linked to cell proliferation and poor survival in estrogen receptor α -positive breast cancer. *Oncogene*
 89. Nishizuka Y. (1995) Protein kinase C and lipid signaling for sustained cellular responses. *FASEB J.* **9**, 484-496.
 90. Liu WS, and Heckman CA. (1998) The sevenfold way of PKC regulation. *Cell Signal* **10**, 529-542.
 91. Livneh E, and Fishman DD. (1997) Linking protein kinase C to cell-cycle control. *Eur J Biochem* **248**, 1-9
 92. Wang C, Wang X, Liang H, Wang T, Yan X, Cao M, Wang N, Zhang S, Zen K, Zhang C, and Chen X. (2013) miR-203 inhibits cell proliferation and migration of lung cancer cells by targeting PKC α . *PLoS One.* **8**, e73985.
 93. Kang JH. (2014) Protein Kinase C (PKC) Isozymes and Cancer. *New Journal of Science* **2014** 1-36.
 94. Smith SD, Enge M, Bao W, Thullberg M, Costa TD, Olofsson H, Gashi B, Selivanova G, and Strömlad S. (2012) Protein kinase C α (PKC α) regulates p53 localization and melanoma cell survival downstream of integrin α v in three-dimensional collagen and in vivo. *J Biol Chem.* **287**, 29336-29347.
 95. Byers HR, Boissel SJ, Tu C, and Park HY. (2010) RNAi-mediated knockdown of protein kinase C- α inhibits cell migration in MM-RU human metastatic melanoma cell line. *Melanoma Res.* **20**, 171-178.
 96. Lahn M, Köhler G, Sundell K, Su C, Li S, Paterson BM, and Bumol TF. (2004) Protein kinase C α expression in breast and ovarian cancer. *Oncology.* **67**, 1-10.

97. Mochly-Rosen D, Das K, and Grimes KV. (2012) Protein kinase C, an elusive therapeutic target? *Nat Rev Drug Discov.* **11**, 937-957.
98. Calin GA, and Croce CM. (2006) MicroRNA signatures in human cancers. *Nat Rev Cancer* **6**, 857-866.
99. Garzon R, Fabbri M, Cimmino A, Calin GA, and Croce CM. (2006) MicroRNA expression and function in cancer. *Trends Mol Med* **12**, 580-587.
100. Medina PP, and FJ., S. (2008) microRNAs and cancer: an overview. *Cell Cycle.* **7**, 2485-2492.
101. Krutovskikh VA, and Z., H. (2010) Oncogenic microRNAs (OncomiRs) as a new class of cancer biomarkers. *Bioessays.* **32**, 894-904.
102. Rovira C, Güida MC, and A., C. (2010) MicroRNAs and other small silencing RNAs in cancer. *IUBMB Life.* **62**, 859-868.
103. Friedman RC, Farh KK, Burge CB, and DP., B. (2009) Most mammalian mRNAs are conserved targets of microRNAs. *Genome Res.* **19**, 92-105.
104. John B, Enright AJ, Aravin A, Tuschl T, Sander C, and DS., M. (2004) Human MicroRNA targets. *PLoS Biol.* **2**, e363.
105. Dweep H, Sticht C, Pandey P, and Gretz N. (2011) miRWalk--database: prediction of possible miRNA binding sites by "walking" the genes of three genomes. *J Biomed Inform.* **44**, 839-847
106. Kanamori H, Krieg S, Mao C, Di Pippo VA, Wang S, Zajchowski DA, and Shapiro DJ. (2000) Proteinase inhibitor 9, an inhibitor of granzyme B-mediated apoptosis, is a primary estrogen-inducible gene in human liver cells. *J Biol Chem.* **275**, 5867-5873.
107. Nakashima S. (2002) Protein kinase C alpha (PKC alpha): regulation and biological function. *J Biochem.* **132**, 669-675.
108. Wen-Sheng W. (2006) Protein kinase C alpha trigger Ras and Raf-independent MEK/ERK activation for TPA-induced growth inhibition of human hepatoma cell HepG2. *Cancer Lett.* **239**, 27-35.
109. Wen-Sheng W, and Jun-Ming H. (2005) Activation of protein kinase C alpha is required for TPA-triggered ERK (MAPK) signaling and growth inhibition of human hepatoma cell HepG2. *J Biomed Sci.* **12**, 289-296.
110. Thorne AM, Jackson TA, Willis VC, and Bradford AP. (2013) Protein Kinase C α Modulates Estrogen-Receptor-Dependent Transcription and Proliferation in Endometrial Cancer Cells. *Obstet Gynecol Int.* **2013**, 537479.

111. Ruvolo PP, Deng X, Carr BK, and May WS. (1998) A functional role for mitochondrial protein kinase Calpha in Bcl2 phosphorylation and suppression of apoptosis. *J Biol Chem.* **273**, 25436-22542.
112. Konopatskaya O, and Poole AW. (2010) Protein kinase Calpha: disease regulator and therapeutic target. *Trends Pharmacol Sci.* **31**, 8-14.
113. Biswas DK, Cruz AP, Gansberger E, and Pardee AB. (2000) Epidermal growth factor-induced nuclear factor kappa B activation: A major pathway of cell-cycle progression in estrogen-receptor negative breast cancer cells. *Proc Natl Acad Sci U S A.* **97**, 8542-8547.
114. Biswas DK, Dai SC, Cruz A, Weiser B, Graner E, and Pardee AB. (2001) The nuclear factor kappa B (NF-kappa B): a potential therapeutic target for estrogen receptor negative breast cancers. **98**, 10386-10391.
115. Biswas DK, Martin KJ, McAlister C, Cruz AP, Graner E, Dai SC, and Pardee AB. (2003) Apoptosis caused by chemotherapeutic inhibition of nuclear factor-kappaB activation. *Cancer Res.* **63**, 290-295.
116. Gupta AK, Galoforo SS, Berns CM, Martinez AA, Corry PM, Guan KL, and Lee YJ. (1996) Elevated levels of ERK2 in human breast carcinoma MCF-7 cells transfected with protein kinase C alpha. *Cell Prolif.* **29**, 655-663.
117. Kim J, Thorne SH, Sun L, Huang B, and Mochly-Rosen D. (2011) Sustained inhibition of PKC α reduces intravasation and lung seeding during mammary tumor metastasis in an in vivo mouse model. *Oncogene* **30**, 323-333.
118. Tan M, Li P, Sun M, Yin G, and Yu D. (2006) Upregulation and activation of PKC alpha by ErbB2 through Src promotes breast cancer cell invasion that can be blocked by combined treatment with PKC alpha and Src inhibitors. *Oncogene*, 3286-3295.
119. Mahanivong C, Chen HM, Yee SW, Pan ZK, Dong Z, and Huang S. (2008) Protein kinase C alpha-CARMA3 signaling axis links Ras to NF-kappa B for lysophosphatidic acid-induced urokinase plasminogen activator expression in ovarian cancer cells. *Oncogene* **27**, 1273-1280.
120. Weichert W, Gekeler V, Denkert C, Dietel M, and Hauptmann S. (2003) Protein kinase C isoform expression in ovarian carcinoma correlates with indicators of poor prognosis. *Int J Oncol.* **23**, 633-639.
121. Putnam AJ, Schulz VV, Freiter EM, Bill HM, and Miranti CK. (2009) Src, PKC α , and PKC δ are required for α v β 3 integrin-mediated metastatic melanoma invasion. *Cell Commun Signal.* **7**, 10.

122. Singhal SS, Yadav S, Singhal J, Drake K, Awasthi YC, and S., A. (2005) The role of PKC α and RLIP76 in transport-mediated doxorubicin-resistance in lung cancer. *FEBS Lett.* . **579**, 4635-4641.
123. Zhou X, Z. C., Lu SX, Chen GG, Li LZ, Liu LL, Yi C, Fu J, Hu W, Wen JM, Yun JP. (2014) miR-625 suppresses tumour migration and invasion by targeting IGF2BP1 in hepatocellular carcinoma. *Oncogene.*, [Epub ahead of print]